HELMINIAK

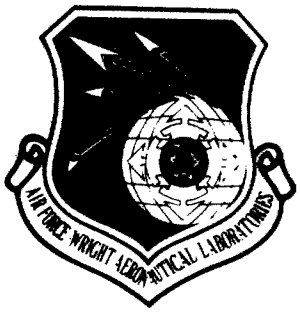

AFWAL-TR-80-4138
ADA 097929

POLYMER/SOLVENT AND POLYMER/POLYMER INTERACTION STUDIES

J. C. Holste
C. J. Glover
K. C. B. Dangayach
T. A. Powell
D. T. Magnuson

Chemical Engineering Department
Texas A&M University
College Station, Texas 77843

June 1980

Technical Report AFWAL-TR-80-4138
Final Report for period June 1979-May 1980

MATERIALS LABORATORY
AIR FORCE WRIGHT AERONAUTICAL LABORATORIES
AIR FORCE SYSTEMS COMMAND
WRIGHT-PATTERSON AIR FORCE BASE, OHIO 45433

NOTICE

When Government drawings, specifications, or other data are used for any purpose other than in connection with a definitely related Government procurement operation, the United States Government thereby incurs no responsibility nor any obligation whatsoever; and the fact that the government may have formulated, furnished, or in any way supplied the said drawings, specifications, or other data, is not to be regarded by implication or otherwise as in any manner licensing the holder or any other person or corporation, or conveying any rights or permission to manufacture use, or sell any patented invention that may in any way be related thereto.

This report has been reviewed by the Office of Public Affairs (ASD/PA) and is releasable to the National Technical Information Service (NTIS). At NTIS, it will be available to the general public, including foreign nations.

This technical report has been review and is approved for publication.

IVAN J. GOLDFARB
Project Monitor

R. L. VANDEUSEN, Chief
Polymer Branch
Nonmetallic Materials Division

FOR THE COMMANDER

F. D. CHERRY, Chief
Nonmetallic Materials Division

"If your address has changed, if you wish to be removed from our mailing list, or if the addressee is no longer employed by your organization please notify AFWAL/ML-BP, W-PAFB, OH 45433 *to help us maintain a current mailing list".*

Copies of this report should not be returned unless return is required by security considerations, contractual obligations, or notice on a specific document.

AIR FORCE/56780/9 April 1981 — 100

SECURITY CLASSIFICATION OF THIS PAGE *(When Data Entered)*

REPORT DOCUMENTATION PAGE

READ INSTRUCTIONS BEFORE COMPLETING FORM

1. REPORT NUMBER: AFWAL-TR-80-4138	2. GOVT ACCESSION NO.
3. RECIPIENT'S CATALOG NUMBER	
4. TITLE *(and Subtitle)*: POLYMER/SOLVENT AND POLYMER/POLYMER INTERACTION STUDIES	5. TYPE OF REPORT & PERIOD COVERED: Final Report June 1979-May 1980
	6. PERFORMING ORG. REPORT NUMBER
7. AUTHOR(s): J.C. Holste, C.J. Glover, K.C.B. Dagayach, T.A. Powell, D.T. Magnuson	8. CONTRACT OR GRANT NUMBER(s): F33615-78-C-5078
9. PERFORMING ORGANIZATION NAME AND ADDRESS: Chemical Engineering Department, Texas A&M University, College Station, TX 77843	10. PROGRAM ELEMENT, PROJECT, TASK AREA & WORK UNIT NUMBERS: Project 2414, Task 241904
11. CONTROLLING OFFICE NAME AND ADDRESS: Air Force Systems Command, Air Materials Laboratory (AFWAL/MLB), Air Force Wright Aeronautical Laboratories, Wright-Patterson Air Force Base, OH 45433	12. REPORT DATE: September 1980
	13. NUMBER OF PAGES: 138
14. MONITORING AGENCY NAME & ADDRESS *(if different from Controlling Office)*	15. SECURITY CLASS. *(of this report)*: Unclassified
	15a. DECLASSIFICATION/DOWNGRADING SCHEDULE

16. DISTRIBUTION STATEMENT *(of this Report)*

Approved for public release; distribution unlimited

17. DISTRIBUTION STATEMENT *(of the abstract entered in Block 20, if different from Report)*

18. SUPPLEMENTARY NOTES

19. KEY WORDS *(Continue on reverse side if necessary and identify by block number)*

Polymers, Solutions, Polysulfones, Radel, P1700, Gas Chromatography, Piezoelectric Sorption, PATS, Acetylene-terminated Sulfone Ternary Mixtures

20. ABSTRACT *(Continue on reverse side if necessary and identify by block number)*

The technique of gas chromatography has been used to investigate the solution properties of many solvents with a propargyl (acetylene-terminated) sulfone (PATS). In this case, unlike previous work on the RADEL polysulfone, no correlation between the strength of the specific interaction parameter and the solubility as determined from beaker tests is found. Furthermore, curing of the PATS at 240°C for 24 hours did not change the measured plasticizer/solvent interactions.

DD FORM 1 JAN 73 1473 EDITION OF 1 NOV 65 IS OBSOLETE

SECURITY CLASSIFICATION OF THIS PAGE *(When Data Entered)*

Piezoelectric sorption techniques were used to study the solution properties of a P1700/ATS/dichloromethane system. Phase equilibrium data are presented for ATS/dichloromethane, P1700/dichloromethane and P1700/ATS/dichloromethane. The ternary system contained 70% P1700 and 30% ATS by weight on a dry basis. Both the Flory-Huggins and corresponding states solutions were used in the data analysis. In both cases, the binary interaction parameter for P1700-ATS interactions indicated strong interactions, in agreement with experimental observations that these polymers form a compatible system.

Gas chromatographic investigations of the Radel polysulfone indicate the presence of a phase transition of undetermined character between 185 and 200°C in addition to the glass transition between 220 and 230°C.

PREFACE

This report is an account of work performed by the Texas A&M Research Foundation, College Station, Texas 77843, on polymer/polymer and polymer/solvent interactions. The work was conducted under contract F33615-78-C-5078 for the Air Force Materials Laboratory. The performance period was 1 June 1979 through 31 May 1980.

The work was performed in the Chemical Engineering Department of Texas A&M University with Dr. James C. Holste and Dr. Charles J. Glover serving as the principal investigators. The PATS measurements were made by Mr. Ted A. Powell; the P1700/ATS/ dichloromethane investigations were done by Dr. Kailash C. B. Dangayach; and the Radel polysulfone research was conducted by Dr. Denise T. Magnuson. The project engineer was Dr. Ivan J. Goldfarb, AFWAL/MLBP, Air force Materials Laboratory, Wright-Patterson Air Force Base, Ohio.

TABLE OF CONTENTS

LIST OF ILLUSTRATIONS

LIST OF TABLES

SECTION I

INTRODUCTION

The principle objective of the research described in this report is the investigation of polymer/polymer and polymer/solvent interactions for polymers of both short-term and long-term practical interest for use as structural materials. The general areas of interest are thermally-stable aromatic heterocyclic polymers, matrix polymer/plasticizer systems, and polymer/polymer miscibilities. Results of previous investigations of these systems have been given in four previous reports.[1-4] In an interim report[1] for this work, we gave the results of experimental investigations for several polymers: a polybenzothiazole, two polysulfones, two sulfone-based plasticizers, and a polysulfone/plasticizer mixture. In addition, we presented theoretical expressions that have been developed during this contract that describe the solution thermodynamics of a ternary mixture containing two solvents and one rigid-rod polymer. In this report, we present the results of experimental investigations on a sulfone-based reactive plasticizer, a polysulfone polymer, and a

---

[1] Holste, J.C., Glover, C.J., Magnuson, D.T., Dangayach, K.C.B., Powell, T.A., Ching, D.W., and Person, D.R., "Polymer/Solvent Polymer/Polymer Interaction Studies," AFML-TR-79-4107, U.S. Air Force Materials Laboratory (1979).

[2] Bonner, D.C., Holste, J.C., Glover, C.J., Magnuson, D.T., Eversdyk, D.A., and Dangayach, K., "Polymer-Polymer Interactions," AFML-TR-78-163, U.S. Air Force Materials Laboratory (1978).

[3] Bonner, D.C., "Determination of Solvents for Thermally Stable Polymers," AFML-TR-77-73, U.S. Air Force Materials Laboratory (1977).

[4] Bonner, D.C., "Determinations of Solvents for Thermally Stable Aromatic Heterocyclic Polymers," AFML-TR-76-51, U.S. Air Force Materials Laboratory (1976).

polysulfone/plasticizer mixture.

Two experimental techniques were used in the investigations of the solution properties for the polymers of interest: gas chromatography and piezoelectric sorption. The gas chromatography measurements are most useful for determining the relative strengths of interaction between a polymer and a large number of solvents, while the piezoelectric sorption apparatus provides the most efficient method for gathering phase equilibrium data between a solvent and one or more polymers at finite solvent concentrations. Gas chromatography also shows great potential as a method for investigating ternary mixtures containing two solvents and a single polymer. Further experimental improvements must be made to obtain acceptable results, but the required improvements appear to be well within the realm of possibility. The experimental techniques are described in some detail in Section II of the previous report[1] which is designed to present a review of our current experimental theory and practice. A brief review of the thermodynamic concepts and relations used in our work also is included.

Acetylene-terminated reactive plasticizers are of interest for use with other matrix polymers or as thermosetting materials in their own right. We have completed an investigation of the interactions of a propargyl(acetylene-terminated)sulfone (PATS), using both gas chromatography and beaker-scale tests. The results of these investigations are given in Section II.

Polymer/polymer miscibility predictions are of extreme interest for predicting the phase behavior of polymer blends. We have completed a theoretical and experimental study of the phase equilibrium behavior of a ternary mixture containing a polysulfone polymer (P1700), a re-

active plasticizer (ATS) and a solvent (dichloromethane). The experimental measurements were made using both gas chromatography and the piezoelectric sorption device. A formulation of Flory's liquid-state (corresponding states) theory appropriate to this system was developed and used to analyze the experimental data. The results of this investigation, which indicated a very strong interaction between the P-1700 and the ATS plasticizer, are presented in Section III.

Finally, in Section IV, we present some final comments regarding our investigations of the Radel polysulfone, and our conclusions regarding the presence of phase transitions in this material.

SECTION II

PATS SOLVENT SCAN RESULTS

Polysulfones are amorphous, mechanically strong polymers with high glass transition temperatures [T_g]. The molding of polysulfones into desired shapes can occur only at temperatures above T_g. Since high T_g polymer melts require excessive energy consumption, alternative processing techniques that lower T_g during formation often are employed. They are:

(1) to mold a polymer-solvent mixture,

(2) to mold a reactive plasticizer, that is similar in structure to the desired polymer, by itself or in a solvent solution, or

(3) to mold a polymer-plasticizer-solvent mixture.

Once the desired shape is obtained, any alternative utilizing a solvent requires the evaporation of the solvent. The second and third alternatives usually are preferred by industry due to the often corrosive and carcinogenic nature of polymer-dissolving solvents. The use of a plasticizer instead of a polymer requires no additional processing steps since the drying operations are at a sufficiently high temperature to cause polymerization.

The purpose of this research was to observe the interaction and solubility of various organic solvents with the reactive sulfone plasticizer, propargyl [acetylene-terminated] sulfone, hereafter referred to as PATS. These numbers are useful both for direct applications in the design of solvent removal equipment and for potential indirect applications such as the prediction of polymer/polymer miscibility behavior.

1. SOLVENT SCAN THEORY

We present here a brief description of the basic concepts of the solvent scan procedure. A detailed description which includes both the gas chromatography theory and the solution thermodynamic theory was presented in an earlier report.[1]

The solvent scan procedure has two principal objectives: the determination of solvents in which the polymer undergoes dissolution, and the measurement of the relative strengths of interaction between the polymer and the individual solvents. In general, a strong interaction is required to overcome the combinatorial effects on the entropy of mixing and permit dissolution. The procedure is based loosely on the approach first described by Hildebrand and Scott[5] where the concept of a solubility parameter is used. This solubility parameter δ represents the cohesive energy density of the condensed phase (in this case the liquid), and it is related to the internal energy change upon vaporization ΔU_v by

$$\delta = \left(\frac{\Delta U_v}{V} \right)^{1/2}, \qquad (1)$$

where V is the molar volume. The cohesive energy contains contributions from hydrogen bonding (or other specific interactions), interactions between permanent dipole moments in the molecules, and interactions between induced dipole moments in the molecules (dispersion or van der Waal's forces). Hansen[6] extended the method of Hildebrand and Scott

---

[5] Hildebrand, J.H. and Scott, R.L., The Solubility of Non-Electrolytes, p. 136, Reinhold (1950).

[6] Hansen, C.N., and Beerbower, A., Encyclopedia of Chemical Technology, Supplement Volume 1971, p. 889, Wiley (1971).

by defining the solubility parameter in terms of components for each of the forces:

$$\delta^2 = \delta_p^2 + \delta_h^2 + \delta_d^2 \ , \qquad (2)$$

where δ_d, δ_p and δ_h represent the dispersion, permanent dipole and hydrogen-bonding components of the solubility parameter. The general approach used by Hansen to predict solubilities was to require that each of these individual components of the solubility parameters for each component be equal, i.e., $\delta_p(1) = \delta_p(2)$, $\delta_h(1) = \delta_h(2)$ and $\delta_d(1) = \delta_d(2)$. The dispersion component is ignored in the present procedure, since the energies of induced dipole interactions will be much smaller than those associated with hydrogen-bonding or other specific interactions. Bonner[4] has pointed out that the hydrogen-bonding parameter may not be a reliable test for mixtures since the polymer/solvent specific interactions may differ appreciably from the solvent/solvent interactions represented by the δ_h value for the solvent. Instead, he proposes that an experimentally determined interaction energy be used in place of the hydrogen-bonding parameter of Hansen. Thus one criterion for solubility would be for both the solvent and the polymer to have identical values for δ_p and to have $\Lambda^{\frac{1}{2}}$ (solvent) = δ_h (polymer), where Λ represents the energy density associated with the specific interaction. The value of the polar solubility parameter can be estimated using the method of Beerbower[6]

$$\delta_p = 18.3\mu/V^{0.5}, \qquad (3)$$

and the specific interaction parameters are determined using a method to be described below. It is possible that even the criterion associated with the polar solubility parameter becomes unimportant if the

specific interactions are sufficiently strong. Such a result may occur in the case of the Radel polysulfone,[2] where the relative efficacy of the solvent appears to follow exactly the order of the relative specific interaction parameter, with no apparent dependence on the polar solubility parameter.

The experimental approach is to define a Gibbs free energy of sorption, and to express this parameter in terms of the experimental observations. (See Ref. 1 for details). This Gibbs energy of sorption then is written as the linear combination of a term directly proportional to the polarizability, a term directly proportional to the permanent dipole moment, and a specific interaction contribution:

$$\Delta G_{ads} = G + a\alpha_1 + b\mu_1 + \Lambda_1, \qquad (4)$$

where G is a constant arising from the choice of reference state, α_1 is the polarizability, μ_1 is the permanent dipole moment, Λ_1 is the specific interaction parameter, and a, b are proportionality constants. The experimental procedure uses a number of non-polar solvents with no specific interactions to establish a dispersion contribution base line, i.e. the proportionality constant a. This contribution then is subtracted to yield the dipole and specific interaction sum

$$\Delta G_{add} = b\mu_1 + \Lambda_1 = \Delta G_{ads} - a\alpha_1 - G. \qquad (5)$$

Then, a group of polar but not specifically interacting solvents is used to evaluate the proportionality constant b in the ΔG_{add} quanity. Considerable uncertainty may arise in this step because of the difficulty in determining whether or not specific interactions are present for a given solvent. In many cases, ethers appear to behave as non-specifically interacting polar compounds, but this probably is not

generally true. Then, specific interaction parameters are calculated for the remaining solvents from

$$\Lambda_1 = \Delta G_{add} - b\mu_1. \tag{6}$$

The solubility criteria following the method of Hansen then can be summarized as follows:

1). $\delta_d(\text{solvent}) \cong \delta_d(\text{polymer})$

2). $\delta_p(\text{solvent}) \cong \delta_d(\text{polymer})$

3). $\sqrt{\Lambda} \cong \delta_h(\text{polymer})$.

(Values of δ_p and δ_h for the polymer may be estimated using the group contribution methods of Fedors.[7,8]) In general, a substantial contribution must be obtained from the specific interactions to accomplish dissolution of the polymer. The solubility criteria only serve to identify potential solvents; beaker tests must be performed as a final step.

2. EXPERIMENTAL DETAILS

The pertinent experimental apparatus and procedures are summarized here. A more detailed description is available elsewhere.[9]

a. Apparatus

The PATS plasticizer measurements were made using the arrangement shown in Figure 1*. The reference column has been eliminated (along with the need for balancing flow rates), by routing the carrier gas

---

[7] Fedors, R.F., Polym. Eng. Sci., 14, 147 (1974).

[8] Fedors, R.F., Polym. Eng. Sci., 14, 472 (1974).

[9] Powell, T.A., "Solvent Interactions with a Cured and Uncured Reactive Sulfone Plasticizer - PATS," M. S. Thesis, Texas A&M University (1979), unpublished.

*Figures and tables are located at end of report.

first through the TCD, then through the column, and finally out through the TCD, solvent trap and soap bubble flow meter. With this arrangement the TCD detects the presence of solvent vapor by comparing the thermal conductivities of the intake and exhaust gases from the column, and the flow rates in both arms of the TCD are balanced automatically. The flow rate through the system now is adjusted using the upstream flow controller (not shown); this is much easier than using a metering valve. In addition, ambiguity concerning the use of the soap bubble flow meter is removed, reducing the probability of operator error. The inlet and outlet temperatures are measured as before. The addition of a capillary by-pass (labeled C on Figure 1b) is a second significant modification to the apparatus. This by-pass allows a small fraction (ideally 5 to 10%) of the injected sample to by-pass the column and pass directly to the detector. The elution time for the portion by-passing the column is proportional to the dead volume outside the column, while the elution time for an inert sample passing through the column is proportional to the sum of the void volume in the column and the dead volume outside the column. The difference in elution times therefore provides a measure of the void volume actually in the column. In addition, manual marking of the injection time on the chart recording no longer is required, thereby eliminating another potential source of significant experimental error. The solvent injections for the PATS measurements were made between the TCD and the capillary by-pass, but these injections also could be made ahead of the TCD inlet. The latter arrangement could be used to detect problems associated with injection technique (these can cause significant errors in GC work).

The solvent injection pumps shown on Figure 1 were not used for

the PATS measurements, but they may be used for ternary system studies. A continuous injection of solvent into the heated inlet line provides a finite concentration of one or more solvents in the vapor phase. The steady-state condition in the column then consists of a stationary phase in equilibrium with a vapor phase, where both phases contain a finite concentration of solvent. The response of the system to a perturbation of this steady state (a solvent injection) provides phase equilibrium information at finite solvent concentrations.

Several comments on experimental procedures and techniques are in order. First, the equations relating the chromatography results to phase equilibrium information are derived assuming zero pressure gradient along the column. The pressure drop across the column therefore must be kept as small as possible to obtain true thermodynamic information. Second, the derivations also depend upon the assumption that thermodynamic equilibrium is attained between the vapor and stationary phases. This requires that both the carrier gas flow rate and the solvent sample size be kept as low as possible. We have assumed that we are truly observing the equilibrium properties when we can detect no dependence of the results upon either the carrier gas flow rate or the sample size. In the case where the sample size dependence cannot be eliminated completely the results are extrapolated to zero sample size. Sample-size dependence occurs more frequently in glassy polymers, particularly for poor solvents, because the mass transfer processes required to achieve thermodynamic equilibrium are hindered in the glassy state.

The most convenient injection procedure is to dip the tip of a one microliter syringe in the solvent of interest, extract the syringe from the solvent, dry the outside of the needle and then draw the needle full

of air. The sample/air combination then is injected into the column. After the peak has eluted from the column, the syringe is drawn full of air and another injection made. The procedure is repeated until there is no solvent in the injected air sample. Each of the successive peaks then represents a smaller sample size and several points for extrapolation to zero sample size can be obtained quite easily and rapidly.

In general, great care must be exercised to assure that equilibrium conditions actually are present in the column when making thermodynamic measurements using gas chromatography. This requires careful experimental procedure and frequent consistency checks. Gas chromatography can be a very powerful tool when used by the cautious experimentor, but it is worse than useless when used carelessly.

The chromatograph column was prepared by packing PATS-coated substrate into a stainless steel tube. The PATS plasticizer was coated on Fluoropak-80 solid support spheres by slowly evaporating dichloromethane from a solution with the support beads and dissolved PATS. The weight ratio of support beads to polysulfone was approximately ten to one [10% loading factor]. The coated spheres were slowly placed in a 1/8 in OD stainless steel tube several feet long with some gentle vibration. The column was formed into a helical shape for placement in the column chamber. Prior to experimental use the column was seasoned using helium.

b. Samples

The PATS polysulfone was supplied by the Polymer Branch of the Materials Laboratory, AFWAL, Wright-Patterson Air Base, Ohio. The column support material for the PATS, Fluoropak-80, was manufactured by the Fluorocarbon Company of Anaheim, California. The injected organic

solvents can be classified as alkanes, cycloalkanes, aromatics, amines, nitriles, ketones, ethers or halogenated hydrocarbons. The solvents were purchased from Aldrich, Pfaultz & Bauer, or Fisher Chemical Company as laboratory or analytical grade. Standard welding grade helium was used as the carrier gas.

c. Procedure

The initially unknown reactive nature of the PATS plasticizer presented a dilemma for column operation. A low column temperature minimizes polymerization during an experimental trial, but column temperatures near the high boiling temperatures of the experimental solvents are required for quality chromatographic results. The experimental procedure used to reconcile these two mutually exclusive requirements was to operate the column at 40°C, 70°C, 100°C, 125°C and 150°C to utilize all the proposed solvents, and to repeat the 40°C trial after each higher temperature trial to determine the extent of polymerization.

At the midpoint of the experiment, PATS kinetic data were obtained from the USAF. These data indicated that no appreciable polymerization should occur at any of the designated operating temperatures within the needed experimental time. The remaining experimental trials were completed as initially designed to insure the accuracy of the kinetic data. In addition, the 150°C trial was partially repeated after curing the PATS column at 240°C for one day.

Prior to the experimental trials, a preliminary experiment was performed to check for solvent equilibrium in the column at 40°C and 70°C. This was done by varying the carrier gas flow rate, and measuring any change in solvent specific retention volumes. The flow

rate range where the retention volumes were constant ($\lesssim$6 cm^3/min) was used in the actual trials.

Secondary experiments were performed during the experimental trials. The first was a repeat of the 40°C and 70°C trials with a second PATS column. This was designed to check the effects of random column packing. The second was to determine the pressure drop characteristics of the various column bypass capillary tubes. These data were used to help calculate the carrier gas flow rate through the column.

The experimental trials used only those solvents whose normal boiling points were less than or equal to the column temperature. Exceptions were made if a higher boiling reference solvent was needed, or if the solvent had a boiling point greater than 150°C. The solvent was injected by using a syringe needle, which was dipped in the solvent and dried with a clean tissue. The syringe plunger was pulled back only for air injections where a measurable quantity [μL] was needed. The injection port temperature was slightly higher [10°-20°C] than the column temperature to insure rapid vaporization of the solvent from the needle, and to help prevent possible condensation. To prevent contamination of the syringe by the various solvents, the syringe was cleaned between solvents by rapidly moving the plunger in air, and, for higher boiling solvents, heating the needle tip. A separate syringe was used to provide only pure air injections.

The detection of the infinitely-diluted solvent injections required the optimization of the Gow-Mac detector sensitivity. Thermal conductivity detector sensitivities increase as the temperature difference between the detector wall and the elements increases. Usually the detector wall temperature is set 20°C higher than the column tempera-

ture to prevent solvent condensation on the walls. The element temperature, which is controlled by the bridge current, is limited by the column temperature and the type of carrier gas used. Generally, as the column temperature increases, the current must decrease to prevent element destruction. It can be concluded, therefore, that the detector sensitivity will decrease as the chromatograph column is operated at higher temperatures.

The detector responses were recorded on a strip chart recorder. Each trial or day began with two air injections followed by the organic solvent injections. Each solvent was injected three times to check for reproducible elution times. Two additional air injections were made at the end of the trial. At the beginning and end of each trial or day (whichever was the shortest) the dependent and independent variables also were recorded. The independent variables were the carrier gas flow rate, column temperature, thermal detector temperature, injector temperature, detector current and the chart recorder speed. The dependent variables were the column inlet pressure, room pressure and room temperature.

The polarizability reference solvents were the n-alkanes (pentane through n-decane) for all aliphatics, and benzene and cyclohexane for all aromatics and cyclic materials respectively. The slopes of the aromatic and cyclic reference lines were assumed equal to the slope of the n-alkane reference line.[10] The dipole reference solvents were chosen to be aliphatic and cyclic ethers [ethyl ether, furan, tetrahy-

---

[10] Eversdyk, D.A., "Solvent Interactions with a Triphenylated Benzoxazole Polymer," M. S. Thesis, Texas A&M University (1977), unpublished.

drofuran, 1,4-dioxane] due to their relatively large [less negative] energy of sorption values.

The analysis of the chart recorder data began by determining the distance between the capillary and column peaks for each injection. This was accomplished by drawing a line parallel to the inflection zone on each side of each peak. The chart distance between the points of the intersecting lines of the two peaks, when divided by the chart speed, gave the elution time of the injection.

The percentage of the total carrier gas flow rate which passed through the column was evaluated by the measurement of the areas under the air injection peaks. The solvent injection peaks were not used since the smaller samples would give less accurate results. The pressure drop characteristic of the column bypass capillary tubes was also used to calculate the column flow rate for comparison with the peak area method.

The retention volumes and thermodynamic values were calculated from the experimental data using a computer. The method of least squares was used to evaluate all of the thermodynamic reference lines.

3. RESULTS AND DISCUSSION

The chromatograph modifications saved experimental time by simplifying its operation. The only complication was caused by the column bypass capillary tube. The capillary tube had to be slowly and irreversibly crimped for each column to set the bypass flow rate between 5% and 45% of the total measured flow rate. The column flow rate was calculated using both the capillary and column peak areas, and the capillary tube pressure drop characteristic. The results from these two methods are shown in Table 4 for comparison purposes.

Three PATS columns were prepared. The first column (named A-PATS) contained 0.32 g PATS in its 1.22 meter (4 ft.) length. This column, however, was never used due to a blockage which created a large pressure drop. The second and third columns (B-PATS, C-PATS) were both 0.91 meters (3 ft.) long, and contained 0.158 g and 0.2079 g PATS respectively.

The molecular weight of the PATS was calculated to be 326.4 g/mole based on the plasticizer structure shown in Figure 2. The density of the plasticizer was observed to be approximately equal to the density of 2,2,2-trifluoroethanol [1.38 g/cm^3] at room temperature, since the undissolved PATS remained suspended in the liquid indefinitely.

The solvent physical properties required for the data analysis are listed in Table 3. The experimental data and results for the two columns at 70°C, 100°C, 116°C and 150°C are listed in Tables 5 through 11. The constants in Equation 4 then are determined as discussed above. The slope of the polarizability reference line (determined from the plot of ΔG_{ads} vs α_1) is a in Equation 4, while the intercept is G. The dipole reference line is established on a plot of ΔG_{add} vs μ_1, where the slope is b in Equation 4, and the intercept should be zero if the analysis is self-consistent. The results describing the reference lines for the various trials are listed in Table 12. In previous work, separate polarizability reference lines were established for aliphatic, aromatic, and cyclic compounds, where the slope was taken to be identical, but separate intercepts were determined. For the case of PATS, there is no statistically significant difference between the three types of solvents, therefore a single reference line would suffice within the accuracy of the data. Note that we also obtain a reasonable agreement for the results obtained from the two different chromatographic columns,

and that the results for the cured sample do not differ significantly from those of the uncured sample.

A chronology of results at 40°C is listed in Table 13, where we present the data that were obtained after successive cycles to the indicated higher temperatures. No significant effects on the reference line parameters are detectable at any time during the experiment.

The relative interaction parameters deduced from the experimental data are shown for 70, 100 and 117°C in Table 14 in order of decreasing specific interaction strength. As the temperature increases, additional solvents appear but the data show no significant temperature dependence of Λ or the relative strength of the specific interactions.

The 145°C measurements on the uncured sample included the greatest variety of solvents. The relative specific interaction parameters for these solvents at 145°C in the uncured PATS are shown in Table 15. In addition, results of beaker tests conducted for comparison to the solvent scan results also are shown in Table 15. For this system, unlike the polymers of large molecular weight previously investigated (e.g. Radel), there is little correlation between the specific interaction strength and the solubility. The solubility plot, where the specific interaction parameter Λ is plotted as a function of the permanent dipole contribution to the solubility parameter δ_p, is shown for this system in Figure 3. The crossed lines are drawn through the point for N,N-dimethylformamide, a solvent which dissolves the PATS instantly, and which also exhibited a very strong interaction with the Radel polysulfone.[2] In this case, the correlation between the permanent dipole energies and solubilities is more pronounced than that between the specific interaction parameter and solubilities. Most likely, the molecular weights of the

PATS molecules, even when cured, are sufficiently small that strong specific interactions are not required to overcome the unfavorable entropy effects.

The specific interaction parameters for a PATS sample cured for 24 hr at 240°C are shown in Table 16. There is essentially no difference between the results for the cured and the uncured samples. It is possible that the curing of this plasticizer in situ results in only a small increase in the molecular weight, and that the solvent molecules have little difficulty in diffusing between and interacting with the polymer molecules.

In summary, several observations concerning the interactions of solvents with PATS are in order. The numerical values of the specific interaction parameters for PATS-solvent interactions are much smaller than those of the Radel or P-1700 polysulfones measured in previous work.[1-4] There appears to be little correlation between the specific interaction parameter and dissolution of the PATS by a solvent, again in contrast to the cases of Radel and P1700. Furthermore, the in situ curing of the plasticizer had no effect on the measured interaction parameters, nor was any temperature dependence observed. In general, however, the solvents which exhibit the strongest interactions with Radel and P1700 tended to interact more strongly with PATS than the other solvents.

SECTION III

P-1700/ATS/DICHLOMETHANE RESULTS

The utility of a polymer in aerospace applications depends largely upon the polymer's mechanical and thermal stability at high temperatures. A polymer used in aircraft or missile systems should not undergo drastic changes in these important properties over the wide temperature ranges that may be encountered in operation.

The Air Force Materials Laboratory has been instrumental in developing a large number of new composite polymeric materials for aerospace applications. A novel polymer alloy which has been given consideration by the AFML and others is a mixture of a thermoplastic polymer with moderate thermal stability and a compatible, cross-linked polymer. The mixture can be made by blending an oligomeric, reactive plasticizer (RPS) with the thermoplastic polymer. The RPS reduces the glass transition temperature for the mixture so that the processing temperature for the mixture is reduced. A piece made from thermoplastic resin containing a reactive plasticizer could be stored almost indefinitely. When ready for use, the RPS is polymerized, thereby forming a thermosetting network in the main thermoplastic matrix. The cured mixture should have thermal stability as good as or better than the thermoplastic alone.

The thermoplastic chosen to demonstrate this approach is UDEL P-1700 polysulfone (PSF), produced by Union Carbide. In general, polysulfones have high glass transition temperatures[11] (185°C - 250°C)

---

[11] Johnson, R. N., Encyclopedia of Polymer Science and Technology, Vol. 11, Wiley-Interscience, N.Y. (1969), p. 447.

and can sustain temperatures up to 450°[12] before serious degradation occurs. They have good hydrolytic stability, good solvent resistance, and excellent thermo-oxidative stability and creep resistance.[11] The chemical structure of the PSF is shown in Figure 1.

The RPS chosen for our work is an acetylene-terminated, sulfonated aromatic oligomer. The RPS which we shall refer to as ATS, was synthesized at AFML. The chemical structure is shown in Figure 2.

Most of the data presented here were obtained using a piezoelectric sorption device, but for the case of the PSF-DCM mixtures some data were obtained using inverse gas chromatography. The agreement between the data obtained from the different experimental techniques is within the combined experimental error. Detailed descriptions of the experimental theory and practice were given in a previous report[1] and elsewhere,[13] and they will not be repeated here.

1. BINARY MIXTURES

In this part of our work we describe sorption studies of dichloromethane (DCM) by UDEL P-1700 polysulfone (PSF) and a reactive plasticizer (ATS) at 40°C and 60°C. DCM has been chosen as a solvent because it is a good solvent for PSF.[14] Qualitative dissolution studies show that DCM and ATS are completely miscible. The sorption data described

---

[12] Jones, E. G., Pedrick, D. L., and Benadum, P. A., Polymer Characterization Using TG-MS Techniques, Technical Report AFML-TR-77-91, U.S. Air Force Materials Laboratory (1977).

[13] Dangayach, K. C. B., "Vapor-Liquid Equilibrium in a Polysulfone-Reactive Plasticizer-Dichloromethane System," Ph.D. Dissertation, Texas A&M University (1979), unpublished.

[14] Dangayach, K. C. B., and Bonner, D. C., Polym. Eng. Sci., in Press.

here are used below, where we describe compatibility studies of the PSF and ATS mixture.

The temperature range of our study is well below the glass transition temperature[11] of PSF (= 190°C), so the polymer is in a glassy stage. However, solvent sorption can plasticize the PSF, thereby reducing the glass transition temperature of the mixture. The solvent concentration range in the PSF solution is kept quite low in our study so that PSF-DCM mixture is still in the glassy state over the temperature range of our experiments. As we show later, the glass transition temperature of ATS is about 20°C. Thus, ATS is in the rubbery state at our experimental temperatures.

Sorption in a glassy polymer is more complex than in rubbery polymers.[15-41] It has been generally agreed that sorption in glassy

---

[15]Berens, A. R., Angew Makromol. Chem., 47, 97 (1975).

[16]Barrer, R. M., Barrie, J. A., and Slater, J. A., J. Polym. Sci., 27, 177 (1958).

[17]Meares, P., J. Amer. Chem. Soc., 76, 3415 (1954).

[18]Meares, P., Trans. Faraday Soc., 53, 101 (1957); 54, 40 (1958).

[19]Michaels, A. S., Vieth, W. R., and Barrie, J. A., J. Appl. Phys., 34, 1 (1963).

[20]Vieth, W. R., Alcady, H. H., and Frabetti, A. J., J. Appl. Polym. Sci., 8, 2125 (1964).

[21]Vieth, W. R., and Sladek, K. J., J. Colloid Sci., 20, 1014 (1965).

[22]Vieth, W. R., Frangoulis, C. S., and Rionda, J. A., J. Colloid Interface Sci., 22, 454 (1966).

[23]Vieth, W. R., Tam, P. M., and Michaels, A. S., J. Colloid Interface Sci., 22, 360 (1966).

[24]Eilenberg, J. A., and Vieth, W. R., in Pae, K. D., Morrow, D. F., and Chen, Y. (Eds.), Advances in Polymer Science and Engineering, Plenum Press, N.Y., 1972, p. 145.

[25]Vieth, W. R., and Eilenberg, J. A., J. Appl. Polym. Sci., 16, 945 (1972).

[26]Vieth, W. R., and Amini, M. A., in Hopfenberg, H. B. (Ed.), Permeability of Plastic Films and Coatings to Gases, Vapors, and Liquids, Plenum Press, N.Y., 1974, p. 49.

[27]Koras, W. J., Paul, D. R., and Rocha, A. A., J. Polym. Sci. Polym. Phys. Ed., 14, 687 (1976).

[28]Paul, D. R., J. Polym. Sci., Pt. A-2, 7, 1811 (1969).

[29]Toi, K., J. Polym. Sci., Polym. Phys. Ed., 11, 1892 (1973).

[30]Fenelon, P. J., in Hopfenberg, H. B. (Ed.), Permeability of Plastic Films and Coatings to Gases, Vapors, and Liquids, Plenum Press, N.Y., 1974, p. 285.

[31]Tshudy, J. A., and von Frarkenberg, C., J. Polym. Sci., Polym. Phys. Ed., 11, 2027 (1973).

[32]Fenelon, P. J., Polym. Eng. Sci., 13, 440 (1973).

[33]Gordon, G. A., and Hsia, P. R., Permeability of Plastics Films and Coatings to Gases, Vapors, and Liquids, Plenum Press, N.Y., 1974, p. 261.

[34]Petropoulos, J. H., J. Polym. Sci., Pt A-2, 8, 1797 (1970).

[35]Koros, W. J., Paul, D. R., Fujii, M., Hopfenberg, H. B., and Stanett, V., J. Appl. Polym. Sci., 21, 2899 (1977).

[36]Berens, A. R., Amer. Chem. Soc. Polym. Preprints, 15, 197 (1974); 15, 203 (1974).

[37]Koros, W. J., and Paul, D. R., J. Polym. Sci., Polym. Phys. Ed., 14, 1903 (1976).

polymers can be described by a combination of Henry's law and a Langmuir "adsorption" term. Barrer et al.[16] were among the first to show this relationship, and it is commonly referred to as the "dual sorption" model. According to this model, holes exist as a stable phase in the polymer below its glass transition temperature. Thus sorption in glassy polymers occurs by two simultaneous mechanisms: ordinary dissolution and hole-filling. In the dual sorption model, the ordinary dissolution contribution is modelled by Henry's law, while the hole-filling contribution is modelled by a Langmuir term. An NMR study of ammonia in glassy polystyrene[41] has shown that there exist two distinct sorption modes in glassy polymers, thus further justifying the "dual sorption" model for the glassy polymers.

Figure 4 is a plot of the pressure dependence of vinyl chloride monomer (VCM) concentration for sorption in glassy PVC.[15] The sorption curve in Figure 4 is a general representation of solvent sorption in a glassy polymer where the solvent acts as a plasticizer for the polymer. Figure 4 shows three different regions: Region I, where the dual sorption model is valid; Region II, a transition region from the glassy to the rubbery state of the mixture; and Region III, where the mixture of the solvent and polymer is in the rubbery state. The dual sorption model is valid for a very small range of solvent concentration. This implies

---

[38]Koros, W. J., Chan, A. H., and Paul, D. R., J. Membrane Sci., 2, 165 (1977).

[39]Chan, A. H., Koros, W. J., and Paul, D. R., J. Membrane Sci., 3, 117 (1978).

[40]Koros, W. J., and Paul, D. R., J. Polym. Sci., Polym. Phys. Ed., 16, 1947 (1978).

[41]Assinik, R. A., J. Polym. Sci., Polym. Phys. Ed., 13, 1665 (1975).

that Henry's law can be used to model the dissolution contribution to glassy sorption only for small solvent concentrations. Region III has been modeled by polymer solution theories. Region II is least understood, and few attempts have been made to model this region. Thus there is no existing single model which can describe the entire glassy sorption curve. In our work we describe an approach by which sorption in glassy polymers for a wide range of solvent concentrations can be modeled. However, we have developed a quantitative model only for Region I.

The number of holes present in glassy polymers is thought to decrease as the glass transition temperature of the mixture is approached and to reach essentially zero at the glass transition temperature. Thus, a first step for a general model which can describe sorption in glassy polymers for a wide range of solvent concentrations is to estimate the sorption in the holes. The dissolution contribution to the glassy sorption can be obtained by subtracting the sorption due to holes from the total sorption. In Region I, where the dual sorption model is valid, the hole-filling contribution is normally represented by a Langmuir term. If we assume that by some procedure one can estimate the hole-filling contribution in Region II, then one can model the dissolution contribution in all three regions by a single polymer solution thermodynamic theory.

In our work, sorption of DCM in the PSF falls well within Region I. Thus we can estimate the dissolution contribution from the dual sorption model. Polymer solution theories are then applied to the dissolution contribution. Polymer solution theories are also used to model the sorption of DCM in ATS.

Our measurements of DCM sorption in PSF are obtained using a piezoelectric sorption apparatus and infinite dilution gas chromatography. The data obtained from these two techniques are compared. The sorption of DCM in ATS is performed on a piezoelectric sorption apparatus.

A. Theory

In this section we describe the dual sorption model, the Flory-Huggins theory and the Cheng and Bonner corresponding states theory.

1. Dual Sorption Model

According to the dual sorption model, the total amount of vapor or gas sorbed in a glassy polymer is represented by[16]

$$C = C_D + C_H \ , \tag{7}$$

and

$$C = k_D P + C_H' \, bP/(1 + bP), \tag{8}$$

where C_D and C_H are the contributions to sorption from ordinary dissolution and hole-filling, respectively. Henry's constant is k_D, P is the pressure in the system, C_H' is the hole saturation constant, and b is the hole affinity constant.

2. Flory-Huggins Theory

The well-known Flory-Huggins theory gives a representation of the solvent chemical potential in a polymer (2)-solvent (1) solution:[42-44]

---

[42]Flory, P. J., J. Chem. Phys., 9, 660 (1941); 10, 51 (1942).

[43]Huggins, M. L., J. Chem. Phys., 9, 440 (1941).

[44]Huggins, M. L., Ann. N.Y. Acad. Sci., 43, 1 (1942).

$$\frac{\mu_1 - \mu_1^\circ}{R\,T} = \ell n \Psi_1 + (1 - \frac{r_1}{r_2})\Psi_2 + \chi_{12}\Psi_2^2 \quad , \tag{9}$$

where

$$\Psi_i = \frac{r_i x_i}{r_1 x_1 + r_2 x_2} \quad . \tag{10-A}$$

Here μ_1 is the chemical potential of solvent at experimental conditions, μ_1° is the chemical potential of pure saturated solvent at absolute temperature T, Ψ_i is the segment fraction of component i, χ_{12} is the Flory-Huggins interaction parameter, r_i is the number of segments per molecule i, and x_i is the mole fraction of component i.

Following the suggestion of Flory,[45] we have computed segment fractions using the relationships:

$$\Psi_i = \frac{w_i \nu^*_{isp}}{w_1 \nu^*_{1sp} + w_2 \nu^*_{2sp}} \tag{10-B}$$

and

$$\frac{r_1}{r_2} = \frac{M_1 \nu^*_{1sp}}{M_2 \nu^*_{2sp}} \quad . \tag{11}$$

Here w_i is the weight fraction of component i, ν^*_{isp} is the specific hard core volume of component i, and M_i is the molecular weight of component i. The specific hard core volume is determined from the PVT properties of a component, as discussed later.

It is of practical interest to determine whether one or two phases exist in the polymer solution. This can be determined by applying

---

[45] Flory, P. J., J. Amer. Chem. Soc., 87, 1833 (1965).

critical conditions to Flory-Huggins theory. The critical conditions at which incipient phase separation occurs are[46]

$$\left(\frac{\partial \mu_1}{\partial \Psi_2}\right)_{T,P} = 0 = \left(\frac{\partial^2 \mu_1}{\partial \Psi_2^2}\right)_{T,P} . \qquad (12)$$

Applying Equation 12 to Equation 9, one obtains[46]

$$\chi_{12,c} = \frac{1}{2}\left[1 + \left(\frac{r_1}{r_2}\right)^{1/2}\right]^2 , \qquad (13)$$

where $\chi_{12,c}$ is the critical value of the Flory-Huggins interaction parameter.

Figure 5 shows χ_{12} as a function of temperature.[47] The dashed curves in Figure 5 give the interactional and free volume contributions as described by Patterson and Robard.[47] The horizontal line corresponds to the critical value of the Flory-Huggins interaction parameter, $\chi_{12,c}$, calculated from Equation 13. The intersection of the χ_{12} curve with the $\chi_{12,c}$ line gives two critical solution temperature, the upper critical solution temperature (UCST) and the lower critical solution temperature (LCST). The UCST is that temperature limit below which values of the χ_{12} parameter are larger than $\chi_{12,c}$. The LCST is that temperature limit above which the values of the χ_{12} parameter are greater than $\chi_{12,c}$. The region in Figure 5 between the UCST and LCST corresponds to a single phase for solvent-polymer mixture.

---

[46]Flory, P. J., Principles of Polymer Chemistry, Cornell University Press, Ithaca, N.Y., 1953.

[47]Patterson, D., and Robard, A., Macromolecules, 11, 690 (1978).

In the Flory-Huggins theory only the interactional contribution to χ_{12} is considered. Thus the Flory-Huggins theory only predicts UCST. In the next section, we discuss the free volume effect and an improved theory which takes into account the free volume effect on thermodynamic properties.

3. Corresponding States Theory

The Flory-Huggins theory is quite simple to use, because it has only one unknown parameter (χ). Although it has successfully modelled many polymer solution systems, it suffers from major shortcomings.[45,47-54] One of its most serious shortcomings is the neglect of the effect of volume changes on mixing. There is a contraction on mixing solvent and polymer molecules because of the differing chain lengths, and this contraction results in an important thermodynamic contribution termed the "free volume" effect. The corresponding states theories of Flory[45] and Patterson[55-56] have considered the free volume effect on thermodynamic properties. In principle, the theories of Flory and Patterson are

---

[48]Patterson, D., Delmas, G., and Somcynsky, T., Polymer, 8, 503 (1967).

[49]Siow, K. S., Delmas, G., and Patterson, D., Macromolecules, 5, 29 (1972).

[50]Zeman, L., Biros, J., Delmas, G., and Patterson, D., J. Phys. Chem., 76, 1206 (1972).

[51]Zeman, L., and Patterson, D., J. Phys. Chem., 76, 1214 (1972).

[52]Bonner, D. C., and Prausnitz, J. M., AIChE J., 19, 943 (1973).

[53]Casassa, E. F., J. Polym. Sci., Polym. Symp., 54, 53 (1976).

[54]Flory, P. J., Disc. Fard. Soc., 49, 7 (1970).

[55]Patterson, D., J. Polym. Sci., Pt. C, 16, 3379 (1968).

[56]Patterson, D., and Delmas, G., Trans. Farad. Soc., 65, 708 (1969).

equivalent. Flory's notation is simpler than Patterson's, and hence we have used Flory's theory in our work. The corresponding-states theories correctly predict the dependence of the χ parameter on composition, while χ is assumed to be composition independent in the Flory-Huggins theory. Also, the corresponding-states theories predict the UCST and LCST for solvent-polymer systems.

According to Prigogine[57-59] the total number of degrees of freedom for r segments can be divided into internal and external degrees of freedom. The internal degrees of freedom are associated with the strong intramolecular forces and thus they are essentially unaffected by the presence of neighbors. The external degrees of freedom are associated with the weak intermolecular van der Waals forces and thus they are significantly affected by the presence of neighbors. The number of external degrees of freedom is taken to be 3c.

The thermodynamic properties of pure fluids and mixtures as obtained from statistical thermodynamics can be divided into two categories:[45] combinatorial and noncombinatorial. The entropy of athermal mixing is taken to be a combinatorial property. The properties arising from the intermolecular forces, such as PVT properties, are taken to be noncombinatorial. In Flory's corresponding states theory, the combinatorial contribution remains the same as that in the Flory-Huggins

---

[57] Prigogine, I. (with the collaboration of A. Bellmans and V. Mathot), The Molecular Theory of Solution, North Holland, Amsterdam, and Interscience, N.Y., 1957.

[58] Prigogine, I., Trappeniers, N., and Mathot, V., Disc. Farad. Soc., 15, 93 (1953).

[59] Prigogine, I., Trappeniers, N., and Mathot, V., J. Chem. Phys., 21, 559 (1953).

theory. The noncombinatorial contribution is determined by a corresponding states theory for polymer solutions, which takes into account the dependence of polymer solution thermodynamics on liquid structure.

One of the limitations of the Flory corresponding states theory is that it is applicable to solutions at high liquid-like density only.[45,60] Cheng and Bonner,[61] using the idea of Beret and Prausnitz,[62] have modified Flory's partition function so that it is applicable to solutions at all densities. The temperatures in our sorption experiments are above the boiling point of dichloromethane, and hence it is appropriate to use the Cheng and Bonner[61] formulations. Their canonical partition function is

$$Z = Z_{comb} \left(\frac{\lambda v^*}{\Lambda^3}\right)^{Nrc} (\tilde{v}^{1/3} - 1)^{3Nrc} \left(\frac{1}{\tilde{v}}\right)^{N(rc-1)} \exp\left(-\frac{NE_o}{kT}\right), \quad (14)$$

where Z is a canonical partition function of a system with total volume V occupied by N molecules at absolute temperature T, Z_{comb} is the combinatorial partition function, $\Lambda = (h/2\pi mkT)^{1/2}$, h is Planck's constant, m is the molecular mass, and k is Boltzmann's constant. Here λ is a constant geometric factor, r is the number of segments per molecule, 3c is the number of external degrees of freedom per segment, and s is the number of intermolecular contact sites per segment. The symbol η/ν is the pair potential operating between two neighboring segments, v^* is the hard core volume per segment. v is the molecular

---

[60] Bonner, D. C., J. Macromol. Sci., Pt. C, 13(2), 263 (1975).

[61] Cheng, Y. L., and Bonner, D. C., J. Polym. Sci., 16, 319 (1978).

[62] Beret, S., and Prausnitz, J. M., AIChE J., 21, 1123 (1976).

volume per segment, $\tilde{v} = v/v^*$, $\tilde{T} = T/T^*$, T^* is the characteristic temperature which represents the kinetic energy per degree of freedom, and $E_o (= - rs\eta/2v)$ is the pair potential energy of the system at rest.

The pressure (P) is directly related to the partition function by[63]

$$P = kT\left(\frac{\partial \ell nZ}{\partial V}\right)_{T,N} \quad . \tag{15}$$

Substituting Equation 14 into Equation 15, we obtain

$$\frac{\tilde{P}\tilde{v}}{\tilde{T}} = \frac{1}{rc} + \frac{1}{\tilde{v}^{1/3} - 1} - \frac{1}{\tilde{v}\tilde{T}} \quad , \tag{16}$$

where

$$\tilde{P} = \frac{P}{P^*} \quad , \qquad \tilde{v} = \frac{v}{v^*} = \frac{v_{sp}}{v^*_{sp}} \quad .$$

Here P^* is the characteristic pressure and v_{sp} is the specific volume.

The characteristic parameters for a pure component are defined by

$$P^* = s\eta/2v^{*2} \quad , \tag{17-A}$$

$$T^* = s\eta/2kv^*c \quad , \tag{17-B}$$

and

$$v^*_{sp} = N_A r v^*/M \quad , \tag{17-C}$$

where N_A is Avogadro's number.

The pure component characteristic parameters are determined using the method of Flory[45,54,64] as applied by Bonner and Prausnitz.[52] We

---

[63] Hill, T. L., An Introduction to Statistical Thermodynamics, Addison-Wesley Publishing Company, Inc., Reading, Massachusetts, 1962, p. 19.

[64] Abe, A., and Flory, P. J., J. Amer. Chem. Soc., 87, 1838 (1965).

have assumed that these parameters are independent of temperature and density over our experimental range.

The thermal pressure coefficient, $\gamma = (\partial P/\partial T)_V$, in the limit as pressure goes to zero, is obtained from Equation 16 as

$$\gamma = \frac{P^*}{\vartheta^2 T} \quad . \tag{18}$$

The thermal expansion coefficient, $\alpha = \frac{1}{v}(\partial v/\partial T)_p$, in the limit as pressure goes to zero is obtained from Equation 16

$$\alpha = \left(\frac{1}{T}\right)\left(\frac{3}{-3 + [(\gamma M v_{sp} - R)/\gamma M v_{sp}][\vartheta^{1/3}/(\vartheta^{1/3} - 1)]}\right) \tag{19}$$

Taking the zero pressure limit of Equation 16 and rearranging, we get

$$T = \frac{T^*}{RT^*\vartheta/P^*Mv_{sp}^* + \vartheta/(\vartheta^{1/3} - 1)} \tag{20}$$

where we have substituted $rc = P^*Mv_{sp}^*/RT^*$.

The parameter v_{sp}^* is obtained from Equation 19 by minimizing the sum of the squares of the percent deviations between the calculated and experimental values of α, over the temperature range. Using the previously determined value of v_{sp}^*, the characteristic pressure P^* is obtained from Equation 18 by minimizing the sum of the squares of the percent deviations between the calculated and experimental values of γ. Note that α and γ used in Equations 19 and 18, respectively are the zero pressure limits of these parameters, which is essentially equivalent to using atmospheric pressure values.

Once v^*_{sp} and P^* are determined, the parameter T^* is obtained from Equation 20 by minimizing the sum of the squares of the percent deviations between the calculated and experimental temperatures.

Following Flory's[45,54] one-fluid model for binary mixtures, Cheng and Bonner[61] have formulated a corresponding states theory for binary mixtures of gases and liquid polymers. The partition function for the mixture of solvent (1) and polymers (2) is given by

$$Z = g(N_1,N_2) \left(\frac{\lambda v^*}{\Lambda^3}\right)^{Nrc} (\tilde{v}^{1/3} - 1)^{3Nrc} \left(\frac{1}{\tilde{v}}\right)^{N(rc-1)} \exp\left(-\frac{NE_o}{kT}\right), \quad (21)$$

where $g(N_1,N_2)$ is the combinatorial factor for the mixture and $\tilde{v}$ is the reduced volume for the mixture. Unsubscripted N, r and c refer to mixture properties. These terms are defined by

$$N = N_1 + N_2 \quad , \quad (22\text{-A})$$

$$r = (r_1N_1 + r_2N_2)/N \quad , \quad (22\text{-B})$$

and

$$c = \Psi_1 c_1 + \Psi_2 c_2 \quad . \quad (22\text{-C})$$

The potential energy term E_o is determined by taking all binary interactions into account and assuming random mixing of segments:[47]

$$-\frac{E_o}{rN} = \frac{P^* v^*}{\tilde{v}} \quad , \quad (23)$$

where

$$P^* = \Psi_1\theta_1 P^*_1 + \Psi_2\theta_2 P^*_2 + 2(\Psi_1\Psi_2\theta_1\theta_2)^{1/2} P^*_{12} \quad . \quad (24)$$

The site fraction θ_i is defined by

$$\theta_i = \frac{s_i r_i N_i}{s_1 r_1 N_1 + s_2 r_2 N_2} = \frac{s_i r_i N_i}{srN} \quad . \tag{25}$$

The binary parameter $P_{12}^* = s\eta_{12}/2\nu^{*2}$ represents the binary intermolecular potential interaction. Cheng and Bonner[61] further have assumed that each segment has the same number of contact sites ($s_1 = s_2 = s$). This leads to

$$\Psi_i = \theta_i \quad , \tag{26}$$

$$P^* = \Psi_1^2 P_1^* + \Psi_2^2 P_2^* + 2\Psi_1\Psi_2 P_{12}^* \quad , \tag{27}$$

and

$$T^* = \frac{P^*}{\frac{\Psi_1 P_1^*}{T_1^*} + \frac{\Psi_2 P_2^*}{T_2^*}} \quad . \tag{28}$$

At low or moderate pressures we can use Flory's approximation[45]

$$\mu_1 \cong -kT \left(\frac{\partial \ell n Z}{\partial N_1}\right)_{T,\tilde{v},N_2} \quad . \tag{29}$$

Substituting Equation 21 into Equation 29 we obtain

$$\frac{\mu_1 - \mu_1^\circ}{RT} = \Psi_2(1 - r_1/r_2) + \ell n \Psi_1 + \frac{3M_1\nu_{1sp}^* P_1^*}{RT_1^*} \ell n\, x \left[\frac{\tilde{v}_1^{1/3} - 1}{\tilde{v}^{1/3} - 1}\right] + \left(\frac{P_1^* M_1 \nu_{1sp}^*}{RT_1^*} - 1\right) \ell n(\tilde{v}/\tilde{v}_1) + \frac{\nu_{1sp}^* M_1 P_1^*}{RT}\left(\frac{1}{\tilde{v}_1} - \frac{1}{\tilde{v}}\right) + \frac{M_1 \nu_{1sp}^* \Psi_2^2}{\tilde{v}\, RT}(X_{12}), \tag{30}$$

where $X_{12} = P_1^* + P_2^* - 2P_{12}^*$.

Note that the polymer solution theories developed in this section are valid for DCM-PSF as well as DCM-ATS systems. In the case of the DCM-ATS system subscript 2 is replaced by 3.

b. Results and Discussion

The solubility data for dichloromethane in polysulfone at 40°C and 60°C as determined by the piezoelectric sorption apparatus are listed in Table 17. Figure 6 shows the solubility as a function of partial pressure of dichloromethane in polysulfone at 40°C and 60°C. At both the temperatures the isotherms are nonlinear, as would be expected for glassy polymers.

Following the suggestion of Paul et al.[27] we have used a non-linear regression analysis to fit Equation 8 to the experimental isotherms of Figure 6. Table 18 lists various dual sorption parameters for dichloromethane in polysulfone with their estimated standard errors at 40°C and 60°C.

The adequacy of the Langmuir term (C_H) for describing the sorption in excess of Henry's law can be demonstrated by plotting $1/C_H$ versus $1/P$.[40] Rearranging the Langmuir term produces

$$\frac{1}{C_H} = \frac{1}{C_H'} + \frac{1}{C_H' bP} \quad , \tag{31}$$

and C_H can be determined from

$$C_H = C_{expt} - k_D P \quad . \tag{32}$$

Here C_{expt} is the experimentally determined total sorption of solvent at each pressure P. The lines in Figure 7 are calculated from Equation

31 using the appropriate parameters from Table 18. It is quite clear in Figure 7 that the calculated line fits the data reasonably well, justifying the use of the Langmuir form. At 40°C the low pressure data deviate more from the straight line than other data points. The deviation is probably within experimental error.

Assuming equilibrium sorption, we can use the van't Hoff equation to calculate enthalpies relative to the free gas state of dichloromethane held in the two sorption modes. The van't Hoff equation is:

$$k_e = k_o \exp(-\Delta H_S/RT) \ , \qquad (33)$$

where k_e is the equilibrium constant at temperature T (e.g., k_D or b), k_o is the equilibrium constant at some reference temperature, and ΔH_S is the enthalpy of sorption. Using the data of Table 18 and Equation 33, the enthalpy of sorption for different modes can be determined. The enthalpy of sorption for the dissolved species is ΔH_D = -29410 Joules/g-mole, while the enthalpy of sorption of the Langmuir species is ΔH_b = -61000 Joules/g-mole. The enthalpy for the Langmuir sorption species is more than double that for the enthalpy of the dissolved species. This indicates that sorption of DCM in PSF may occur by two distinct mechanisms.

The large difference in enthalpies between Langmuir sorption and ordinary dissolution has been explained by Barrer et al.[16] and Michaels et al.[19] by considering the morphology of glassy polymers. According to them, sorption in the Langmuir mode occurs in preexisting holes. There are no such holes available for ordinary dissolution. Hence considerable energy is utilized in creating space for the solvent molecules in the ordinary dissolution. Thus, it is expected that the energy

of sorption in the ordinary dissolution mode would be less exothermic than in the Langmuir mode. Our data agree with this concept.

Application of Polymer Solution Thermodynamic Theories

Figure 8 shows the specific volume (ν) as a function of temperature (T) for a typical amorphous polymer.[65,40] When an amorphous polymer is cooled from the rubbery state, the slope of the line on ν versus T changes at the glass transition temperature (T_g). The slope of the line below T_g depends on the rate of cooling. A polymer cooled at an infinitely slow rate will have a value of ν obtained by extrapolating the specific volume line in the rubbery region to temperatures below T_g. In Figure 8 this corresponds to the dotted line. The deviation from the extrapolated value is directly proportional to the rate of cooling.[40] Hence, in the glassy region, amorphous polymers are nonequilibrium solids. The relaxation of a nonequilibrium solid polymer to a more uniform liquid-like state is a very slow process, and the change may be imperceptible on the usual experimental time scale.

At any particular temperature T below T_g the real specific volume of the polymer is denoted by ν_g, and the extrapolated value corresponding to the liquid-like state is denoted by ν_ℓ, as shown in Figure 8. The difference ($\nu_g - \nu_\ell$) corresponds to the unrelaxed volume for an amorphous polymer. Koros and Paul[40] have shown that there is a fundamental quantitative relationship between ($\nu_g - \nu_\ell$) and the Langmuir capacity (C_H'). This implies that the nonequilibrium contribution to the sorption in glassy polymers is due to the Langmuir sorption only.

---

[65] Hutchinson, J. M., and Kovacs, A. J., J. Polym. Sci., Polym. Phys. Ed., 14, 1575 (1976).

Thus if we can subtract the Langmuir sorption from total sorption, the remaining sorption contribution must correspond to equilibrium sorption to which all equilibrium polymer solution thermodynamic theories would be applicable. A similar idea has been used in the past by several authors[19,20,23,66] to correlate the solubility constants (k_D) for dissolution of gases in polymers with the Lennard-Jones energy constant parameters (ε/k). We discuss below the application of polymer solution thermodynamic theories to amorphous polymers in the glassy state.

In the dual sorption approach which we have used to describe the sorption of dichloromethane in polysulfone, the hole-filling contribution is modelled by the Langmuir term. In the Langmuir model the basic assumption is that a uniform, unimolecular layer of solvent is formed on the adsorbing surface (polymer in our case). Thus the hole-filling capacity also represents the fraction of total polymer contributed by the holes. We can convert C_H' from cm^3 (STP) of solvent per cm^3 of polymer to cm^3 of solvent per cm^3 of polymer at the experimental conditions by following equation[38]

$$f = C_H' \left(\frac{M_1}{22400\ \rho_1} \right) , \qquad (34)$$

where f is the fraction of total polymer volume due to holes, and ρ_1 is the solvent density as it exists in the holes. The experimental temperatures in our study are much below the critical temperature of DCM. Hence it is justified to use the saturated density of DCM at the experimental temperature to compute ρ_1 in eq. (34). The saturated

---

[66] Michaels, A. S., and Bixler, H. J., J. Polym. Sci., 50, 413 (1961).

density of DCM is determined by Bondi's[67] group contribution method to be given by

$$\rho_1 = 2.449[0.727 - 5.993\text{x}10^{-4}T - 1.110\text{x}10^{-7}T^2]. \qquad (35)$$

In the application of polymer solution thermodynamics theories, weight fractions of the solvent in the polymer solution are required. In our analysis we plan to apply polymer solution theories to the liquid-like sorption in the glassy polymer. Hence the weight fraction of the solvent in the liquid-like phase of the glassy polymer must be separated from the total sorption. From the dual sorption model we can determine the ordinary dissolution contribution (C_D) to the total sorption of a solvent in the glassy polymer. The value of C_D is normally expressed in terms of cm^3 (STP) of solvent per cm^3 of polymer. We calculate the weight fraction of the solvent in the liquid-like phase of the glassy polymer from C_D in two steps. First we calculate the grams of solvent in the liquid-like phase per gram of the liquid-like polymer by

$$\frac{w_1}{w_2} = C_D\left(\frac{M_1 P^\circ}{RT^\circ}\right)\left(\frac{1}{1 - f}\right)\left(\frac{1}{\rho_{2ext}}\right) . \qquad (36)$$

Here we assume that the solvent vapor obeys the ideal gas law. P° is standard pressure, 1 atm.

From Equation 36 the weight fraction of solvent (w_1) in the liquid-like phase can be determined by

---

[67] Bondi, A., Physical Properties of Molecular Crystals, Liquids, and Gases, Wiley, N.Y., 1968.

$$w_1 = \frac{(w_1/w_2)}{1 + (w_1/w_2)} \quad . \tag{37}$$

Tables 19 and 20 give the weight fraction of DCM in the liquid-like phase of PSF at 40°C and 60°C, respectively.

Flory-Huggins interaction parameters for DCM-PSF (χ_{12}) and for DCM-ATS (χ_{13}) calculated from Equations 4 and 9 are plotted in Figures 9 and 10, respectively. In Tables 19 and 20 we list the values of the χ_{12} parameter at 40°C and 60°C, respectively. In Table 21 we list the values of the χ_{13} parameter.

The specific hard core volumes for DCM, PSF and RPS are determined from the corresponding states theory of Cheng and Bonner[61] and PVT properties, and they are listed in Table 22. The mathematical details involved in determining hard core volumes are discussed later.

From Figure 9 we can see that χ_{12} is a function of composition at both 40°C and 60°C. The curves which best describe the χ_{12} data are

$$\chi_{12} = -0.185 + 1.200\ w_1 + 3.890\ w_1^2 \qquad (40°C) \tag{38}$$

$$\chi_{12} = -0.167 + 1.227\ w_1 + 3.660\ w_1^2 \qquad (60°C) \tag{39}$$

The critical value of χ_{12} for the DCM-PSF system calculated from eq. (13) is 0.640. At both 40°C and 60°C χ_{12} is less than 0.10 for the concentration range of our experiments. At low concentrations χ_{12} becomes negative at both temperatures. This means that a single phase exists at both temperatures for the concentration range of our experiment. The increase in χ_{12} with solvent concentration can be explained as follows. DCM is a proton donor while PSF is the proton acceptor due to presence of the $-SO_2$ and -O- groups. Hence, initially sorbed molecules of DCM are very tightly bound, resulting in a

negative value of χ_{12}. The available sites on the PSF molecules deplete rapidly with increasing DCM concentration. This means that with an increase of solvent concentration, the sorption of solvent molecules occurs due to a nonspecific interaction with the polymer molecules.[68] This process results in an increasing value of χ_{12}.

There is a slight increase in χ_{12} at a particular weight fraction of DCM as the temperature is increased. The difference is quite small, and it is probably within experimental error. It is not possible at present to draw any conclusions about the temperature dependence of the χ_{12} parameter.

Figure 10 shows that χ_{13} is a function of DCM weight fraction at both temperatures. The curves which best describe the χ_{13} data are

$$\chi_{13} = 0.323 - 0.355\ w_1 \qquad (40°C) \qquad (40)$$

$$\chi_{13} = 0.235 - 0.899\ w_1 \qquad (60°C) \qquad (41)$$

The error involved in determining χ_{13} is about 15% due to uncertainties in the weight fraction and the activity of the solvent. The critical value of χ_{13} is 0.955. At both temperatures χ_{13} is less than 0.350 for the concentration range of our experiments. This implies that one phase exists at the conditions of our experiments. The decrease in χ_{13} with increasing DCM concentration at both temperatures indicates that the solubility of RPS is enhanced as more solvent is introduced into the RPS solution.

Pure component characteristic parameters for DCM, PSF and ATS are determined from Equations 18 through 20, and they are listed in Table

---

[68] Zimm, B. H., and Lundberg, J. L., J. Phys. Chem., 21, 934 (1953).

22. PVT properties for PSF are obtained from Zoller.[69] PVT properties for DCM are calculated from Bondi's[67] correlation by fitting the density equation to one experimental density at 20°C. In our work the temperature range of validity of characteristic parameters of DCM is 0°C to 40°C, because Bondi's correlation is limited to the boiling point of a solvent. However, we have assumed that the same characteristic parameters apply up to 60°C, which is a safe extrapolation. PVT properties for ATS are calculated from Bondi's[67] correlation.

Vapor sorption data for DCM-PSF and DCM-ATS systems are modelled by Equation 30 at 40°C and 60°C. The optimum values of P_{12}^* and P_{13}^* are determined by a least squares fit of Equation 30 to the experimental activities. P_{12}^* and P_{13}^* are assumed independent of pressure and composition at a particular temperature. Figures 11 and 12 for DCM-PSF and Figure 13 for DCM-ATS show that the experimental data are correlated well by Equation 30 for these systems. If we define P_{ij}^* as

$$P_{ij}^* = (P_i^* P_j^*)^{1/2} (1 - \Delta), \qquad (42)$$

then Δ represents the deviation of P_{12}^* from the geometric mean $(P_i^* P_j^*)^{1/2}$. Table 23 lists P_{ij}^*, Δ and Flory's interaction parameter X_{ij} for the DCM-PSF and DCM-RPS systems. The values of Δ and X_{ij} give essentially the same information about the molecular interactions. In both systems, the values of Δ and X_{ij} are negative. Hence the interaction between segments of type i-j is much more favorable than i-i or j-j types interactions in the solution of i and j components.

---

[69]Zoller, P., J. Polym. Sci., Polym. Phys. Ed., 16, 1261 (1978).

Flory and collaborators[70-71] have suggested that a negative value of X_{ij} determined from heat of mixing data, does not necessarily mean favorable interactions between the components from the standpoint of the free energy. The reason for this is that in the case of specifically interacting components, the entropy of mixing is also negative due to molecular ordering. Flory and collaborators[70-71] have introduced an empirical parameter, Q_{12}, which has entropic significance.

Patterson and Robard[47] have suggested that the X_{12} parameter must be replaced by an "effective" value, $X_{12} - TQ_{12}\tilde{v}_1$, which has Gibbs energy of mixing significance. In our calculation of X_{12} from Equation 30, we actually calculate an "effective" X_{12} which characterizes free energy of interactions. Thus all the conclusions regarding compatibility of components are valid. To determine the Q_{12} parameter, we would need heat of mixing data. Then, the Q_{12} parameter could be estimated from an "effective" X_{12} and the X_{12} value determined from heat of mixing.

In the next section we describe the comparison of GC data with the piezoelectric sorption data for DCM-PSF system.

C. Comparison of GC Data with Piezoelectric Sorption Data

There have been few studies reported in which GC data are compared with other methods.[72-76] Most of these studies have not made a compar-

---

[70] Orwoll, R. A., and Flory, P. J., J. Amer. Chem. Soc., 89, 6822 (1967).

[71] Eichinger, B. E., and Flory, P. J., Trans. Fard. Soc., 64, 2035 (1968).

[72] Patterson, D., Tewari, Y. B., Schreiber, H. P., and Guillet, J. E., Macromolecules, 4, 356 (1971).

[73] Schreiber, H. P., Tewari, Y. B., and Patterson, D., J. Polym. Sci., Pt. A-2, 11, 15 (1973).

ison of data using GC and other methods in the glassy state. The reason for this is that slow diffusion of solvent vapor or gas in glassy polymers inhibits the attainment of equilibrium in GC experiments. However, according to Courval and Gray,[77] reaching equilibrium in inverse GC depends upon a kinetic parameter involving the thickness of the polymer layer, the carrier gas flow rate, and the diffusivity of the solvent molecules in the polymer.

Berens[78] has compared GC data on glassy PVC powder with other methods. Berens[78] has considered three types of solvents: solvents which have high, medium, and low diffusivity in PVC powder. His study shows that for solvents with high diffusivity sorption, GC experiments correspond to equilibrium sorption, as the data obtained from GC experiments and those obtained from gravimetric or volumetric methods are comparable. For solvents with medium diffusivity, equilibrium conditions are obtained only if the GC sorption experiments are performed at a relatively high temperature or by using small PVC particles. In the case of low diffusivity solvents, equilibrium conditions are unattainable below the glass transition temperature of PVC powder, irrespective of the particle size of PVC powder. Thus the Berens[78] study agrees with the Courval and Gray[77] notion.

---

[74]Summers, W. R., Tewari, Y. B., and Schreiber, H. P., Macromolecules, 5, 12 (1972).

[75]Tewari, Y. B., and Schreiber, H. P., Macromolecules, 5, 329 (1972).

[76]Newman, R. D., and Prausnitz, J. M., J. Phys. Chem., 76, 1492 (1972).

[77]Courval, G. J., and Gray, D. G., Macromolecules, 8, 916 (1975).

[78]Berens, A. R., Organic Coating and Plastic Chemistry Preprints, 39, 236 (1978).

Recently Tait and Abushihada[79] have compared GC data with vapor pressure data for poly (vinyl chloride), polystyrene and poly (methyl methacrylate) in different solvents. Their study shows that Flory-Huggins interaction parameters calculated from GC experiments and vapor pressure measurements (values obtained by extrapolating to zero solvent concentration) are comparable. In the Tait and Abushihada[79] study, the experimental temperature for all three polymers was below the glass transition temperature of the polymer, and all three polymers were glassy. In their vapor pressure measurements, the solvent concentrations are quite large (Region III in Figure 4), thus plasticizing the polymer and reducing the glass transition temperature of the mixture below that of the experiment. Therefore in the vapor pressure measurements, the solvent concentrations are quite large (Region III in Figure 4), thus plasticizing the polymer and reducing the glass transition temperature of the mixture below that of the experiment. Therefore in the vapor pressure measurements, the polymer-solvent mixtures are in true solution. The Flory-Huggins interaction parameters determined by extrapolating to zero solvent concentration correspond to values for which the polymer-solvent mixture is in a hypothetical liquid state. It is rather remarkable that the Flory-Huggins interaction parameter from the GC measurements (polymer in glassy state) and from vapor pressure measurements (polymer in liquid state) are comparable. Tait and Abushihada[79] have not offered any explanation for this behavior. Here we offer a tentative explanation for this comparison and support our explanation with our sorption results for DCM in PSF.

---

[79] Tait, P. J. T., and Abushihada, A. M., Polymer, 18, 610 (1977).

Berens[78] has suggested a simple method to compare GC data with data from other methods. From specific retention volume V_g°, we can calculate a "solubility coefficient," K, using the relation

$$K = \frac{V_g^\circ M_1}{RT^\circ} \quad . \tag{43}$$

If equilibrium conditions are attained in the GC experiments, K represents the reciprocal of the slope of the sorption isotherm plotted as weight of vapor sorbed per gm. of polymer versus gas pressure.

In our work V_g° data for DCM-PSF at 100.5°C, 105.5°C and 110.3°C are determined as listed in Table 24. We obtain a straight line equation for $\ell n V_g^\circ$ versus 1/T:

$$\ell n V_g^\circ = 4.424 \times 10^3 (1/T) - 9.007. \tag{44}$$

The values of V_g° at 40°C and 60°C are determined from Equation 44 on the assumption that this equation is valid to 40°C.

Table 25 shows a comparison of GC data with piezoelectric sorption data. The "solubility coefficient" K is determined from Equation 43 for GC experiments. Henry's law constant k_d is determined from piezoelectric sorption measurements by assuming that sorption data in the glassy PSF can be modelled by the dual sorption model.[16] As we have already discussed, sorption in a glassy polymer occurs due to two concurrent mechanisms: hole-filling and ordinary dissolution. In the dual sorption model at the low solvent concentrations, the ordinary dissolution contribution can be modelled by Henry's law. Thus Henry's law constant k_d is the "solubility coefficient" for DCM in PSF for the liquid-like phase of the glassy PSF.

Table 25 shows that the difference between K and k_d is less than 10 percent at 40°C and 60°C. The sum of errors involved in determining k_d, are more than 10 percent. Thus K and k_d are comparable.

The similarity of K and k_d implies that in our GC experiments, DCM is sorbed only in the liquid-like phase of the glassy PSF. That is the holes present in the glassy polysulfone do not contribute to the sorption mechanism in our GC experiments. This is reasonable since at the low diffusion rates encountered in DCM sorption in PSF, only surface sorption can occur, precluding hole-filling. We can explain the Tait and Abushihada[79] results by applying the same reasoning. In the Tait and Abushihada[79] GC experiments, the sorption of solvents probably takes place only in the liquid-like phase of the glassy polymers. In vapor pressure measurements, polymers are plasticized by the presence of solvents so that the polymers are in the liquid state. Thus the Flory-Huggins interaction parameters calculated from GC experiments and from vapor pressure measurements both apply to the same physical state (liquid) of polymers, therefore they are comparable.

2. TERNARY MIXTURE

In this part of our work we describe the sorption of dichloromethane (DCM) in a mixture of P-1700 and a reactive plasticizer (ATS). Polysulfones are thermoplastics with high glass transition temperatures (185°C - 250°C) and with moderate thermal stability. One of the ways to reduce the glass transition temperature (T_g) and therefore the processing temperature of the PSF is to plasticize the PSF with a reactive plasticizer.

The choice of a plasticizer depends upon its compatibility with the PSF before and after curing. A mixture of PSF and RPS can be

stored nearly indefinitely. When ready for use, a piece made from PSF-RPS mixture can be cured by heating. Curing of this mixture results in the formation of a thermoset network in the thermoplastic matrix. For an appropriate choice of plasticizer the cured mixture will have as good or better thermal stability than the thermoplastic polymer (PSF).

Figure 14[80] shows T_g for PSF-ATS mixtures as a function of composition. The ATS is temperature sensitive and temperatures in excess of 80°C[81] are not recommended, because the ATS polymerization reaction is quite rapid above 80°C. Hence, the composition of PSF-ATS mixture should be selected so that the mixture T_g is substantially less than 80°C. A mixture of PSF-ATS containing 30 percent by weight of ATS has a T_g of about 65°C. Hence in this work we investigate the compatibility of a mixture containing 70 wt % PSF and 30 wt % ATS.

It has long been known that many mixtures of two polymers form two-phase or "incompatible" systems at least at some temperatures.[82] From a thermodynamic standpoint, two polymers are mutually compatible with one another only if the Gibbs free energy of mixing (ΔG^M) satisfies the following criterion:

$$\left(\frac{\partial^2 \Delta G^M}{\partial \phi^2}\right)_{T,P} > 0 \quad . \tag{45}$$

Here ϕ is the volume fraction.

---

[80] Goldfarb, I. J., (Air Force Materials Laboratory, Ohio), Unpublished.

[81] Goldfarb, I. J., (Air Force Materials Laboratory, Ohio), Personal communication.

[82] Krause, S., J. Macromol. Sci., Rev. Macromol. Chem., C7, 251 (1972).

Koningsveld et al.[83] have given an excellent account of why, in general, mixtures of two polymers are incompatible. They have considered a lattice representation of three cases: a binary small-molecule mixture, a polymer solution and a polymer mixture. Entropy of mixing can be calculated by considering the number of possible arrangements of molecules in a lattice. In equal volumes, the number of possible arrangements in binary small-molecule mixtures is much larger than the polymer solution. There is a further drastic decrease in the number of possible arrangements in the case of a polymer mixture. The enthalpy of mixing can be calculated approximately by considering the number of nearest neighbor contacts. In equal volumes, the number of nearest neighbor contacts is nearly the same in all three cases, and hence the enthalpy of mixing in all the three cases is nearly the same. The entropy of mixing in a polymer mixture therefore is very small and it does not contribute significantly to the Gibbs free energy of mixing. Additionally, the necessary condition of a zero or negative Gibbs free energy of mixing requires the enthalpy of mixing to be either very small or negative in mixtures of compatible polymers. This is possible only if there is a specific interaction such as hydrogen bonding or charge transfer between the two different polymer molecules. The validity of this concept has been shown by many researchers.[84-98].

---

[83]Koningsveld, R., Kleintjens, L. A., and Schoffelers, H. M., Pure Appl. Chem., 39, 1 (1974).

[84]Wahrmund, D. C., Paul, D. R., and Barlow, J. W., J. Appl. Polym. Sci., 22, 2125 (1978).

Slonimskii et al.[99-102] have measured the heat of mixing of many polymer pairs. They have found that most pairs mix endothermically and

---

[85]Wahrmund, D. C., Bernstein, R. E., Barlow, J. W., and Paul, D. R., Polym. Eng. Sci., 18, 677 (1978).

[86]Bernstein, R. E., Paul, D. R., and Barlow, J. W., Polym. Eng. Sci., 18, 683 (1978).

[87]Robeson, L. M., and Furtek, A. B., J. Appl. Polym. Sci., 23, 645 (1979).

[88]Hoffman, A. S., Lewis, R. W., and Michaels, A. S., Organic Coating and Plastic Chemistry Preprints, 29, 236 (1969).

[89]Michaels, A. S., Ind. Eng. Chem., 57, 32 (1965).

[90]Michaels, A. S., and Miekka, R. G., J. Phys. Chem., 65, 1765 (1961).

[91]Smith, K. L., Winslow, A. E., and Petersen, D. E., Ind. Eng. Chem., 51, 1361 (1959).

[92]Osada, Y., and Sato, M., J. Polym. Sci., Polym. Lett. Ed., 14, 129 (1976).

[93]Bimendina, L. A., Roganov, V. V., and Bekturov, Y. A., Vysokomal. Soedin., A16, 2810 (1974).

[94]Sulzberg, T., and Cotter, R. L., J. Polym. Sci., Pt. A-1, 8, 2747 (1970).

[95]Matzner, M., Schober, D. L., Johnson, R. N., Robeson, L. M., and McGrath, J. E., Permeability of Plastic Films and Coatings to Gases, Vapors and Liquids, Plenum Press, N.Y., 1975.

[96]Robeson, L. M., and McGrath, J. E., Paper Presented at the 82nd National Meetinp of AIChE, Atlantic City, New Jersey, August 31, 1976.

[97]Olabisi, O., Macromolecules, 8, 316 (1975).

[98]Hickman, J. J., and Ikeda, R. M., J. Polym. Sci., Polym. Phys. Ed., 311, 1713 (1973).

[99]Komskaya, N. F., and Slonimskii, G. L., J. Phys. Chem. SSSR, 30, 1529 (1956).

[100]Slonimskii, G. L., and Komskaya, N. F., J. Phys. Chem., SSR, 30, 1746 (1956).

[101]Struminskii, G. V., and Slonimskii, G. L., J. Phys. Chem. SSR, 30, 1941 (1956).

hence form an incompatible polymer mixture. An exception is the polystyrene-polybutadiene system. For polystyrene-polybutadiene, mixing is endothermic - yet this system shows partial miscibility. This observation has been explained by considering the non-combinatorial contribution to the entropy of mixing. This contribution can be calculated from any liquid mixture theory which takes into account the volume change upon mixing. McMaster[103] and Patterson and Robard[47] have applied Flory's[45] corresponding states theory to polymer mixtures to explain the compatibility of polymer mixtures. Recently Sanchez and Lacombe[104-107] have developed a new theory of liquid mixtures which accounts for free volume effects, and they have applied it to polymer mixtures.

Mixing of polymers is usually performed in a melt phase or sometimes from solution. However, a mixture of two polymers in an amorphous state is highly viscous, thereby impeding the attainment of equilibrium. This means that macroscopic phase separation may not occur in a polymer mixture even if the equilibrium state consists of two phases. Thus kinetic effects play an important part in polymer compatibility behavior.

---

[102] Slonimskii, G. L., and Struminskii, G. V., J. Phys. Chem. SSR, 30, 2144 (1956).

[103] McMaster, L. P., Macromolecules, 6, 760 (1973).

[104] Sanchez, I. C., and Lacombe, R. H., J. Phys. Chem., 80, 2352 (1976).

[105] Lacombe, R. H., and Sanchez, I. C., J. Phys. Chem., 80, 26568 (1976).

[106] Sanchez, I. C., and Lacombe, R. H., J. Polym. Sci., Polym. Lett. Ed., 15, 71 (1977).

[107] Sanchez, I. C., and Lacombe, R. H., Macromolecules, 11, 1145 (1978).

The kinetic effects on the polymer compatibility can be minimized by studying the polymer properties in solution. The presence of a solvent enhances the establishment of equilibrium between different phases. Thus the structure of each phase separately and of the mixture as a whole can be studied.

The solvent effect on polymer compatibility has been recognized by many investigators.[108-114] It generally has been agreed that a small difference in polymer-solvent interactions may have a marked effect on polymer compatibility. Thus the results obtained from a solvent-polymer-polymer system must be used very cautiously to understand the polymer-polymer compatibility.

Mixing ATS and PSF in the melt phase is ruled out as a processing operation because of the thermal sensitivty of ATS. A simple alternative is to mix ATS and PSF in a solvent, but here sorption data on ATS and PSF will be required for proper engineering design of devolatilization units.

---

[108] Hugelin, C., and Dondos, A., Makromol. Chem., 126, 206 (1969).

[109] Banks, M., Leffingwell, J., and Thies, C., Macromolecules, 4, 43 (1971).

[110] Kern, R. J., J. Polym. Sci., 21, 19 (1956).

[111] Zeman, L., and Patterson, D., Macromolecules, 5, 513 (1972).

[112] Hsu, C. C., and Prausnitz, J. M., Macromolecules, 7, 320 (1974).

[113] Sheehan, C. J., and Bisio, A. L., Rubber Chem. Technol., 39, 149 (1966).

[114] Paxton, T. R., J. Appl. Polym. Sci., 7, 1499 (1963).

In our work the sorption of DCM in a mixture of PSF-ATS has been measured using a piezoelectric sorption apparatus. The sorption of DCM in PSF and ATS is described above. The sorption data for the ternary mixture are analyzed using two polymer solution theories. One is Scott's[115] extension of Flory-Huggins theory to three components. Scott's[115] theory is approximate but quite simple to use and it yields some useful information about PSF-RPS compatibility. The other theory is the extension of the Cheng and Bonner[33] corresponding states theory to three components. This theory is more accurate than Scott's theory in modeling data.

A. Theory

1. Flory-Huggins Theory

Scott[115] has extended Flory-Huggins theory to three components. In Scott's three-component extension of Flory-Huggins theory, the binary interaction parameters are related to the difference in chemical potential of solvent by the following equation

$$\frac{\mu_1 - \mu_1^{\circ}}{RT} = \ell n\Psi_1 + \ell n(1 - \Psi_1) - \Psi_2\left(\frac{r_1}{r_2}\right) - \Psi_3\left(\frac{r_1}{r_3}\right)$$

$$+ [(\chi_{12}\Psi_2 + \chi_{13}\Psi_3)(\Psi_2 + \Psi_3)] - \chi_{23}\frac{r_1}{r_3}\Psi_2\Psi_3 \quad , \qquad (46)$$

where

$$\Psi_i = \frac{r_i x_i}{r_1 x_1 + r_2 x_2 + r_3 x_3} \quad . \qquad (47\text{-A})$$

Here subscripts 1, 2, and 3 denote DCM, PSF and ATS, respectively. The chemical potential of solvent at experimental conditions is μ_1, μ_1°

---

[115] Scott, R. L., J. Chem. Phys., 17, 279 (1949).

is the chemical potential of pure saturated solvent at absolute temperature T, Ψ_i is the segment fraction of component i, χ_{ij} is the Flory-Huggins interaction parameter between components i and j, r_i is the number of segments per molecule i, and x_i is the mole fraction of component i.

Following the suggestion of Flory,[45] we have computed segment fractions using the relationships:

$$\Psi_i = \frac{w_i \nu^*_{isp}}{w_1 \nu^*_{1sp} + w_2 \nu^*_{2sp} + w_3 \nu^*_{3sp}} , \qquad (47\text{-B})$$

and

$$\frac{r_i}{r_j} = \frac{M_i \nu^*_{isp}}{M_j \nu^*_{jsp}} . \qquad (48)$$

Here w_i is the weight fraction of component i, ν^*_{isp} is the hard core volume of component i, and M_i is the molecular weight of component i.

To evaluate the compatibility between polymer and plasticizer it is of interest to determine the Flory-Huggins interactions parameter χ_{23}, between polymer and plasticizer. From Equation 9 we can determine χ_{12} and χ_{13} as a function of solvent concentration. Thus χ_{23} can be determined from Equation 46.

Deshpande *et al.*[116] and Su *et al.*[117] have pointed out that χ_{23} is not a convenient parameter for understanding the compatibility of a polymer-polymer system. According to these references the most con-

---

[116] Deshpande, D., Patterson, D., Schreiber, H. P., and Su, C. S., Macromolecules, 7, 530 (1974).

[117] Su, C. S., Patterson, D., and Schreiber, H. P., J. Appl. Polym. Sci., 20, 1025 (1974).

venient parameter is $r_1\chi_{23}/r_2 (= \chi_{23}^+)$. The χ_{23}^+ parameter is normalized to correspond to the number of polymer-polymer contacts equal to that in a mole of the solvent. The same normalization is used for the χ_{12} and χ_{13} parameters.

The critical value of the χ_{23}^+ parameter (above which phase separation occurs) can be found from Equation 12. The result is

$$\chi_{23,c}^+ = \frac{1}{2}\left[\left(\frac{M_1 \nu^*_{1sp}}{M_2 \nu^*_{2sp}}\right)^{1/2} + \left(\frac{M_1 \nu^*_{1sp}}{M_3 \nu^*_{3sp}}\right)^{1/2}\right] . \qquad (49)$$

Equation 49 is symmetric with respect to components 2 and 3, thus it does not matter which polymer is chosen to be 2 or 3.

2. Corresponding States Theory

The estimation of pure component characteristic parameters for DCM, PSF and RPS, and the corresponding states theory of Cheng and Bonner[61] for binary mixtures are discussed in Section II. Here we describe the extension of the Cheng and Bonner corresponding states theory to ternary mixtures.

Bonner and Brockmeier[118] have extended Flory's[45] corresponding states theory to three components. We have followed the same procedure to extend the Cheng and Bonner corresponding states theory to three components. For the sake of continuity we repeat some of the derivation of Bonner and Brockmeier.

The canonical partition function for three components becomes:

$$Z = g(N_1, N_2, N_3) \left(\frac{\lambda \nu^*}{3}\right)^{Nrc} (\tilde{v}^{1/3} - 1)^{3Nrc} \left(\frac{1}{\tilde{v}}\right)^{N(rc-1)} \exp\left(-\frac{NE_o}{kT}\right) , \qquad (50)$$

[118] Bonner, D. C., and Brockmeier, N. F., Ind. Eng. Chem., Process Des. Dev., 16, 428 (1977).

where $g(N_1,N_2,N_3)$ is the combinatorial partition function for three components and $\tilde{v}$ is the reduced volume for the mixture. We use the Flory-Huggins[46] expression for combinatorial factor.

The potential energy E_o is determined by considering all the binary interactions among three components

$$-E_o = \frac{1}{v}[A_{11}\eta_{11} + A_{22}\eta_{22} + A_{33}\eta_{33} + A_{12}\eta_{12} + A_{13}\eta_{13} + A_{23}\eta_{23}] \quad , \tag{51}$$

where A_{ij} represents the number of contact pairs between components i and j, and η_{ij}/v is the energy associated with contact pair i and j.

Defininig s_i as the molecular surface of contact per segment for component i, we get

$$\begin{aligned} 2A_{11} + A_{12} + A_{13} &= s_1 r_1 N_1 \quad , \\ 2A_{22} + A_{12} + A_{23} &= s_2 r_2 N_2 \quad , \\ 2A_{33} + A_{13} + A_{23} &= s_3 r_3 N_3 \quad . \end{aligned} \tag{52}$$

Substituting for A_{11}, A_{22} and A_{33} from Equation 52 in Equation 5 we get

$$\begin{aligned} -E_o = \frac{1}{v}[&s_1 r_1 \eta_{11} N_1 + s_2 r_2 \eta_{22} N_2 + s_3 r_3 \eta_{33} N_3 \\ &- A_{12}(\eta_{11} + \eta_{22} - 2\eta_{12}) - A_{13}(\eta_{11} + \eta_{33} - 2\eta_{13}) \\ &- A_{23}(\eta_{22} + \eta_{33} - 2\eta_{23})] \quad . \end{aligned} \tag{53}$$

The site fraction θ_i is defined by

$$\theta_i = \frac{s_i r_i N_i}{s_1 r_1 N_1 + s_2 r_2 N_2 + s_3 r_3 N_3} \quad . \tag{54}$$

From eq. 51 we define

$$A_{ij} = s_i r_i N_i \theta_j \quad . \tag{55}$$

We assume that all the molecules have equal molecular surface of contact per segment ($s_1 = s_2 = s_3$), and define segment fraction Ψ_i in this manner

$$\Psi_i = \frac{r_i N_i}{r_1 N_1 + r_2 N_2 + r_3 N_3} \quad . \tag{56}$$

A more useful definition of segment fraction Ψ_i is

$$\Psi_i = \frac{w_i \nu^*_{isp}}{w_1 \nu^*_{1sp} + w_2 \nu^*_{2sp} + w_3 \nu^*_{3sp}} \quad . \tag{57}$$

The expression for E_o then becomes

$$-\frac{E_o}{rN} = \frac{s}{2}[\Psi_1 \eta_{11} + \Psi_2 \eta_{22} + \Psi_3 \eta_{33} - \Psi_1 \eta_2 \Delta\eta_{12} - \Psi_1 \Psi_3 \Delta\eta_{13} - \Psi_2 \Psi_3 \Delta\eta_{23}] \quad , \tag{58}$$

where

$$\Delta\eta_{ij} = \eta_{ii} + \eta_{jj} - 2\eta_{ij} \tag{59}$$

$$rN = r_1 N_1 + r_2 N_2 + r_3 N_3 \quad . \tag{60}$$

As shown by Flory[45]

$$-\frac{E_o}{rN} = \frac{P^* \nu^*}{\tilde{v}} = \frac{ckT^*}{\tilde{v}} \quad , \tag{61}$$

where

$$c = \Psi_1 c_1 + \Psi_2 c_2 + \Psi_3 c_3 \quad . \tag{62}$$

Defining

$$P_i^* = \frac{s_i \eta_{ii}}{2\nu^{*2}} \quad , \tag{63}$$

we get

$$-\frac{E_o}{rN} = \frac{\nu^*}{\tilde{\nu}}[\Psi_1^2 P_1^* + \Psi_2^2 P_2^* + \Psi_3^2 P_3^* + 2\Psi_1\Psi_2 P_{12}^* + 2\Psi_1\Psi_3 P_{13}^* + 2\Psi_2\Psi_3 P_{23}^*] \quad , \tag{64}$$

where

$$P_{ij}^* = \frac{s_i \Delta\eta_{ij}}{2\nu^{*2}} \quad . \tag{65}$$

Combining Equations 61 and 64, we obtain

$$P^* = \Psi_1^2 P_1^* + \Psi_2^2 P_2^* + \Psi_3^2 P_3^* + 2\Psi_1\Psi_2 P_{12}^* + 2\Psi_1\Psi_3 P_{13}^* \tag{66}$$

and

$$T^* = P^*/(\Psi_1 P_1^*/T_1^* + \Psi_2 P_2^*/T_2^* + \Psi_3 P_3^*/T_3^*) \quad . \tag{67}$$

At low or moderate pressures we can use Flory's approximation[45]

$$\mu_1 = -kT \left(\frac{\partial \ell n Z}{\partial N_1}\right)_{T,\tilde{v},N_2,N_3} \quad . \tag{68}$$

Substitution into eq. (50) produces:

$$\frac{\mu_1 - \mu_1^\circ}{RT} = \Psi_2 \left(1 - \frac{r_1}{r_2}\right) + \Psi_3 \left(1 - \frac{r_1}{r_3}\right) + \ell n \Psi_1 + \frac{3P_1^* M_1 \nu_{1sp}^*}{R\, T_1^*} \ell n \left(\frac{(\nu_1^{1/3} - 1)}{(\nu^{1/3} - 1)}\right)$$

$$- \left[\frac{M_1 \nu_{1sp}^* P_1^*}{R T_1^*} - 1\right] \ln \frac{\tilde{v}_1}{\tilde{v}} + \frac{M_1 \nu_{1sp}^* P_1^*}{} \left(\frac{1}{\tilde{v}_1} - \frac{1}{}\right) \qquad (69)$$

$$+ \frac{M_1 \nu_{1sp}^* P_1}{\tilde{v} RT} \Big[(\Psi_2 + \Psi_3)^2 P_1^* + \Psi_2^2 P_2^* + \Psi_3^2 P_3^*$$

$$- 2(\Psi_2^2 + \Psi_2\Psi_3) P_{12}^* - 2(\Psi_3^2 + \Psi_2\Psi_3) P_{13}^*$$

$$+ 2\Psi_2\Psi_3 P_{23}^* \Big] .$$

B. Results and Discussion

The experimental results for the ternary mixture are listed in Table 26, where we give the solvent activities as a function of the weight fraction of solvent in the liquid phase. In addition, χ_{23}^+ values calculated from Equations 4 and 46 are listed in Table 26. Figure 15 shows χ_{23}^+ as a function of DCM weight fraction at 40°C and 60°C. In our calculation of χ_{23}^+, we have assumed that DCM plasticizes the PSF-RPS mixture so that the T_g of the DCM-PSF-RPS mixture is below the experimental temperature. The values of χ_{12} used in Equation 45 are from Equations 38 and 39 at 40°C and 60°C, respectively. The values of χ_{13} used are from Equations 40 and 41 at 40°C and 60°C, respectively.

At both temperatures the values of χ_{23}^+ are large negative numbers. The critical value of χ_{23}^+ is 0.132 as calculated from Equation 48. This implies that ATS and PSF form a single phase in the presence of DCM. The compatibility of ATS and PSF is probably due to van der Waal's forces. The chains of ATS and PSF are flat and thus they can be parallel to each other. Hence the van der Waals forces may result in strong interaction between ATS and PSF.

The difference between χ_{23}^{+} at two temperatures at a particular weight fraction is small and is probably within the experimental error. Hence it is not feasible at present to draw any conclusion on the temperature dependence of the χ_{23}^{+} parameter.

The vapor sorption data for the DCM-PSF-RPS systems also can be modelled using the corresponding states theory using Equation 69. The pure component parameters for DCM, and ATS are from Table 22. The optimum values of binary interaction parameters are given above. The optimum value of P_{23}^{*} is determined by a least squares fit of Equation 69 to the experimental activities. P_{23}^{*} is assumed independent of pressure and composition at a particular temperature.

Figure 16 compares the experimental activities with those predicted using Equation 69. The maximum differences between the experimental and calculated activities at 40°C are 22 percent at lower concentration and 15 percent at higher concentration, while at 60°C they are 10 percent at both the lower and the higher concentrations. The detailed numerical comparison is presented in Table 26.

The difference between the experimental and calculated activities can be explained by considering the errors involved in our measurements and analysis. The errors involved are due to fluctuations in resonant frequency in the determination of weight fraction of DCM in the mixture, temperature uncertainties in the measurement of activities, and the use of binary sorption data of P_{12}^{*} and P_{13}^{*}. Considering these errors, the corresponding states theory in the simplified form models the data reasonably well.

From Equation 42 we can calculate the deviation of P_{23}^{*} from the geometric mean $(P_2^{*} P_3^{*})^{1/2}$. The values of P_{23}^{*} are 1.694 G Pa

and 1.711 G Pa at 40°C and 60°C, respectively. The values of Δ which represent the deviation of P_{23}^* from $(P_2^* P_3^*)^{1/2}$ are -0.9823 and -1.0000 at 40°C and 60°C, respectively. The values of Δ are exceptionally large negative numbers. This indicates that the interaction of type ATS-PSF is strong and much more favorable than ATS-ATS or PSF-PSF types.

3. SUMMARY

A general model of vapor or gas sorption in glassy polymers has been proposed. According to this model, sorption of a gas or vapor is first analyzed using the "dual sorption" model. In the dual sorption model it is envisioned that sorption in glassy polymers occurs due to two distinct mechanisms: hole-filling and ordinary dissolution. The nonequilibrium behavior of sorption in a glassy polymer is due to the hole-filling mechanisms. Thus if the hole-filling contribution is subtracted from the total sorption, the remaining sorption contribution (ordinary dissolution) is due to the equilibrium liquid-like sorption. In the proposed model, it has been suggested that the equilibrium polymer solution should be applicable to the ordinary dissolution contribution obtained from the "dual sorption" model.

The proposed model of glassy sorption has been applied to the sorption of dichloromethane in the glassy PSF at 40°C and 60°C. Use of the dual sorption concept allows us to estimate hole-filling and ordinary dissolution contributions. The Flory-Huggins theory and the corresponding states theory of Cheng and Bonner have been applied to the dissolution contribution. These theories have also been applied to the sorption of DCM in the ATS.

The values of the Flory-Huggins interaction parameters for DCM-PSF and DCM-RPS systems are quite small at both temperatures. Small values of Flory-Huggins interaction parameters indicate that in these systems a single phase is formed and that there are very strong interactions between the participating components.

The corresponding states theory of Cheng and Bonner models the dissolution contribution of sorption of DCM in PSF quite well. In case of DCM sorption in the RPS, the difference between the experimental activities and those calculated from the Cheng and Bonner theory are within the experimental errors. The values of Δ which represent the deviation of binary interaction parameter (P_{ij}^{*}) from the geometric mean are negative for both the systems at both temperatures. The negative value of Δ indicates that the interactions between the participating components are more favorable than the interactions between the pure components.

It has been found that the "solubility coefficients" determined by gas chromatography and those by dissolution contribution of sorption of DCM in PSF are comparable. This implies that the sorption of DCM in PSF in gas chromatography technique occurs only in the liquid-like phase of glassy PSF.

The values of the Flory-Huggins interaction parameter χ_{23}^{+} determined from Scott's theory are large negative numbers at both temperatures. This indicates that PSF and RPS are compatible in the presence of DCM at the experimental temperatures.

Our extension of the Cheng and Bonner theory to three components models the sorption of DCM in the mixture of PSF and RPS within the experimental errors. The exceptionally large negative values of Δ for

this system imply PSF-ATS interactions are much more favorable than are PSF-PSF or ATS-ATS interactions.

SECTION IV

RADEL POLYSULFONE

Radel is a commercially available (Union Carbide) polysulfone polymer which has attractive mechanical and thermal properties in addition to a high glass transition temperature and excellent resistance to water degradation. The structure of this polymer is shown in Figure 2. We previously have reported[1,2] both a complete solvent scan which identified several potential solvents, and the results of saturation concentration measurements for Radel in the most promising solvents. We report here the results of further analysis on our gas chromatography data, which indicate the presence of at least one transition of unknown character in addition to the glass transition temperature for this polymer.

Several comments concerning the saturation concentration measurements are in order. These measurements were made by placing the dry polymer into a vial containing a known amount of the solvent of interest, and dissolution was determined by visual observation. A recent series of papers by Blackadder and Ghavamikia[119-121] describing experiments on a polyethersulfone polymer quite similar in structure to both the Radel and the P1700 indicates that a large degree of aggregation exists among the polymer molecules even in solutions which appear to the naked eye to be completely dissolved. They further report some rather unusual

---

[119] Blackadder, D. A., and Ghavamikia, H., "Dissolution of Polyether sulfone in Chloroform," Polymer, 20, 523 (1979).

[120] Blackadder, D. A., and Ghavamikia, H., "Evidence for Crystallinity in Poly(ether sulphone)," Polymer, 20, 781 (1979).

[121] Blackadder, D. A., and Ghavamikia, H., "Crystallinity in Polyethersulphone: A Problem of Definition," Polymer, 1432 (1979).

results indicating possible crystallinity in polymer samples obtained by slowly evaporating methylene chloride and chloroform from the polymer at room temperature. It is not clear that complete dissolution in the molecular sense actually is required in the processing of polysulfone into desired structural shapes, and further investigations in this area are warranted.

We have discussed the use of inverse gas chromatography as a method of identifying various types of transitions in polymeric materials in a previous report,[2] where the more important of a wide body of sources in the literature are identified. Here we summarize the results of a series of experiments on the Radel polysulfone which indicate the presence of a transition of unknown character some 20 to 40 K below the accepted glass transition temperature for this material. These data were obtained using three separate gas chromatograph columns and Radel polysulfone from two separate batches, thereby minimizing effects that might be ascribed to sample preparation techniques.

The chromatography results are summarized in Figures 17 through 20, where the natural logarithm of the retention volume is plotted as a function of inverse temperature. In the absence of phase transitions or other peculiar solution behavior, a linear relation should exist between these variables. Figure 17 shows results for Radel/chloroform in Column 1, Figures 18 and 19 show Radel/dichloromethane and Radel/N,N-dimethylformamide results, respectively, for Column 2, and Figure 20 shows the Radel/DMF behavior observed in Column 3. The chloroform results (Figure 17) exhibit significantly more scatter than the others, but a change in slope clearly exists near 200°C. The glass transition temperature, determined from torsion pendulum measurements to be

220°C,[122] cannot be resolved in this case. In all other cases, a distinct break in the curve occurs between 220 and 230°C, in excellent agreement with the accepted T_g. In all cases, we observe distinctly anamolous behavior between 185 and 200°C, which strongly suggests the presence of an additional phase transition of undetermined character in this temperature range. Further research in this area appears to be of interest, particularly in light of unusual behavior in polysulfone solutions observed by Blackadder and Ghavamikia.[119-121]

---

[122]Dominie, J., Union Carbide Corporation, Bound Brook, NJ, private communication.

REFERENCES

1. Holste, J.C., Glover, C.J., Magnuson, D.T., Dangayach, K.C.B., Powell, T.A., Ching, D.W., and Person, D.R., "Polymer-Solvent Polymer/Polymer Interaction Studies," AFML-TR-79-4107, U.S. Air Force Materials Laboratory (1979).

2. Bonner, D.C., Holste, J.C., Glover, C.J., Magnuson, D.T., Eversdyk, D.A., and Dangayach, K., "Polymer-Polymer Interactions," AFML-TR-78-163, U.S. Air Force Materials Laboratory (1978).

3. Bonner, D.C., "Determination of Solvents for Thermally Stable Polymers," AFML-TR-77-73, U.S. Air Force Materials Laboratory (1977).

4. Bonner, D.C., "Determinations of Solvents for Thermally Stable Aromatic Heterocyclic Polymers," AFML-TR-76-51, U.S. Air Force Materials Laboratory (1976).

5. Hildebrand, J.H., and Scott, R.L., The Solubility of Non-Electrolytes, p. 136, Reinhold (1950).

6. Hanson, C.N., and Beerbower, A., Encyclopedia of Chemical Technology, Supplement Volume 1971, p. 889, Wiley (1971).

7. Fedors, R.F., Polym. Eng. Sci., 14, 147 (1974).

8. Fedors, R.F., Polym. Eng. Sci., 14, 472 (1974).

9. Powell, T.A., "Solvent Interactions with a Cured and Uncured Reactive Sulfone Plasticizer - PATS," M. S. Thesis, Texas A&M University (1979), unpublished.

10. Eversdyk, D.A., "Solvent Interactions with a Triphenylated Benzoxazole Polymer," M. S. Thesis, Texas A&M University (1977), unpublished.

11. Johnson, R.N., Encyclopedia of Polymer Science and Technology, Vol. 11, Wiley-Interscience, N.Y. (1969), p. 447.

12. Jones, E.G., Pedrick, D.L., and Benadum, P.A., Polymer Characterization Using TG-MS Techniques, Technical Report AFML-TR-77-91, U.S. Air Force Materials Laboratory (1977).

13. Dangayach, K.C.B., "Vapor-Liquid Equilibrium in a Polysulfone-Reactive Plasticizer-Dichloromethane System," Ph.D. Dissertation, Texas A&M University (1979), unpublished.

14. Dangayach, K.C.B., and Bonner, D.C., Polym. Eng. Sci., in Press.

15. Berens, A.R., Angew Makromol. Chem., 47, 97 (1975).

16. Barrer, R.M., Barrie, J.A., and Slater, J.A., J. Polym. Sci., 27, 177 (1958).

17. Meares, P., J. Amer. Chem. Soc., 76, 3415 (1954).

18. Meares, P., Trans. Faraday Soc., 53, 101 (1957); 54, 40 (1958).

19. Michaels, A.S., Vieth, W.R., and Barrie, J.A., J. Appl. Phys., 34, 1 (1963).

20. Vieth, W.R., Alcady, H.H., and Frabetti, A.J., J. Appl. Polym. Sci., 8, 2125 (1964).

21. Vieth, W.R., and Sladek, K.J., J. Colloid Sci., 20, 1014 (1965).

22. Vieth, W.R., Frangoulis, C.S., and Rionda, J.A., J. Colloid Interface Sci., 22, 454 (1966).

23. Vieth, W.R., Tam, P.M., and Michaels, A.S., J. Colloid Interface Sci., 22, 360 (1966).

24. Eilenberg, J.A., and Vieth, W.R., in Pae, K.D., Morrow, D.F., and Chen, Y. (Eds.), Advances in Polymer Science and Engineering, Plenum Press, N.Y., 1972, p. 145.

25. Vieth, W.R., and Eilenberg, J.A., J. Appl. Polym. Sci., 16, 945 (1972).

26. Vieth, W.R., and Amini, M.A., in Hopfenberg, H.B. (Ed.), Permeability of Plastic Films and Coatings to Gases, Vapors, and Liquids, Plenum Press, N.Y., 1974, p. 49.

27. Koras, W.J., Paul, D.R., and Rocha, A.A., J. Polym. Sci. Polym. Phys. Ed., 14, 687 (1976).

28. Paul, D.R., J. Polym. Sci., Pt. A-2, 7, 1811 (1969).

29. Toi, K., J. Polym. Sci., Polym. Phys. Ed., 11, 1892 (1973).

30. Fenelon, P.J., in Hopfenberg, H.B. (Ed.), Permeability of Plastic Films and Coatings to Gases, Vapors, and Liquids, Plenum Press, N.Y., 1974, p. 285.

31. Tshudy, J.A., and von Frarkenberg, C., J. Polym. Sci., Polym. Phys. Ed., 11, 2027 (1973).

32. Fenelon, P.J., Polym. Eng. Sci., 13, 440 (1973).

33. Gordon, G.A., and Hsia, P.R., Permeability of Plastics Films and Coatings to Gases, Vapors, and Liquids, Plenum Press, N.Y., 1974, p. 261.

34. Petropoulos, J.H., J. Polym. Sci., Pt A-2, 8, 1797 (1970).

35. Koros, W.J., Paul, D.R., Fujii, M., Hopfenberg, H.B., and Stanett, V., J. Appl. Polym. Sci., 21, 2899 (1977).

36. Berens, A.R., Amer. Chem. Soc. Polym. Preprints, 15, 197 (1974); 15, 203 (1974).

37. Koros, W.J., and Paul, D.R., J. Polym. Sci., Polym. Phys. Ed., 14, 1903 (1976).

38. Koros, W.J., Chan, A.H., and Paul, D.R., J. Membrane Sci., 2, 165 (1977).

39. Chan, A.H., Koros, W.J., and Paul, D.R., J. Membrane Sci., 3, 117 (1978).

40. Koros, W.J., and Paul, D.R., J. Polym. Sci., Polym. Phys. Ed., 16, 1947 (1978).

41. Assinik, R.A., J. Polym. Sci., Polym. Phys. Ed., 13, 1665 (1975).

42. Flory, P.J., J. Chem. Phys., 9, 660 (1941); 10, 51 (1942).

43. Huggins, M.L., J. Chem. Phys., 9, 440 (1941).

44. Huggins, M.L., Ann. N.Y. Acad. Sci., 43, 1 (1942).

45. Flory, P.J., J. Amer. Chem. Soc., 87, 1833 (1965).

46. Flory, P.J., Principles of Polymer Chemistry, Cornell University Press, Ithaca, N.Y., 1953.

47. Patterson, D., and Robard, A., Macromolecules, 11, 690 (1978).

48. Patterson, D., Delmas, G., and Somcynsky, T., Polymer, 8, 503 (1967).

49. Siow, K.S., Delmas, G., and Patterson, D., Macromolecules, 5, 29 (1972).

50. Zeman, L., Biros, J., Delmas, G., and Patterson, D., J. Phys. Chem., 76, 1206 (1972).

51. Zeman, L., and Patterson, D., J. Phys. Chem., 76, 1214 (1972).

52. Bonner, D.C., and Prausnitz, J.M., AIChE J., 19, 943 (1973).

53. Casassa, E.F., J. Polym. Sci., Polym. Symp., 54, 53 (1976).

54. Flory, P.J., Disc. Fard. Soc., 49, 7 (1970).

55. Patterson, D., J. Polym. Sci., Pt. C, 16, 3379 (1968).

56. Patterson, D., and Delmas, G., Trans. Farad. Soc., 65, 708 (1969).

57. Prigogine, I. (with the collaboration of A. Bellmans and V. Mathot), The Molecular Theory of Solution, North Holland, Amsterdam, and Interscience, N.Y., 1957.

58. Prigogine, I., Trappeniers, N., and Mathot, V., Disc. Fard. Soc., 15, 93 (1953).

59. Prigogine, I., Trappeniers, N., and Mathot, V., J. Chem. Phys., 21, 559 (1953).

60. Bonner, D.C., J. Macromol. Sci., Pt. C, 13(2), 263 (1975).

61. Cheng, Y.L., and Bonner, D.C., J. Polym. Sci., 16, 319 (1978).

62. Beret, S., and Prausnitz, J.M., AIChE J., 21, 1123 (1976).

63. Hill, T.L., An Introduction to Statistical Thermodynamics, Addison-Wesley Publishing Company, Inc. Reading, Massachusetts, 1962, p. 19.

64. Abe, A., and Flory, P.J., J. Amer. Chem. Soc., 87, 1838 (1965).

65. Hutchnison, J.M., and Kovacs, A.J., J. Polym. Sci., Polym. Phys. Ed., 14, 1575 (1976).

66. Michaels, A.S., and Bixler, H.J., J. Polym. Sci., 50, 413 (1961).

67. Bondi, A., Physical Properties of Molecular Crystals, Liquids, and Gases, Wiley, N.Y., 1968.

68. Zimm, B.H., and Lundberg, J.L., J. Phys. Chem., 21, 934 (1953).

69. Zoller, P., J. Polym. Sci., Polym. Phys. Ed., 16, 1261 (1978).

70. Orwoll, R.A., and Flory, P.J., J. Amer. Chem. Soc., 89, 6822 (1967).

71. Eichinger, B.E., and Flory, P.J., Trans. Fard. Soc., 64, 2035 (1968).

72. Patterson, D., Tewari, Y.B., Schreiber, H.P., and Guillet, J.E., Macromolecules, 4, 356 (1971).

73. Schreiber, H.P., Tewari, Y.B., and Patterson, D., J. Polym. Sci., Pt. A-2, 11, 15 (1973).

74. Summers, W.R., Tewari, Y.B., and Schreiber, H.P., Macromolecules, 5, 12 (1972).

75. Tewari, Y.B., and Schreiber, H.P., Macromolecules, 5, 329 (1972).

76. Newman, R.D., and Prausnitz, J.M., J. Phys. Chem., 76, 1492 (1972).

77. Courval, G.J., and Gray, D.G., Macromolecules, 8, 916 (1975).

78. Berens, A.R., Organic Coating and Plastic Chemistry Preprints, 39, 236 (1978).

79. Tait, P.J.T., and Abushihada, A.M., Polymer, 18, 610 (1977).

80. Goldfarb, I.J., (Air Force Materials Laboratory, Ohio), Unpublished.

81. Goldfarb, I.J., (Air Force Materials Laboratory, Ohio), Personal Communication.

82. Krause, S., J. Macromol. Sci., Rev. Macromol. Chem., C7, 251 (1972).

83. Koningsveld, R., Kleintjens, L.A., and Schoffelers, H.M., Pure Appl. Chem., 39, 1 (1974).

84. Wahrmund, D.C., Paul, D.R., and Barlow, J.W., J. Appl. Polym. Sci., 22, 2125 (1978).

85. Wahrmund, D.C., Bernstein, R.E., Barlow, J.W., and Paul, D.R., Polym. Eng. Sci., 18, 677 (1978).

86. Bernstein, R.E., Paul, D.R., and Barlow, J.W., Polym. Eng. Sci., 18, 683 (1978).

87. Robeson, L.M., and Furtek, A.B., J. Appl. Polym. Sci., 23, 645 (1979).

88. Hoffman, A.S., Lewis, R.W., and Michaels, A.S., Organic Coating and Plastic Chemistry Preprints, 29, 236 (1969).

89. Michaels, A.S., Ind. Eng. Chem., 57, 32 (1965).

90. Michaels, A.S., and Miekka, R.G., J. Phys. Chem., 65, 1765 (1961).

91. Smith, K.L., Winslow, A.E., and Petersen, D.E., Ind. Eng. Chem., 51, 1361 (1959).

92. Osada, Y., and Sato, M., J. Polym. Sci., Polym. Lett. Ed., 14, 129 (1976).

93. Bimendina, L.A., Roganov, V.V., and Bekturov, Y.A., Vysokomal. Soedin., A16, 2810 (1974).

94. Sulzberg, T., and Cotter, R.L., J. Polym. Sci., Pt. A-1, 8, 2747 (1970).

95. Matzner, M., Schober, D.L., Johnson, R.N., Robeson, L.M., and McGrath, J.E., Permeability of Plastic Films and Coatings to Gases, Vapors and Liquids, Plenum Press, N.Y., 1975.

96. Robeson, L.M., and McGrath, J.E., Paper Presented at the 82nd National Meeting of AIChE, Atlantic City, New Jersey, August 31, 1976.

97. Olabisi, O., Macromolecules, 8, 316 (1975).

98. Hickman, J.J., and Ikeda, R.M., J. Polym. Sci., Polym. Phys. Ed., 311, 1713 (1973).

99. Komskaya, N.F., and Slonimskii, G.L., J. Phys. Chem. SSSR, 30, 1529 (1956).

100. Slonimskii, G.L., and Komskaya, N.F., J. Phys. Chem. SSSR, 30, 1746 (1956).

101. Struminskii, G.V., and Slonimskii, G.L., J. Phys. Chem. SSSR, 30, 1941 (1956).

102. Slonimskii, G.L., and Struminskii, G.V., J. Phys. Chem. SSSR, 30, 2144 (1956).

103. McMaster, L.P., Macromolecules, 6, 760 (1973).

104. Sanchez, I.C., and Lacombe, R.H., J. Phys. Chem., 80, 2352 (1976).

105. Lacombe, R.H., and Sanchez, I.C., J. Phys. Chem., 80, 26568 (1976).

106. Sanchez, I.C., and Lacombe, R.H., J. Polym. Sci., Polym. Lett. Ed., 15, 71 (1977).

107. Sanchez, I.C., and Lacombe, R.H., Macromolecules, 11, 1145 (1978).

108. Hugelin, C., and Dondos, A., Makromol. Chem., 126, 206 (1969).

109. Banks, M., Leffingwell, J., and Thies, C., Macromolecules, 4, 43 (1971).

110. Kern, R.J., J. Polym. Sci., 21, 19 (1956).

111. Zeman, L., and Patterson, D., Macromolecules, 5, 513 (1972).

112. Hsu, C.C., and Prausnitz, J.M., Macromolecules, 7, 320 (1974).

113. Sheehan, C.J., and Bisio, A.L., Rubber Chem. Technol., 39, 149 (1966).

114. Paxton, T.R., J. Appl. Polym. Sci., 7, 1499 (1963).

115. Scott, R.L., J. Chem. Phys., 17, 279 (1949).

116. Deshpande, D., Patterson, D., Schreiber, H.P., and Su, C.S., Macromolecules, 7, 530 (1974).

117. Su, C.S., Patterson, D., and Schreiber, H.P., J. Appl. Polym. Sci., 20, 1025 (1974).

118. Bonner, D.C., and Brockmeier, N.F., Ind. Eng. Chem., Process Des. Dev., 16, 428 (1977).

119. Blackadder, D.A., and Ghavamikia, H., "Dissolution of Polyether sulfone in Chloroform," Polymer, 20, 523 (1979).

120. Blackadder, D.A., and Ghavamikia, H., "Evidence for Crystallinity in Poly(ether sulphone)," Polymer, 20, 781 (1979).

121. Blackadder, D.A., and Ghavamikia, H., "Crystallinity in Polyether-sulphone: A Problem of Definition," Polymer, 1432 (1979).

122. Dominie, J., Union Carbide Corporation, Bound Brook, NJ, private communication.

TABLE 1

SOLVENT GROUP DESIGNATIONS

Code:	Solvent Group:
A	Acyclic saturated unbranched hydrocarbons
B	Acyclic saturated branched hydrocarbons
C	Acyclic unsaturated hydrocarbons (branched and unbranched)
D	Monocyclic hydrocarbons (saturated and unsaturated, with or without side chains)
E	Aromatic hydrocarbons (with or without side chains)
F	Cyclic compound with one or more hetero atoms
G	Carboxylic acids and anhydrides; Acids containing S or N
H	Monohydric alcohols
I	Polyhydric alcohols and phenols
J	Halogenated solvents
K	Ketones
L	Aldehydes and esters
M	Ethers
N	Amines
O	Nitro compounds and nitriles
P	Miscellaneous solvents

TABLE 2

CODE DESIGNATIONS FOR SOLVENTS

Code:	Solvent:	Code:	Solvent:
A1	Methane	G1	Formic acid
A2	Ethane	G2	Acetic acid
A3	n-Propane	G3	n-Propionic acid
A4	n-Butane	G4	n-Butyric acid
A5	n-Pentane	G5	Oxalic acid
A6	n-Hexane	G6	Pthalic acid
A7	n-Heptane	G7	Acetic anhydride
A8	n-Octane	G8	Propionic anhydride
A9	n-Nonane	G9	Pthalic anhydride
A10	n-Decane	G10	Methane sulfonic acid
A11	n-Undecane	G11	Nitric acid
A12	n-Dodecane	G12	Sulfuric acid
		G13	Benzene sulfonic acid
B1	2,2-Dimethyl-butane		
B2	2-Methyl pentane	H1	Methanol
B3	2-Methyl hexane	H2	Ethanol
B4	i-Octane	H3	1-Propanol
		H4	2-Propanol
C1	Ethylene	H5	1-Butanol
C2	Allene	H6	2-Butanol
C3	2-Hexene	H7	i-Butanol
C4	2-Heptene	H8	1-Pentanol
C5	1-Octene	H9	1-Hexanol
C6	2-Octene	H10	Cyclohexanol
C7	2,6-Dimethyl-3-heptene	H11	Allyl alcohol
		H12	Benzyl alcohol
D1	Cyclopentane		
D2	Cyclohexane	I1	Phenol
D3	Methyl cyclohexane	I2	o-Cresol
D4	Ethyl cyclohexane	I3	m-Cresol
		I4	p-Cresol
E1	Benzene	I5	Resorcinol
E2	Toluene	I6	m-Methoxyl phenol
E3	m-Xylene	I7	Propylene glycol
E4	Ethyl benzene	I8	Resorcinol monoacetate
		I9	Ethylene glycol
F1	Furan	I10	1,5-Pentanediol
F2	Tetrahydrofuran		
F3	Pyrrole		
F4	Pyrrolidine		
F5	1,3-Dioxolane		
F6	p-Dioxane		
F7	Pyridine		
F8	Quinoline		
F9	Quinoxaline		

TABLE 2 (Continued)

Code:	Solvent:	Code:	Solvent:
J1	Dichloromethane	L10	Propyl formate
J2	1,2-Dichloroethane	L11	Dioctyl phthalate
J3	1-Chloropropane	L12	m-Dimethoxy benzene
J4	Chloroform	L13	n-Butyl acetate
J5	Carbon tetrachloride		
J6	1-Chlorobutane	M1	Diethyl ether
J7	2-Chlorobutane	M2	Phenyl ether
J8	1-Bromobutane	M3	Di(i-propyl) ether
J9	2-Bromobutane	M4	Di(n-propyl) ether
J10	Chlorobenzene	M5	2-Methoxy pentane (Methyl i-Butyl ether)
J11	Bromobenzene		
J12	Fluorobenzene		
J13	Iodobenzene	N1	N-acetyl ethanolamine
J14	Benzyl chloride	N2	Aniline
J15	o-Chlorophenol	N3	n-Butyl amine
J16	Hexafluoro-iso-propanol	N4	Diethyl amine
J17	Trifluoromethanol	N5	Diethylene triamine
J18	2,2,2-Trifluoroethanol	N6	Dimethyl acetamide
J19	Chlorosulfonic acid	N7	N,N-Dimethyl formamide
J20	Hydrochloric acid	N8	N-Ethyl acetamide
J21	Hydrofluoric acid	N9	Ethylene diamine
J22	Perfluorotributylamine	N10	Formamide
J23	Dio-idomethane	N11	1,2-Propane diamine
J24	Pentachloroethane	N12	Tetramethyl urea
J25	Tetrachloroethylene	N13	N-Methyl formamide
J26	α,α-Dichlorotoluene	N14	i-Butyl amine
J27	Benzoyl chloride		
J28	p-Chlorophenol	O1	Acetonitile
		O2	Acrylonitrile
K1	Acetone	O3	Propionitrile
K2	2,4-Dimethyl-3-pentanone	O4	Butyronitrile
K3	3-Methyl-2-butanone	O5	Hydracrylonitrile
K4	Methyl ethyl ketone	O6	Nitrobenzene
K5	Methyl isobutyl ketone	O7	Nitromethane
K6	Diethyl ketone	O8	Nitroethane
K7	Cyclohexanone	O9	1-Nitropropane
K8	1-Methyl-2-pyrrolidone	O10	2-Nitropropane
L1	Acetaldehyde	P1	2-Dimethyl amino ethanol
L2	Propionaldehyde	P2	Dimethyl sulfoxide
L3	Butyraldehyde	P3	2-Ethoxy ethanol
L4	Benzaldehyde	P4	Ethylene carbonate
L5	Methyl acetate	P5	Hexamethyl phosphate triamide
L6	Ethyl acetate		
L7	n-Propyl acetate	P6	Monoethanolamine
L8	Methyl formate	P7	Sulfanilimide
L9	Ethyl formate	P8	Triethyl phosphate
		P9	Water

TABLE 3

PHYSICAL PROPERTIES OF SOLVENTS AT 25° C

Solvent	Code	MW	T_b (K)	$\alpha x10^{18}$ (m^{-3})	$\mu x10^{30}$[a] (C•m)	δ $(kJ/mol)^{1/2}$	δ_p $(kJ/mol)^{1/2}$
Acetaldehyde	L1	44.05	294.00	4.60	9.07	---	---
Acetic acid	G2	60.05	391.15	5.11	5.80	---	---
Acetic anhydride	G7	102.09	412.15	8.88	10.71	---	---
Acetone	K1	58.08	329.70	6.42	9.61	5.08	2.79
Acetonitrile	O1	41.05	354.75	4.40	13.14	5.38	4.01
N-Acetyl ethanolamine	N1	103.12	428.15	10.22	14.18	---	---
Acrylonitrile	O2	53.06	350.15	6.19	12.78	---	---
Allyl alcohol	H11	58.08	369.00	6.74	5.17	---	---
Aniline	N2	93.13	457.15	12.13	5.04	---	---
Benzene	E1	73.11	353.30	10.38	0.0	5.57	0.30
Benzene sulfonic acid	G13	158.18	---	---	---	---	---
Benzoyl chloride	J27	140.57	470.35	14.60	10.54	7.46	3.46
Benzyl alcohol	H12	108.15	478.50	12.25	5.77	8.16	1.89
Benzyl chloride	J14	126.59	452.45	14.34	4.47	6.74	2.38
Bromobenzene	J11	157.06	429.20	13.48	5.67	6.46	1.77
1-Bromobutane	J8	137.03	374.75	11.22	6.94	6.29	---
2-Bromobutane	J9	137.03	364.15	11.26	7.44	---	---
1-Butanol	H5	74.12	390.80	8.76	5.54	7.13	1.33
2-Butanol	H6	74.12	372.7	8.66	5.47	6.74	1.32
i-Butanol	H7	74.12	381.0	8.60	9.24	---	---
n-Butyl acetate	L13	116.16	399.2	12.51	6.24	---	---
i-Butyl amine	N14	73.14	340.6	9.55	4.80	---	---
n-Butyl amine	N3	73.14	350.6	9.71	3.34	5.88	1.44
Butyraldehyde	L3	72.10	348.0	8.17	9.01	---	---
n-Butyric acid	G4	88.10	436.4	8.81	5.50	6.90	1.76
Butyronitrile	O4	69.10	391.0	8.02	13.58	---	---
Carbon tetrachloride	J5	153.82	349.7	10.24	0.00	5.48	0.00
Chlorobenzene	J10	112.56	404.9	12.33	5.40	6.19	1.36
1-Chlorobutane	J6	42.57	351.6	10.07	6.84	5.52	1.77

TABLE 3 (Continued)

Solvent	Code	MW	T_b (K)	$\alpha x10^{18}$ (m^{-3})	$\mu x10^{30}$[a] (C•m)	δ (kJ/mol)1/2	δ_p $(kJ/mol)^{1/2}$
Chloroform	J4	119.38	334.3	8.48	3.37	---	---
o-Chlorophenol	J15	128.56	448.05	12.96	4.54	8.50	1.47
p-Chlorophenol	J28	128.56	492.90	12.97	7.47	8.55	---
1-Chloropropane	J3	78.54	319.6	8.17	6.84	---	---
m-Cresol	I3	108.14	475.4	13.11	4.94	7.94	1.96
o-Cresol	I2	108.14	464.2	13.11	4.70	---	---
p-Cresol	I4	108.14	475.1	13.11	5.21	---	---
Cyclohexane	D2	84.16	353.9	10.71	0.00	5.47	0.00
n-Decane	A10	142.28	447.30	19.30	0.00	6.84	0.00
1,2-Dichloroethane	J2	98.96	356.6	8.34	5.01	5.36	1.54
α,α-Dichlorotoluene	J26	161.03	478.35	16.18	6.90	7.43	2.26
Diethyl amine	N4	73.14	328.6	9.63	3.97	5.37	0.74
Diethyl ether	M1	74.12	307.7	8.92	3.84	---	---
Diethyl ketone	K6	86.13	375.1	9.91	9.10	6.15	2.56
Di-iodomethane	J23	267.84	455.15	12.89	3.64	4.72	1.20
m-Dimethoxy benzene	L12	138.17	490.25	14.85	5.34	6.69	---
N,N-Dimethyl formamide	N7	73.10	426.15	7.84	11.34	6.62	3.65
p-Dioxane	F6	88.11	374.15	8.58	1.44	5.73	0.42
1,3-Dioxolane	F5	74.08	351.15	8.56	4.74	5.95	1.45
Ethanol	H2	46.07	351.40	5.02	5.64	6.15	1.36
Ethyl acetate	L6	88.10	350.30	8.33	5.94	5.64	---
Ethyl formate	L9	74.08	327.50	7.06	6.44	5.37	2.34
Ethylene glycol	I9	62.06	470.40	5.72	7.34	8.18	2.36
Fluorobenzene	J12	96.10	358.25	10.40	5.24	5.47	---
Formic acid	G1	46.03	373.95	3.28	5.07	---	---
Furan	F1	68.08	304.52	7.60	2.30	5.32	0.56
n-Heptane	A7	100.20	371.60	13.71	0.00	5.87	0.00
n-Hexane	A6	86.18	342.15	11.85	0.00	5.31	0.00
Methane sulfonic acid	G10	96.11	440.15	---	---	---	---
Methanol	H1	32.04	337.80	3.23	5.71	5.68	1.37

TABLE 3 (Continued)

Solvent	Code	MW	T_b (K)	$\alpha x10^{18}$ (m^{-3})	$\mu x10^{30}$ [a] (C·m)	δ $(kJ/mol)^{1/2}$	δ_p $(kJ/mol)^{1/2}$
m-Methoxy phenol	I6	124.15	517.45	13.77	6.17	8.43	2.03
Methyl acetate	L5	74.08	330.15	6.94	5.60	5.46	1.67
Methyl ethyl ketone	K4	72.10	352.80	8.24	9.24	5.71	---
N-Methyl formamide	N13	59.07	453.65	5.99	12.78	8.77	4.17
Methyl formate	L8	60.05	304.70	5.10	5.91	4.95	1.63
i-Octane	B4	114.23	390.8	15.44	0.00	6.03	0.00
2-Methyl hexane	B3	100.20	363.2	13.67	0.00	5.73	0.00
Methyl isobutyl ketone	K5	100.16	389.60	11.83	9.34	5.91	---
1-Methyl-2-pyrrolidone	K8	99.13	475.15	10.64	13.64	6.63	3.96
Dichloromethane	J1	84.93	313.05	6.58	5.21	4.97	1.26
Nitrobenzene	O6	123.11	483.65	12.96	14.14	7.43	4.65
Nitroethane	O8	75.07	387.15	6.74	11.81	6.07	3.71
Nitromethane	O7	61.04	374.00	4.95	11.91	5.96	3.74
1-Nitropropane	O9	89.09	403.65	8.43	11.98	8.75	3.95
n-Nonane	A9	128.25	424.00	17.42	0.00	6.56	0.00
n-Octane	A8	114.23	398.90	15.54	0.00	6.20	0.00
1-Octane	C5	112.21	394.4	15.36	1.13	6.07	0.00
Oxalic acid	G5	90.04	430.15	---	8.77	---	---
Pentachloroethane	J24	202.30	435.15	14.08	3.07	6.54	0.99
1,5-Pentanediol	I10	104.15	533.15	11.16	12.14	6.76	4.08
1,2-Propane diamine	N11	74.13	393.65	9.46	6.54	6.21	---
1-Propanol	H3	60.09	370.40	6.90	5.60	6.69	1.35
Propionaldehyde	L2	58.08	321.00	6.35	9.17	4.38	---
Propionitrile	O3	55.08	370.50	6.26	13.44	5.62	4.15
n-Propyl acetate	L7	102.13	374.80	10.67	6.00	5.98	---
Pyridine	F7	79.10	388.50	9.51	7.67	6.35	2.57
Quinoline	F8	129.16	513.20	15.35	7.31	7.36	---
Quinoxaline	F9	130.15	502.65	14.74	1.70	8.92	0.56
Tetrachloroethylene	J25	165.83	394.3	12.02	0.00	6.10	1.97
Tetrahydrofuran	F2	72.12	340.15	7.97	5.84	5.11	1.41

TABLE 3 (Continued)

Solvent	Code	MW	T_b (K)	$\alpha x10^{18}$ (m^{-3})	$\mu x10^{30}$[a] (C•m)	δ $(kJ/mol)^{1/2}$	δ_p $(kJ/mol)^{1/2}$
Tetramethyl urea	N12	116.16	450.15	13.04	11.67	7.17	3.13
Toluene	E2	92.13	383.80	12.33	1.20	5.89	0.29
Triethyl phosphate	P8	182.16	488.15	16.50	10.01	6.44	3.32
m-Xylene	E3	106.17	412.25	13.91	1.17	6.31	0.28

[a] 1 Debye = $3.3356x10^{-30}$ C•m.

TABLE 4
COMPARISON OF COLUMN AND CAPILLARY FLOW RATES

Experimental Date	Total Gas[a] Flow Rate (cm^3/min)	Column Gas[b] Flow Rate (F) (cm^3/min)	Column Gas[c] Flow Rate (F) (cm^3/min)
4/6/79	5.42	3.75	3.75
4/19/79	2.78	1.93	1.90
5/7/79	2.05	1.92	1.98
5/9-11/79	2.55	2.42	2.45
6/2-5/79	2.78	1.67	1.53
6/11-14/79	2.72	1.50	1.50

[a]Measured by bubble flow meter and stop watch

[b]Determined from the areas under the capillary and column peaks recorded from an air injection

$$F = \left(\begin{array}{l} \text{total gas} \\ \text{flow rate} \end{array} \right) \frac{\text{area under column peak}}{\text{sum of area under column and capillary peaks}}$$

[c]Determined by using the pressure drop characteristic of the bypass (ΔP versus capillary flow rate) and the experimentally measured pressure drop ($P_I - P_R$). This flow rate value is considered the most accurate.

TABLE 5

UNCURED PATS RESULTS AT 74°C (Column B)

Solvent:	Code	$(t_g - t_g^a)$: (min)	V_N^c: (cm^3/g)	$\Delta G:_{ads}$ (kJ/mol)	$\Delta G:_{add}$ (kJ/mol)	Λ: (kJ/mol)	Ω_{12}^{∞}:	χ_{12}^{∞}:
Acetaldehyde	L1	0.21	4.18	13.9	- 5.9	- 1.95	20.	1.8
Acetone	K1	0.13	2.63	14.4	- 3.0	1.2	75.	3.1
Acetonitrile	O1	---	---	---	---	---	---	---
Acrylonitrile	O2	---	---	---	---	---	---	---
Allyl alcohol	H11	---	---	---	---	---	---	---
Aniline	N2	---	---	---	---	---	---	---
Benzene[b]	E1	0.33	6.60	10.9	0.0	0.0	50.	2.9
Bromobenzene	J11	---	---	---	---	---	---	---
1-Butanol	H5	---	---	---	---	---	---	---
Carbon tetrachloride	J5	---	---	---	---	---	---	---
Chlorobenzene	J10	---	---	---	---	---	---	---
1-Chlorobutane	J6	---	---	---	---	---	---	---
Chloroform	J4	0.25	5.15	10.4	- 4.5	- 3.2	25.	2.6
Cyclohexane[b]	D2	0.28	5.76	11.1	0.0	0.0	55.	2.9
n-Decane[b,c]	A10	---	---	---	---	---	---	---
1,2-Dichloroethane	J2	---	---	---	---	---	---	---
Diethylamine	N4	1.42	18.4	8.1	- 5.1	- 3.45	8.5	1.0
Diethylketone	K6	---	---	---	---	---	---	---
1,4-Dimethoxybenzene	E5	---	---	---	---	---	---	---
Dimethylformamide	N7	---	---	---	---	---	---	---
p-Dioxane[c]	F6	---	---	---	---	---	---	---
Ethanol	H2	---	---	---	---	---	---	---
Ethyl-acetate	L6	---	---	---	---	---	---	---
Ethyl-benzene	E4	---	---	---	---	---	---	---
Ethylcyanide	O3	---	---	---	---	---	---	---
Ethyl ether[c]	M1	0.12	2.40	14.0	- 0.93	0.6	33.	2.4
Ethyl formate	L9	0.16	3.27	13.1	- 3.5	- 0.7	45.	2.8
Fluorobenzene	J12	---	---	---	---	---	---	---
Furan[c]	F1	0.11	2.26	14.4	- 0.1	0.73	37.	2.5
n-Heptane[b,c]	A7	0.80	16.1	7.6	- 0.2	- 0.4	30.	2.3

TABLE 5 (Continued)

Solvent:	Code:	$(t - t)^a$: (min)	V°_N: (cm^3/gl)	$\Delta G:_{ads}$ (kJ/mol)	$\Delta G:_{add}$ (kJ/mol)	Λ: (kJ/mol)	Ω^∞_{12}:	χ^∞_{12}:
n-Hexane[b,c]	A6	0.33	6.59	10.6	0.4	0.15	30.	2.3
Isobutylamine	N14	1.74	35.18	6.3	- 7.0	- 5.0	7.	0.7
Isooctane	B4	---	---	---	---	---	---	---
Methanol	H1	2.0	40.26	8.2	-13.3	-10.9	11.5	1.1
Methyl acetate	L5	0.16	3.34	13.2	- 3.4	- 1.0	55.	2.9
3-Methyl-2-Butanone	K3	---	---	---	---	---	---	---
Methylcyclohexane	D3	---	---	---	---	---	---	---
Methylene chloride	J1	0.18	3.6	12.4	- 5.0	- 2.8	23.	2.4
Methylethylketone	K4	---	---	---	---	---	---	---
n-Nonane[b,c]	A9	---	---	---	---	---	---	---
n-Octane[b,c]	A8	---	---	---	---	---	---	---
n-Pentane[b,c]	A5	0.17	3.47	13.0	- 0.2	- 0.4	25.	2.0
Propanol	H3	---	---	---	---	---	---	---
2-Propanol	H4	---	---	---	---	---	---	---
Propionic acid	G3	---	---	---	---	---	---	---
Tetrahydrofuran[c]	F2	0.28	5.72	11.5	- 3.15	- 0.7	40.	2.6
Toluene	E2	---	---	---	---	---	---	---
2,2,2,-Triflouroethanol	J18	---	---	---	---	---	---	---
m-Xylene	E3	---	---	---	---	---	---	---

[a]The average of the four air elution times subtracted from the average of the three solvents elution times.
[b]Polarizability reference solvent.
[c]Dipole reference solvent.

Experimental Data: Date Performed = 4/6/79; Column Temperature = 74.25°C; Room Temperature = 22.95°C; Inlet Pressure = 2.45 psig; Room Pressure = 29.860 in Hg; Column Helium Flow Rate = 3.75 cm^3/min.

TABLE 6
UNCURED PATS RESULTS AT 69%C (Column B)
Gas Chromatograph Date and Results for Uncured Column B-PATS at 69%C

Solvent:	Code:	$(t_g - t_a)^a$: (min)	V^o_N: (cm^3/g)	ΔG: ads (kJ/mol)	ΔG: add (kJ/mol)	Λ: (kJ/mol)	Ω^∞_{12}	χ^∞_{12}
Acetaldehyde	L1	0.65	6.85	12.3	- 7.7	- 4.9	14.	1.5
Acetone	K1	0.32	3.32	13.6	- 3.8	- 0.87	70.	3.0
Acetonitrile	O1	---	---	---	---	---	---	---
Acrylonitrile	O2	---	---	---	---	---	---	---
Allyl alcohol	H11	---	---	---	---	---	---	---
Aniline	N2	---	---	---	---	---	---	---
Benzene[b]	E1	0.72	7.52	10.4	0.0	0.0	50.	2.8
Bromobenzene	J11	---	---	---	---	---	---	---
1-Butanol	H5	---	---	---	---	---	---	---
Carbon tetrachloride	J5	---	---	---	---	---	---	---
Chlorobenzene	J10	---	---	---	---	---	---	---
1-Chlorobutane	J6	---	---	---	---	---	---	---
Chloroform	J4	0.52	5.42	10.1	- 4.6	- 3.6	25.	2.7
Cyclohexane[b]	D2	0.60	6.34	10.6	0.0	0.0	60.	2.9
n-Decane[b,c]	A10	---	---	---	---	---	---	---
1,2-Dichloroethane	J2	---	---	---	---	---	---	---
Diethylamine	N4	3.57	37.56	6.0	- 6.9	- 5.7	5.0	0.4
Diethylketone	K6	---	---	---	---	---	---	---
1,4-Dimethoxybenzene	E5	---	---	---	---	---	---	---
Dimethylformamide	N7	---	---	---	---	---	---	---
p-Dioxane[c]	F6	---	---	---	---	---	---	---
Ethanol	H2	---	---	---	---	---	---	---
Ethyl acetate	L6	---	---	---	---	---	---	---
Ethyl benzene	E4	---	---	---	---	---	---	---
Ethylcyanide	O3	---	---	---	---	---	---	---
Ethyl ether[c]	M1	0.24	2.51	13.7	- 1.0	0.16	40.	2.5
Ethyl formate	L9	0.35	3.67	12.6	- 3.9	- 1.9	50.	2.8
Fluorobenzene	J12	---	---	---	---	---	---	---
Furan[c]	F1	0.29	3.11	13.3	- 1.0	- 0.26	30.	2.4
n-Heptane[b,c]	A7	1.83	19.25	7.0	- 0.14	- 0.1	30.	2.2
n-Hexane[b,c]	A6	0.74	7.77	10.0	0.25	0.29	30.	2.3

TABLE 6 (Continued)

Solvent:	Code:	(t_g-t_a):[a] (min)	V_N^o: (cm^3/g)	$\Delta G:_{ads}$ (kJ/mol)	$\Delta G:_{add}$ (kJ/mol)	Λ: (kJ/mol)	Ω_{12}^{∞}	X_{12}^{∞}
Isobutylamine	N14	4.62	48.6	5.2	- 7.7	- 6.3	6.	0.5
Isooctane	B4	---	---	---	---	---	---	---
Methanol	H1	5.17	54.32	7.3	-14.6	-12.8	10.	0.9
Methyl acetate	L5	0.38	3.95	12.4	- 4.2	- 2.4	50.	2.8
3-Methyl-2-Butanone	K3	---	---	---	---	---	---	---
Methylcyclohexane	D3	---	---	---	---	---	---	---
Methylene chloride	J1	0.38	4.00	11.9	- 5.5	- 3.9	25.	2.45
Methylethylketone	K4	---	---	---	---	---	---	---
n-Nonane[b,c]	A9	---	---	---	---	---	---	---
n-Octane[b,c]	A8	---	---	---	---	---	---	---
n-Pentane[b,c]	A5	0.34	3.56	12.8	- 0.35	- 0.1	30.	2.1
Propanol	H3	---	---	---	---	---	---	---
2-propanol	H4	---	---	---	---	---	---	---
Propionic acid	G3	---	---	---	---	---	---	---
Tetrahydrofuran[c]	F2	0.35	3.63	12.7	- 1.8	- 0.01	75.	3.2
Toluene	E2	---	---	---	---	---	---	---
2,2,2-Trifluoroethanol	J18	---	---	---	---	---	---	---
m-Xylene	E3	---	---	---	---	---	---	---

[a] The average of the four air elution times subtracted from the average of the three solvents elution times.
[b] Polarizability reference solvent.
[c] Dipole reference solvent.

Experimental Data: Date Performed = 4/19/79; Column Temperature = 69.4°C; Room Temperature = 26.0°C; Inlet Pressure = 1.30 psig; Room Pressure = 29.707 in Hg; Column Helium Flow Rate = 1.9 cm^3/min.

TABLE 7
UNCURED PATS RESULTS AT 70°C (Column C)

Solvent:	Code:	$(t_g - t_a)^a$: (min)	V°_N: (cm^3/g)	$\Delta G:_{ads}$ (kJ/mol)	$\Delta G:_{add}$ (kJ/mol)	Λ: (kJ/mol)	Ω^∞_{12}	χ^∞_{12}
Acetaldehyde	L1	0.83	8.87	11.6	- 9.9	- 5.1	10.	1.2
Acetone	K1	0.32	2.65	14.2	- 4.4	0.7	90.	3.3
Acetonitrile	O1	---	---	---	---	---	---	---
Acrylonitrile	O2	---	---	---	---	---	---	---
Allyl alcohol	H11	---	---	---	---	---	---	---
Aniline	N2	---	---	---	---	---	---	---
Benzene[b]	E1	0.81	6.62	10.8	0.0	0.0	60.	3.0
Bromobenzene	J11	---	---	---	---	---	---	---
1-Butanol	H5	---	---	---	---	---	---	---
Carbon tetrachloride	J5	---	---	---	---	---	---	---
Chlorobenzene	J10	---	---	---	---	---	---	---
1-Chlorobutane	J6	---	---	---	---	---	---	---
Chloroform	J4	0.54	4.46	10.7	- 5.1	- 3.5	30.	2.8
Cyclohexane[b]	D2	0.65	5.34	11.1	0.0	0.0	70.	3.1
n-Decane[b,c]	A10	---	---	---	---	---	---	---
1,2-Dichloroethane	J2	---	---	---	---	---	---	---
Diethylamine	N4	2.72	22.37	7.5	- 6.3	- 4.3	8.0	0.9
Diethylketone	K6	---	---	---	---	---	---	---
1,4-Dimethoxybenzene	E5	---	---	---	---	---	---	---
Dimethylformamide	N7	---	---	---	---	---	---	---
p-Dioxane[c]	F6	---	---	---	---	---	---	---
Ethanol	H2	---	---	---	---	---	---	---
Ethyl acetate	L6	---	---	---	---	---	---	---
Ethyl benzene	E4	---	---	---	---	---	---	---
Ethylcyanide	O3	---	---	---	---	---	---	---
Ethyl ether[c]	M1	0.24	1.96	14.5	- 1.3	0.5	50.	2.7
Ethyl formate	L9	0.35	2.85	13.3	- 4.4	- 1.0	60.	3.0
Fluorobenzene	J12	---	---	---	---	---	---	---
Furan[c]	F1	0.28	2.29	14.2	- 0.80	0.16	40.	2.7
n-Heptane[b,c]	A7	2.00	16.39	7.5	- 0.02	- 0.38	33.	2.4
n-Hexane[b,c]	A6	0.84	6.87	10.4	0.03	- 0.34	35.	2.4

TABLE 7 (Continued)

Solvent:	Code:	$(t_g - t_a)^a$: (min)	V°_N: (cm^3/g)	$\Delta G:_{ads}$ (kJ/mol)	$\Delta G:_{add}$ (kJ/mol)	Λ: (kJ/mol)	Ω^∞_{12}	χ^∞_{12}
Isobutylamine	N14	3.20	26.29	7.0	- 6.9	0 4.5	10.	1.1
Isooctane	B4	---	---	---	---	---	---	---
Methanol	H1	6.19	50.85	7.5	-16.1	-13.2	10.	1.0
Methyl acetate	L5	0.34	2.77	13.4	- 4.3	- 1.4	65.	3.2
2-Methyl-2-Butanone	K3	---	---	---	---	---	---	---
Methylcyclohexane	D3	1.19	9.74	9.0	1.2	0.81	60.	3.1
Methylene chloride	J1	0.50	4.12	11.9	- 6.8	- 4.2	20.	2.4
Methylethylketone	K4	---	---	---	---	---	---	---
n-Nonane[b,c]	A9	---	---	---	---	---	---	---
n-Octane[b,c]	A8	---	---	---	---	---	---	---
n-Pentane[b,c]	A5	0.32	2.59	13.7	- 0.01	- 0.38	40.	2.4
Propanol	H3	---	---	---	---	---	---	---
2-Propanol	H4	---	---	---	---	---	---	---
Propionic acid	G3	---	---	---	---	---	---	---
Tetrahydrofuran[c]	F2	0.58	4.72	12.0	- 3.4	- 0.4	55.	2.9
Toluene	E2	---	---	---	---	---	---	---
2,2,2,-Trifluoroethanol	J18	---	---	---	---	---	---	---
m-Xylene	E3	---	---	---	---	---	---	---

[a]The average of the four air elution times subtracted from the average of the three solvents elution times.
[b]Polarizability reference solvent.
[c]Dipole reference solvent.

Experiment Data: Date Performed = 5/7/79; Column Temperature = 70° C; Room Temperature = 25.7° C; Inlet Pressure = 1,653 psig; Room Pressure = 29.454 in Hg; Column Helium Flow Rate = 1.98 cm^3/min.

TABLE 8
UNCURED PATS RESULTS AT 102°C (Column C)

Solvent:	Code:	$(t_g - t_a)^a$: (min)	V°_N: (cm^3/g)	$\Delta G:_{ads}$ (kJ/mol)	$\Delta G:_{add}$ (kJ/mol)	Λ (kJ/mol)	Ω^∞_{12}	χ^∞_{12}
Acetaldehyde	L1	0.38	3.75	15.3	- 7.9	- 7.5	11.2	1.3
Acetone	K1	0.16	1.62	17.1	- 4.0	- 3.6	60.	2.8
Acetonitrile	O1	0.94	9.37	12.7	-10.8	-10.3	20.	2.2
Acrylonitrile	O2	0.44	4.36	14.3	- 7.2	- 6.6	45.	2.6
Allyl alcohol	H11	0.30	3.00	15.1	- 5.6	- 5.5	105.	3.5
Aniline	N2	---	---	---	---	---	---	---
Benzene[b]	E1	0.31	3.14	14.1	0.0	0.0	45.	2.9
Bromobenzene	J11	---	---	---	---	---	---	---
1-Butanol	H5	---	---	---	---	---	---	---
Carbon Tetrachloride	J5	0.28	2.82	12.3	- 6.7	- 6.7	25.	2.8
Chlorobenzene	J10	---	---	---	---	---	---	---
1-Chlorobutane	J6	0.21	2.12	14.8	- 2.1	- 1.5	55.	3.1
Chloroform	J4	0.16	1.59	14.9	- 4.1	- 4.0	35.	3.0
Cyclohexane[b]	D2	0.29	2.88	14.1	0.0	0.0	48.	2.8
n-Decane[b,c]	A10	---	---	---	---	---	---	---
1,2-Dichloroethane	J2	0.23	2.27	14.4	- 4.6	- 4.4	58.	3.3
Diethylamine	N4	1.54	15.37	9.3	- 8.2	- 8.0	5.	0.4
Diethylketone	K6	---	---	---	---	---	---	---
1,4-Dimethoxybenzene	E5	---	---	---	---	---	---	---
Dimethylformamide	N7	---	---	---	---	---	---	---
p-Dioxane[c]	F6	---	---	---	---	---	---	---
Ethanol	H2	0.46	4.61	14.5	- 8.2	- 8.0	40.	2.5
Ethylacetate	L6	0.14	1.37	16.3	- 2.1	- 1.9	85.	3.5
Ethylbenzene	E4	---	---	---	---	---	---	---
Ethylcyanide	O3	0.30	2.68	15.3	- 6.0	- 5.5	115.	3.5
Ethyl ether[c]	M1	0.05	0.46	20.2	1.3	1.4	90.	3.3
Ethyl formate	L9	0.95	1.36	16.9	- 3.5	- 3.3	50.	2.9
Fluorobenzene	J12	0.33	3.32	13.2	- 0.91	- 0.75	40.	2.9
Furan[c]	F1	0.12	1.20	17.5	0.25	0.3	30.	2.5
n-Heptane[b,c]	A7	0.38	4.89	12.7	- 0.07	- 0.01	50.	2.8
n-Hexane[b,c]	A6	0.21	2.08	15.1	- 0.1	- 0.05	45.	2.7
Isobutylamine	N14	0.87	11.0	10.4	- 7.2	- 7.0	9.	1.1

TABLE 8 (Continued)

Solvent:	Code:	$(t_g - t_a)^a$: (min)	V_N°: (cm^3/g)	$\Delta G:_{ads}$ (kJ/mol)	$\Delta G:_{add}$ (kJ/mol)	Λ: (kJ/mol)	Ω^∞: 12	χ^∞: 12
Isooctane	B4	0.27	2.73	13.3	3.1	3.0	60.	3.2
Methanol	H1	1.15	11.5	12.8	-12.0	-11.8	15.	1.4
Methyl acetate	L5	0.17	1.65	16.3	- 4.1	- 3.9	45.	2.8
3-Methyl-2-Butanone	K3	0.27	2.65	14.3	- 2.6	- 2.3	75.	3.3
Methylcyclohexane	D3	---	---	---	---	---	---	---
Methylene chloride	J1	0.17	1.69	15.8	- 5.4	- 5.2	25.	2.5
Methylethylketone	K4	0.16	1.62	16.4	- 2.7	- 2.3	95.	3.5
n-Nonane[b,c]	A9	---	---	---	---	---	---	---
n-Octane[b,c]	A8	---	---	---	---	---	---	---
n-Pentane[b,c]	A5	0.13	1.25	17.4	- 0.06	- 0.01	40.	2.4
Propanol	H3	0.17	1.73	16.7	- 3.8	- 3.6	180.	4.0
2-Propanol	H4	0.15	1.46	17.4	- 3.1	-2.9	125.	3.6
Propionic acid	G3	---	---	---	---	---	---	---
Tetrahydrofuran[c]	F2	0.19	1.85	16.0	- 1.2	- 1.0	60.	3.0
Toluene	E2	---	---	---	---	---	---	---
2,2,2-Triflouroethanol	J18	0.09	0.88	17.3	- 5.7	- 5.5	560.	5.6
m-Xylene	E3	---	---	---	---	---	---	---

[a]The average of the four air elution times subtracted from the average of the three solvents elution times.
[b]Polarizability reference solvent.
[c]Dipole reference solvent.

Experiment Data: Date Performed = 5/9,10,11/79; Column Temperature = 101.6°C; Room Temperature = 25.3°C; Inlet Pressure = 2.35 psig; Room Pressure = 29.488 in Hg; Column Helium Flow Rate = 2.45 cm^3/min.

TABLE 9
UNCURED PATS RESULTS AT 117°C (Column C)

Solvents:	Code:	$(t_g - t_a)$[a]: (min)	V°_N: (cm^3/g)	$\Delta G:_{ads}$ (kJ/mol)	$\Delta G:_{add}$ (kJ/mol)	Λ: (kJ/mol)	Ω^∞: 12	χ^∞: 12
Acetaldehyde	L1	0.24	1.50	18.9	-10.3	- 4.6	20.	1.9
Acetone	K1	0.13	0.85	19.8	- 6.6	- 0.6	72.	3.1
Acetonitrile	O1	0.67	4.22	15.8	-13.7	- 6.6	43.	2.5
Acrylonitrile	O2	0.39	2.49	16.6	-10.2	- 2.5	51.	2.8
Allyl alcohol	H11	0.33	2.10	16.9	- 9.1	- 5.7	90.	3.3
Aniline	N2	0.99	6.27	11.8	- 4.0	- 0.5	323.	4.9
Benzene[b]	E1	0.15	0.98	18.4	0.0	0.0	101.	3.6
Bromobenzene	J11	---	---	---	---	---	---	---
1-Butanol	H5	0.14	0.80	19.2	- 3.8	0.1	380.	4.8
Carbon tetrachloride	J5	0.23	1.48	14.9	- 8.7	- 8.3	32.	3.1
Chlorobenzene	J10	---	---	---	---	---	---	---
1-Chlorobutane	J6	0.14	0.92	18.2	- 2.8	1.5	90.	3.5
Chloroform	J4	0.14	0.9	17.3	- 6.3	- 4.0	43.	3.2
Cyclohexane[b]	D2	0.13	0.84	18.8	0.0	0.0	120.	3.7
n-Decane[b,c]	A10	---	---	---	---	---	---	---
1,2-Dichloroethane	J2	0.16	1.04	17.4	- 6.2	- 2.3	82.	3.6
Diethylamine	N4	0.53	3.39	14.6	- 7.1	- 4.4	15.	1.5
Diethylketone	K6	0.21	1.33	17.1	- 4.2	1.5	120.	3.7
1,4-Dimethoxybenzene	E5	---	---	---	---	---	---	---
Dimethylformamide	N7	---	---	---	---	---	---	---
p-dioxane[c]	F6	0.20	1.28	17.1	- 4.8	- 3.6	122.	3.9
Ethanol	H2	0.46	2.93	16.6	-11.9	- 8.2	40.	2.5
Ethyl acetate	L6	0.13	0.82	18.6	- 4.2	- 0.4	93.	3.6
Ethyl benzene	E4	---	---	---	---	---	---	---
Ethylcyanide	O3	0.26	1.63	17.9	- 8.8	- 1.2	140.	3.7
Ethyl ether[c]	M1	0.04	0.28	22.9	- 0.8	1.86	110.	3.6
Ethyl formate	L9	0.13	0.80	19.4	- 6.1	- 2.0	60.	3.1
Fluorobenzene	J12	0.21	1.32	16.8	- 1.8	1.4	70.	3.4
Furan[c]	F1	0.10	0.63	20.5	- 2.1	- 0.3	48.	2.8
n-Heptane[b,c]	A7	0.29	1.82	15.6	- 0.02	0.4	70.	3.2
n-Hexane[b,c]	A6	0.15	0.93	18.4	0.06	0.5	80.	3.2

TABLE 9 (Continued)

Solvent:	Code:	$(t_g - t_a)^a$: (min)	V°_N: (cm^3/g)	$\Delta G:_{ads}$ (kJ/mol)	$\Delta G:_{add}$ (kJ/mol)	Λ: (kJ/mol)	Ω^∞: 12	χ^∞: 12
Isobutylamine	N14	0.53	3.36	14.6	- 7.2	- 4.0	20.	1.9
Isooctane	B4	0.23	1.46	15.5	3.7	4.1	80.	3.4
Methanol	H1	0.86	5.47	15.7	-15.5	-11.8	20.	1.7
Methyl acetate	L5	0.15	1.41	18.8	- 6.8	- 3.0	54.	3.0
3-Methyl-2-Butanone	K3	0.18	1.11	17.7	- 3.3	2.5	120.	3.7
Methylcyclohexane	D3	0.30	1.87	15.6	0.03	0.5	75.	3.3
Methylene chloride	J1	0.17	1.10	17.8	- 8.6	- 5.2	26.	2.6
Methylethylketone	K4	0.12	0.73	19.6	- 4.1	1.62	140.	3.9
n-Nonane[b,c]	A9	---	---	---	---	---	---	---
n-Octane[b,c]	A8	0.58	3.68	12.6	- 0.01	0.4	65.	3.2
n-Pentane[b,c]	A5	0.07	0.42	21.6	- 0.03	0.01	90.	3.2
Propanol	H3	0.15	0.94	19.6	- 6.1	- 2.4	220.	4.1
2-Propanol	H4	0.09	0.58	21.2	- 4.4	- 0.7	208.	4.0
Propionic acid	G3	0.72	4.53	13.6	-12.1	- 8.3	150.	4.0
Tetrahydrofuran[c]	F2	0.15	0.94	18.8	- 4.0	- 0.3	75.	3.3
Toluene	E2	0.21	1.31	16.9	1.4	2.6	150.	4.0
2,2,2-Trifluoroethanol	J18	0.04	0.26	21.9	- 7.0	- 2.6	1000.	6.8
m-Xylene	E3	0.56	3.57	13.23	0.04	1.1	110.	3.8

[a] The average of the four air elution times subtracted from the average of the three solvents elution times.
[b] Polarizability reference solvent.
[c] Dipole reference solvent.

Experiment Data: Date Performed = 6/2,3,5/79; Column Temperature = 116.7°C; Room Temperature = 25.2°C; Inlet Pressure = 1.745 psig; Room Pressure = 29.603 in Hg; Column Helium Flow Rate = 1.52 cm^3/min.

TABLE 10
UNCURED PATS RESULTS AT 145°C (Column C)

Solvent:	Code:	$(t_g - t_a)^a$: (min)	V_N^o: (cm^3/g)	$\Delta G:_{ads}$ (kJ/mol)	$\Delta G:_{add}$ (kJ/mol)	Λ: (kJ/mol)	Ω^∞: 12	χ^∞: 12
Acetaldehyde	L1	0.13	0.79	22.5	-12.9	-3.7	21.	2.0
Acetone	K1	0.05	0.29	25.6	- 7.0	2.6	150.	3.8
Acetonitrile	O1	0.23	1.36	20.8	-14.8	-3.3	65.	2.9
Acrylonitrile	O2	0.12	0.73	22.2	-10.9	1.6	90.	3.5
Allyl alcohol	H11	0.10	0.63	22.3	- 9.8	-4.3	130.	3.7
Aniline	N2	0.52	3.15	15.08	- 4.7	1.0	230.	4.5
Benzene[b]	E1	0.08	0.47	22.3	0.0	0.0	108.	3.7
Bromobenzene	J11	0.32	1.94	15.0	- 2.8	2.6	96.	4.1
1-Butanol	H5	0.04	0.22	25.7	- 3.5	2.8	720.	5.4
Carbon tetrachloride	J5	0.08	0.47	19.9	- 9.9	-9.0	51.	3.5
Chlorobenzene	J10	0.22	1.3	17.5	- 2.0	3.7	102.	3.9
1-Chlorobutane	J6	0.02	0.12	26.4	- 0.8	6.2	325.	4.9
Chloroform	J4	0.05	0.27	23.7	- 6.15	-2.2	124.	4.1
Cyclohexane[b]	D2	0.04	0.24	24.8	0.0	0.0	260.	4.4
n-Decane[b,c]	A10	0.46	2.77	14.	0.33	1.1	121.	4.0
1,2-Dichloroethane	J2	0.17	0.43	21.9	- 7.9	-1.6	107.	3.9
Diethylamine	N4	0.07	1.01	19.9	- 8.1	-3.6	24.7	2.1
Diethylketone	K6	0.05	0.32	23.8	- 3.8	5.3	317.	4.6
1,4-Dimethoxybenzene	E5	1.09	6.58	11.1	- 4.6	1.1	5.	0.78
Dimethylformamide	N7	0.51	3.08	16.0	-14.6	-3.3	123.	3.7
p-Dioxane[c]	F6	0.10	0.63	20.9	- 7.09	-5.1	119.	3.9
Ethanol	H2	0.18	1.08	21.3	-13.4	-7.4	46.	2.6
Ethyl acetate	L6	0.04	0.22	24.7	- 4.4	1.9	191.	4.3
Ethyl benzene	E4	0.20	1.2	18.0	1.2	3.2	134.	4.0
Ethyl cyanide	O3	0.11	0.68	22.5	-10.4	1.7	180.	3.9
Ethyl ether[c]	M1	0.02	0.09	28.2	- 1.72	2.6	160.	4.1
Ethyl formate	L9	0.05	0.32	24.3	- 7.4	-0.7	100.	3.5
Fluorobenzene	J12	0.11	0.64	20.5	- 1.9	3.2	70.	3.4
Furan	F1	0.07	0.4	23.65	- 2.8	0.15	45.	2.8
n-Heptane[b,c]	A7	0.04	0.4	22.1	0.2	1.0	165.	4.0
n-Hexane[b,c]	A6	0.02	0.24	25.1	0.4	1.2	200.	4.1

TABLE 10 (Continued)

Solvent:	Code:	$(t_g - t_a)^a$: (min)	V°_N: (cm^3/g)	$\Delta G:_{ads}$ (kJ/mol)	$\Delta G:_{add}$ (kJ/mol)	Λ: (kJ/mol)	Ω^∞: 12	χ^∞: 12
Isobutylamine	N14	0.09	0.55	22.2	- 5.8	-0.6	75.	3.1
Isooctane	B4	0.02	0.12	25.7	7.1	7.9	465.	5.3
Methanol	H1	0.22	1.33	21.8	-15.5	-9.5	38.	2.3
Methyl acetate	L5	0.07	0.39	23.3	- 8.5	-2.4	71.	3.3
3-Methyl-2-Butanone	K3	0.03	0.17	25.7	- 1.5	7.8	467.	5.1
Methylcyclohexane	D3	0.12	0.73	20.0	- 1.6	-0.8	99.	3.6
Methylene chloride	J1	0.1	0.61	21.5	-11.2	-5.6	30.	2.7
Methylethylketone	K4	0.06	0.37	23.4	- 6.5	2.7	140.	3.9
n-Nonane[b,c]	A9	0.28	1.68	16.1	- 0.3	0.5	115.	3.8
n-Octane[b,c]	A8	0.15	0.91	18.7	- 0.5	0.3	120.	3.9
n-Pentane[b,c]	A5	0.02	0.12	27.3	- 0.7	0.1	140.	3.8
Propanol	H3	0.06	0.37	24.1	- 7.9	-1.9	200.	4.1
2-Propanol	H4	0.02	0.12	27.9	- 4.0	2.0	335.	4.7
Propionic acid	G3	0.4	2.42	16.8	-15.1	-9.0	107.	3.6
Tetrahydrofuran[c]	F2	0.07	0.41	23.2	- 5.6	0.5	100.	3.5
Toluene	E2	0.10	0.80	19.7	0.4	2.5	110.	3.7
2,2,2-Trifluoroethanol	J18	0.03	0.19	24.7	-10.3	-3.3	1000.	7.0
m-Xylene	E3	0.21	1.25	17.9	0.8	2.51	140.	4.1

[a] The average of the four air elution times subtracted from the average of the three solvents elution times.
[b] Polarizability reference solvent.
[c] Dipole reference solvent.

Experiment Data: Date Performed = 6/11,12,13,14/79; Column Temperature = 145°C; Room Temperature = 25.7°C; Inlet Pressure = 1.91 psig; Room pressure = 29.815 in Hg; Column Helium Flow Rate = 1.47 cm^3/min.

TABLE 11

CURED PATS RESULTS AT 150°C (COLUMN C)

Solvent:	Code:	$[t_g - t_a]^a$: [min]	V_N°: [cm^3/g]	G_{ads}: [kJ/mol]	G_{add}: [kJ/mol]	Λ: [kJ/mol]	Ω_{12}^∞:	χ_{12}^∞:
Acetaldehyde	L1	---	---	---	---	---	---	---
Acetone	K1	---	---	---	---	---	---	---
Acetonitrile	O1	0.59	5.12	16.4	-17.7	-6.7	15.	1.5
Acrylonitrile	O2	---	---	---	---	---	---	---
Allyl alcohol	H11	---	---	---	---	---	---	---
Aniline	N2	1.14	11.	10.9	- 7.0	-1.5	55.	3.1
Benzene[b]	E1	0.12	1.04	20.1	0.0	0.0	50.	2.9
Bromobenzene	J11	---	---	---	---	---	---	---
1-Butanol	H5	---	---	---	---	---	---	---
Carbon tetrachloride	J5	---	---	---	---	---	---	---
Chlorobenzene	J10	---	---	---	---	---	---	---
1-Chlorobutane	J6	---	---	---	---	---	---	---
Chloroform	J4	---	---	---	---	---	---	---
Cyclohexane[b]	D2	0.04	0.36	23.3	0.0	0.0	118.	3.7
N-Decane[b,c]	A10	0.26	2.77	14.9	- 0.7	0.8	125.	4.0
1,2-Dichloroethane	J2	---	---	---	---	---	---	---
Diethylamine	N4	0.32	3.8	15.4	-12.0	- 7.7	6.0	0.7
Diethylketone	K6	---	---	---	---	---	---	---
1,4-Dimethoxybenzene	E5	0.98	9.78	9.9	- 4.4	1.1	3.2	0.3
Dimethylformamide	N7	1.63	16.21	10.4	-19.4	- 8.7	20.	1.9
p-Dioxane[c]	F6	0.12	1.03	19.4	- 6.6	- 4.6	65.	3.3
Ethanol	H2	---	---	---	---	---	---	---
Ethyl acetate	L6	---	---	---	---	---	---	---

TABLE 11 (Continued)

Solvent:	Code:	$[t_g - t_a]^a$: [min]	V_N°: [cm^3/g]	G_{ads}: [kJ/mol]	G_{add}: [kJ/mol]	: [kJ/mol]	Ω_{12}^∞:	χ_{12}^∞:
Ethyl benzene	E4	---	---	---	---	---	---	---
Ethyl cyanide	03	---	---	---	---	---	---	---
Ethyl ether[c]	M1	0.04	0.35	24.8	- 5.3	-1.1	40.	2.6
Ethyl formate	L9	---	---	---	---	---	---	---
Fluorobenzene	J12	---	---	---	---	---	---	---
Furan[c]	F1	---	---	---	---	---	---	---
n-Heptane[b,c]	A7	0.04	0.37	22.6	0.43	1.27	150.	4.0
n-Hexane[b,c]	A6	---	---	---	---	---	---	---
Isobutylamine	N14	---	---	---	---	---	---	---
Isooctane	B4	---	---	---	---	---	---	---
Methanol	H1	0.32	2.80	19.45	-16.2	-10.4	15.	1.4
Methyl acetate	L5	---	---	---	---	---	---	---
3-Methyl-2-Butanone	K3	---	---	---	---	---	---	---
Methylcyclohexane	D3	---	---	---	---	---	---	---
Methylene chloride	J1	---	---	---	---	---	---	---
Methylethylketone	K4	---	---	---	---	---	---	---
n-Nonane[b,c]	A9	0.13	1.1	17.9	0.5	1.4	160.	4.2
n-Octane[b,c]	A8	0.11	0.96	18.9	- 0.9	-0.04	110.	3.7
n-Pentane[b,c]	A5	0.02	0.13	27.4	- 0.02	0.82	120.	3.6
Propanol	H3	---	---	---	---	---	---	---
2-Propanol	H4	---	---	---	---	---	---	---
Propionic acid	G3	0.31	2.65	16.7	-14.2	- 8.3	80.	3.4
Tetrahydrofuran[c]	F2	0.07	0.8	21.1	- 5.7	0.2	41.	2.7
Toluene	E2	---	---	---	---	---	---	---
2,2,2-Trifluoroethanol	J18	---	---	---	---	---	---	---
m-Xylene	E3	---	---	---	---	---	---	---

[a]The average of the four air elution times subtracted from the average of the three solvent elution times.

[b]Polarizability reference solvent. [c]Dipole reference solvent.

Experiment Data: Date Performed = 6/28/79; Column Temperature = 150.8°C; Room Temperature = 26°C; Inlet Pressure = 0.38 psig; Room Pressure = 29.761 in Hg; Column Flow Rate = 2.0 cm^3/min.

TABLE 12

PATS POLARIZABILITY AND DIPOLE REFERENCE LINE PARAMETERS

Date: Column:	Polarizability Reference Line Slope: [All] [$X10^{-24}$ kJ-cm^3/mol]	Intercepts: [Aliphatic]: [kJ/mol]	[Aromatic]: [kJ/mol]	[Cyclic]: [kJ/mol]	Dipole Reference Line: Slope: [kJ-D/mol]	Intercept: [kJ/mol]
T = 70°C:						
4/6 B-PATS	-1.32±0.08	25.8±0.9	24.5	25.2	-1.53±0.23	0.22±0.21
4/19 B-PATS	-1.41±0.07	26.4±0.9	25.0	25.7	-1.01±0.16	-0.03±0.15
5/7 C-PATS	-1.54±0.09	28.5±1.0	26.7	27.6	-1.92±0.23	0.37±0.19
T = 100°C:						
5/9-11 C-PATS	-1.14±0.10	28.5±1.2	25.9	26.3	-0.16±0.28	0.07±0.18
T = 116°C:						
6/2-5 C-PATS	-1.49±0.11	36.0±1.5	33.9	34.7	-1.92±0.54	-0.44±0.4
T = 150°C:						
6/11-14 C-PATS	-1.47±0.13	42.0±2.0	37.6	40.6	-3.06±0.85	-0.81±0.62
6/28[a] C-PATS	-1.28±0.11	39.8±1.8	33.4	37.0	-2.89±0.80	-0.84±0.59

[a]After cure at 240°C for 24 hrs.

TABLE 13

CHRONOLOGY OF POLARIZABILITY AND DIPOLE REFERENCE

LINE PARAMETERS FOR PATS AT 40°C

		Aliphatic Polarizability Line:		Dipole Line:	
Date:	Column:	Slope: [X10^{-24}kJ-cm^3/mol]	Intercept[a]: [kJ/mol]	Slope: [kJ-D/mol]	Intercept: [kJ/mol]
Initial:					
4/5	B-PATS	-1.66±0.04	25.1±0.5	-2.04±0.08	0.0±0.05
After 70°C Trial:					
4/13	B-PATS	-1.65±0.06	25.1±0.7	-1.88±0.14	0.0±0.08
After 2nd 70°C Trial:					
4/23	B-PATS	-1.69±0.05	25.8±0.6	-1.89±0.11	0.02±0.07
Initial:					
4/25	C-PATS	-1.62±0.06	25.1±0.7	01.78±0.13	0.02±0.08
After 70°C Trial:					
5/8	C-PATS	-1.49±0.01	23.3±0.7	-1.36±0.16	0.08±0.11
After 100°C Trial:					
5/24	C-PATS	-1.56±0.03	25.5±0.4	-1.47±0.10	0.02±0.06
After 116°C Trial:					
6/7	C-PATS	-1.51±0.06	24.6±0.6	-1.39±0.11	0.0±0.07
After 145°C Trial:					
6/15	C-PATS	-1.45±0.04	24.4±0.5	-1.63±0.1	0.0±0.07
After 200°C Curing:					
7/2	C-PATS	-1.48±0.05	23.6±0.6	-2.13±0.14	0.0±0.08

[a] Aromatic and cyclic reference lines are parallel to the aliphatic line by definition. Their intercepts differed by as much as 6%.

TABLE 14

RANKED SPECIFIC INTERACTION PARAMETERS FOR UNCURED PATS AT 70, 100 AND 117°C

T = 70°C Solvent:	Λ^a: [kJ/cm^3]	T = 100°C Solvent:	Λ^a: [kJ/cm^3]	T = 117°C Solvent:	Λ^a: [kJ/cm^3]
Column B-PATS[b]		Column C-PATS		Column C-PATS	
Methanol	-0.316	Methanol	-0.291	Methanol	-0.291
Acetaldehyde	-0.087	Acetonitrile	-0.196	Ethanol	-0.140
Isobutylamine	-0.063	Ethanol	-0.136	Acetonitrile	-0.125
Methylene chloride	-0.060	Acetaldehyde	-0.132	Propionic acid	-0.111
Diethylamine	-0.055	Acrylonitrile	-0.10	Carbon tetrachloride	-0.085
Chloroform	-0.045	Allyl alcohol	-0.081	Ally alcohol	-0.084
Methyl acetate	-0.030	Methylene chloride	-0.081	Acetaldehyde	-0.081
Ethyl formate	-0.024	Ethyl cyanide	-0.078	Methylene chloride	-0.081
		Diethylamine	-0.077	Chloroform	-0.050
Column C-PATS[c]		222 Trifluoroethanol	-0.076	Diethylamine	-0.042
Methanol	-0.326	Isobutylamine	-0.070	1,4-Dioxane	-0.042
Acetaldehyde	-0.090	Carbon tetrachloride	-0.069	Isobutylamine	-0.040
Methylene chloride	-0.065	1,2 Dichloroethane	-0.055	Acrylanitrile	-0.038
Isobutylamine	-0.045	Chloroform	-0.050	Methyl acetate	-0.038
Chloroform	-0.044	Acetone	-0.049	222 Trifluoroethanol	-0.036
Diethylamine	-0.041	Methyl acetate	-0.049	Propanol	-0.032
Methyl acetate	-0.030	Propanol	-0.048	1,2 Dichloroethane	-0.029
Ethyl formate	-0.024	Ethyl formate	-0.041	Ethyl formate	-0.025
		2-Propanol	-0.038	Ethyl cyanide	-0.017

[a]Average value from the three injections for each solvent.

[b]Column flow rate = 1.90 cm^3/min.

[c]Column flow rate = 1.98 cm^3/min.

TABLE 15

SPECIFIC INTERACTION PARAMETERS FOR PATS AT 145°C

AND 25°C BEAKER TEST RESULTS

Solvent	$[kJ/cm^3]$	Dissolving Rate: Fast[a]	Slow[b]	None	Comments
Methanol	-0.235			x	d
Ethanol	-0.126			x	d
Propionic acid	-0.121			x	d
Carbon tetrachloride	-0.0927			x	e
Methylene chloride	-0.0868	x			
Acetaldehyde	-0.0655	x			
Allyl alcohol	-0.0632		x		
Acetonitrile	-0.0627	x			
1,4-Dioxane	-0.0597	x			
2,2,2-Trifluoroethanol	-0.0455			x	d
N,N-Dimethylformamide	-0.0426	x			c
Diethylamine	-0.0348		x		
Methyl acetate	-0.0302	x			
Chloroform	-0.0275	x			
Propanol	-0.0255			x	e
1,2-Dichloroethane	-0.0202	x			
Ethyl formate	-0.009	x			
Isobutylamine	-0.006			x	
Benzene	0.0		x		
Cyclohexane	0.0			x	e
Pentane	0.001			x	e
Furan	0.002		x		
Tetrahydrofuran	0.006			x	e
1,4-Dimethoxybenzene	0.008	x			
Aniline	0.011	x			
m-Xylene	0.0204			x	e
Acrylonitrile	0.0243	x			
m-Bromobenzene	0.0247	x			
Ethyl ether	0.0250			x	e
Ethyl benzene	0.0261			x	d
Isopropanol	0.0262			x	e
Acetone	0.0354	x			
Diethylketone	0.0500	x			

[a] Needed mixing at most.

[b] Dissolved after few hours or days.

[c] Dissolved without mixing. Almost instantaneous.

[d] Some swelling suspected due to stringy appearance of solids.

[e] No interaction. Solids had powder appearance.

TABLE 16

SPECIFIC INTERACTION PARAMETERS FOR CURED PATS AT 150°C

Solvent[a]:	Λ^b: (kJ/cm^3)
Methanol	-0.257
Acetonitrile	-0.127
N,N Dimethylformamide	-0.112
Propionic acid	-0.111
Diethylamine	-0.074
1,4 Dioxane	-0.054

[a]Only reference solvents and solvents with long elution times were injected.

[b]Average value from the three injections for each solvent.

TABLE 17

PARTIAL PRESSURE OF DICHLOROMETHANE AS A FUNCTION OF CONCENTRATION IN POLYSULFONE SOLUTION

40°C		60°C	
Partial Pressure[a]: (kPa)	Concentration[b]: $\left[\frac{cm^3\ (STP)}{cm^3\ polymer}\right]$	Partial Pressure[a]: (kPa)	Concentration[b]: $\left[\frac{cm^3\ (STP)}{cm^3\ polymer}\right]$
0.66	4.34	1.68	4.09
0.69	4.44	1.87	4.62
0.95	6.42	2.05	5.16
1.01	6.80	2.93	6.33
1.64	8.53	3.49	7.81
1.66	8.78	4.56	9.25
2.64	10.51	6.03	10.31
2.82	11.01	7.54	12.56
3.88	13.36	9.23	13.89
5.58	16.19	14.99	19.68
6.99	18.89	19.25	23.77
10.08	24.58	20.60	25.27
15.18	34.08	22.30	26.70
19.70	42.18	26.23	30.41
24.46	52.01	30.23	33.93
26.44	55.50	31.90	35.79
30.61	63.00	37.09	40.36
		47.83	51.53

[a] The error involved in determining P_1 is less than 1% due to temperature fluctuations of ±0.1°C of ethanol bath and the water bath.

[b] The error involved in determining C is about 3% at lower pressure due to frequency fluctuations of ±1 Hz, while at higher perssure the error is about 1% due to frequency fluctuations of ±5 Hz.

TABLE 18

DUAL SORPTION PARAMETERS[a] FOR DICHLOROMETHANE IN POLYSUFONE

T: (°C)	k_D: $\left[\frac{cm^3\ (STP)\ solvent}{cm^3\ polymer\ \ Pa}\right]$	C_H': $\left[\frac{cm^3\ (STP)\ solvent}{cm^3\ polymer}\right]$	b: (Pa^{-1})
40	$1.84 \times 10^{-3} \pm 1.83 \times 10^{-5}$	6.68 ± 0.40	$2.01 \times 10^{-3} \pm 4.76 \times 10^{-4}$
60	$9.34 \times 10^{-4} \pm 1.26 \times 10^{-5}$	6.48 ± 0.47	$4.91 \times 10^{-4} \pm 9.57 \times 10^{-5}$

[a]Error in the estimated parameter is the standard error.

TABLE 19

DICHLOROMETHANE-POLYSULFONE EXPERIMENTAL SORPTION RESULTS AT 40°C

Solvent[a] Weight Fraction:	Solvent Activity:	Predicted[b] Activity:	χ_{12}[c]:
0.0037	0.0067	0.0067	-0.181
0.0038	0.0069	0.0070	-0.181
0.0053	0.0096	0.0097	-0.179
0.0056	0.0103	0.0103	-0.179
0.0090	0.0166	0.0167	-0.175
0.0091	0.0167	0.0168	-0.174
0.0144	0.0266	0.0267	-0.168
0.0154	0.0284	0.0286	-0.166
0.0211	0.0391	0.0392	-0.158
0.0300	0.0562	0.0564	-0.146
0.0373	0.0704	0.0705	-0.135
0.0529	0.1014	0.1013	-0.110
0.0776	0.1525	0.1516	-0.069
0.0985	0.1976	0.1956	-0.030
0.1194	0.2450	0.2413	0.013
0.1279	0.2647	0.2602	0.031
0.1451	0.3060	0.2991	0.072

[a] Weight fraction of dichloromethane in the liquid-like phase of polysulfone.

[b] Activity of dichloromethane in polysulfone solution predicted by the Cheng and Bonner corresponding states theory (Chapter II, eq. 30).

[c] The error involved in χ_{12} is about 5% due to solvent weight fraction uncertainties of about 1% and activity uncertainties of less than 1%.

TABLE 20

DICHLOROMETHANE-POLYSULFONE EXPERIMENTAL SORPTION RESULTS AT 60°C.

Solvent[a] Weight Fraction:	Solvent[b] Activity:	Predicted Activity:	χ_{12}[c]:
0.0047	0.0088	0.0089	-0.161
0.0053	0.0098	0.0099	-0.161
0.0058	0.0108	0.0108	-0.160
0.0082	0.0154	0.0155	-0.157
0.0098	0.0184	0.0185	-0.155
0.0128	0.0240	0.0241	-0.151
0.0168	0.0317	0.0319	-0.145
0.0210	0.0396	0.0399	-0.140
0.0256	0.0485	0.0487	-0.133
0.0408	0.0787	0.0787	-0.110
0.0518	0.1009	0.1008	-0.093
0.0553	0.1080	0.1077	-0.088
0.0596	0.1169	0.1164	-0.081
0.0693	0.1373	0.1365	-0.064
0.0791	0.1581	0.1568	-0.047
0.0831	0.1668	0.1652	-0.040
0.0953	0.1937	0.1912	-0.017
0.1196	0.2493	0.2444	0.033

[a] Weight fraction dichloromethane in the liquid-like phase of polysulfone.

[b] Activity of dichloromethane in polysulfone solution predicted by the Cheng and Bonner corresponding states theory (Chapter II, eq. 30).

[c] The error involved in χ_{12} is about 5% due to solvent weight fraction uncertainties of about 1% and activity uncertainties of less than 1%.

TABLE 21

DICHLOROMETHANE-REACTIVE PLASTICIZER EXPERIMENTAL SORPTION RESULTS

40°C				60°C			
Solvent Weight Fraction:	Solvent Activity:	Predicted Activity:	χ_{13} [a]:	Solvent Weight Fraction:	Solvent Activity:	Predicted Activity:	χ_{13} [a]:
0.0139	0.0342	0.0310	0.312	0.0097	0.0227	0.0197	0.257
0.0274	0.0664	0.0622	0.317	0.0147	0.0332	0.0300	0.231
0.0396	0.0955	0.9164	0.313	0.0233	0.0500	0.0482	0.182
0.0510	0.1211	0.1203	0.300	0.0346	0.0747	0.0729	0.201
0.0675	0.0155	0.1623	0.289	0.0432	0.0919	0.0925	0.189
0.0772	0.1751	0.1863	0.288	0.0517	0.1070	0.1125	0.165
0.0882	0.1974	0.2146	0.308	0.0603	0.1257	0.1333	0.182
				0.0702	0.1444	0.1561	0.169
				0.0757	0.1581	0.1691	0.194

[a] Estimated error in χ_{13} is about 15% due to weight fraction uncertainties of less than 3% and activity uncertainties of less than 1%.

TABLE 22

PURE-COMPONENT CHARACTERISTIC PARAMETERS

Component:	ν^*: (cm^3/gm)	P*: (GPa)	T*: (K)	Range: (K)
Dichloromethane	0.5602	0.593	3792.6	273.15 - 313.15
Polysulfone	0.6827	0.680	7972.8	273.15 - 373.15
Reactive Plasticizer (ATS)	0.7243	1.070	14925.0	298.15 - 378.15

TABLE 23

INTERACTION PARAMETERS DETERMINED FROM CORRESPONDING STATES THEORY

System	$P_{ij}^{*} \times 10^{-5}$: (kPa)		Δ:		$X_{ij} \times 10^{-4}$: (kPa)	
	40°C	60°C	40°C	60°C	40°C	60°C
DCM-PSF	6.6860	6.7140	-0.0533	-0.0573	-6.4546	-7.0168
DCM-ATS	8.8826	8.9603	-0.1127	-0.1124	-10.8821	-12.4358

TABLE 24

SPECIFIC RETENTION VOLUMES OF DICHLOROMETHANE IN POLYSULFONE

Temp: (°C)	V_g° [a] : (cm^3/gm polym)
100.5	16.94
105.5	14.24
110.3	12.31

[a] The error in V_g° values is about 2%.

TABLE 25

COMPARISON OF GC AND PIEZOELECTRIC SORPTION RESULTS

FOR POLYSULFONE-DICHLOROMETHANE

Temp (°C)	V_g°: (cm^3/gm polym)	K: $\left[\frac{\text{gm solvent}}{(\text{kPa})(\text{gm polym})}\right]$	k_d: $\left[\frac{\text{gm solvent}}{(\text{kPa})(\text{gm polym})}\right]$	$\left(\frac{K-k_d}{K}\right)$x100:
40	167.18	5.68×10^{-3}	6.19×10^{-3}	8.24
60	71.54	2.73×10^{-3}	2.63×10^{-3}	3.66

TABLE 26

DICHLOROMETHANE-POLYSULFONE-REACTIVE PLASTICIZER EXPERIMENTAL SORPTION RESULTS

40°C				60°C			
Solvent Weight Fraction:	Solvent Activity:	Predicted Activity:	χ_{23}^{+} [a]:	Solvent Weight Fraction:	Solvent Activity:	Predicted Activity:	χ_{23}^{+} [a]:
0.0262	0.0432	0.0529	-3.75	0.0145	0.0280	0.0305	-4.57
0.0383	0.0704	0.0760	-4.31	0.0211	0.0422	0.0439	-4.76
0.0472	0.0947	0.0926	-4.77	0.0250	0.0488	0.0517	-4.67
0.0617	0.1256	0.1187	-4.88	0.0306	0.0614	0.0629	-4.82
0.0743	0.1544	0.1406	-5.03	0.0445	0.0879	0.0897	-4.79
0.0873	0.1866	0.1623	-5.21	0.0559	0.1166	0.1110	-5.10
0.0930	0.2027	0.1717	-5.34	0.0573	0.1214	0.1136	-5.19
				0.0658	0.1414	0.1290	-5.29
				0.0750	0.1599	0.1452	-5.29

[a] A rough estimate of the error involved in χ_{23}^{+} suggests that the error is less than 10% due to solvent weight fraction uncertainties of 3%, activity uncertainties of less than 1%, and the error involved in χ_{12} and χ_{13} parameters.

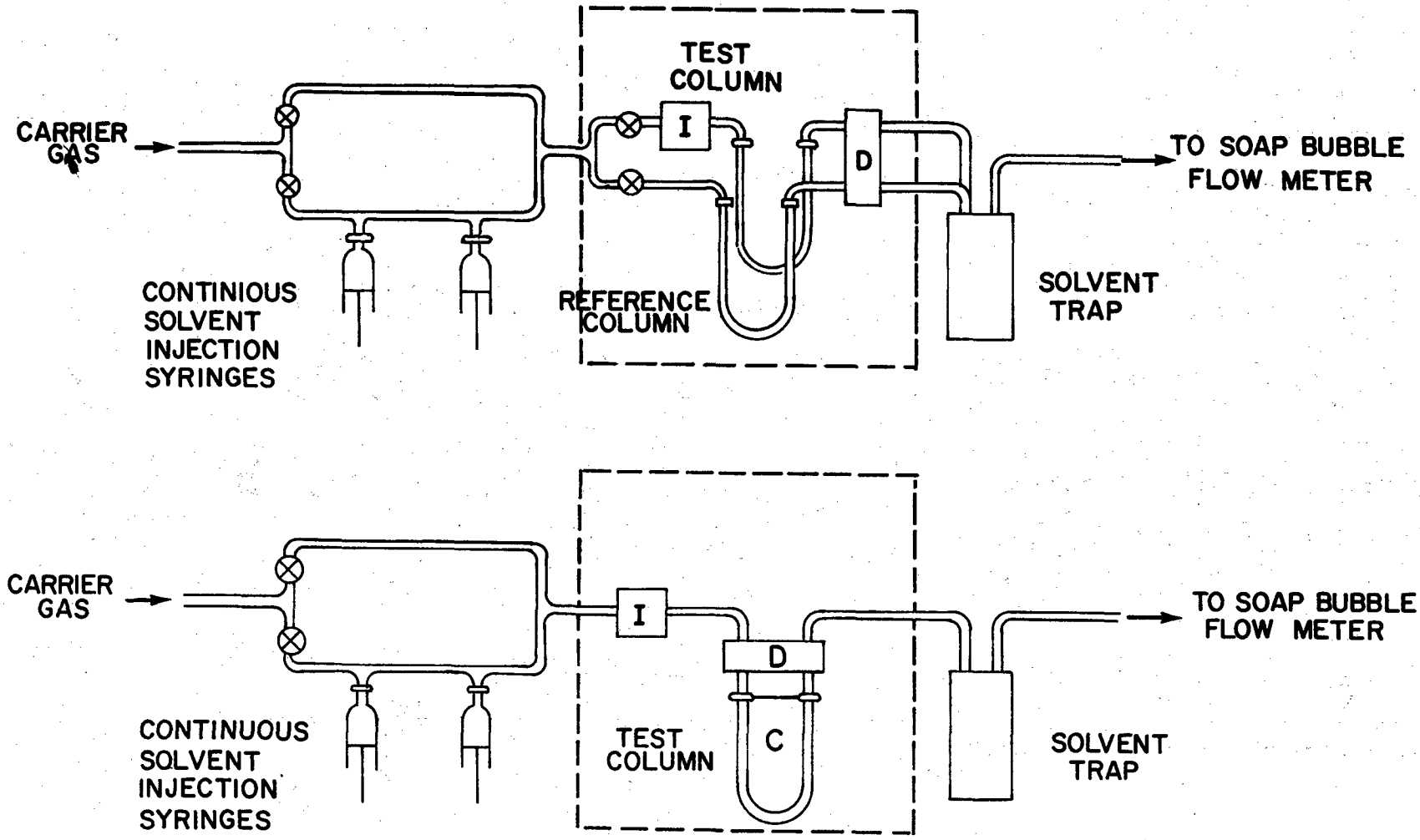

Figure I. Gas Chromatography Apparatus

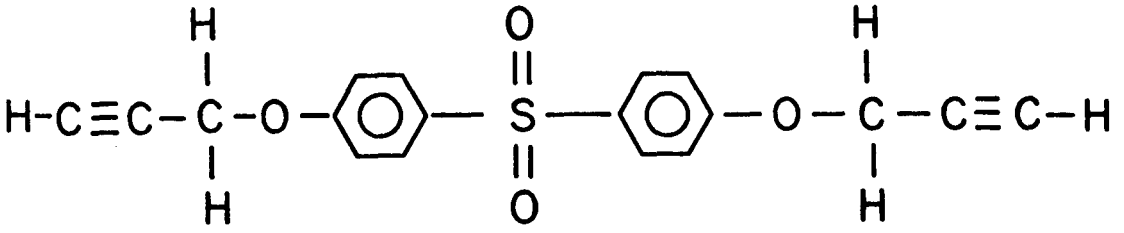

PATS

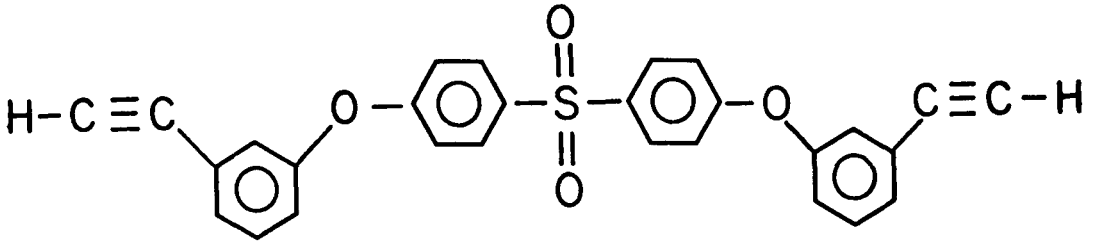

ATS

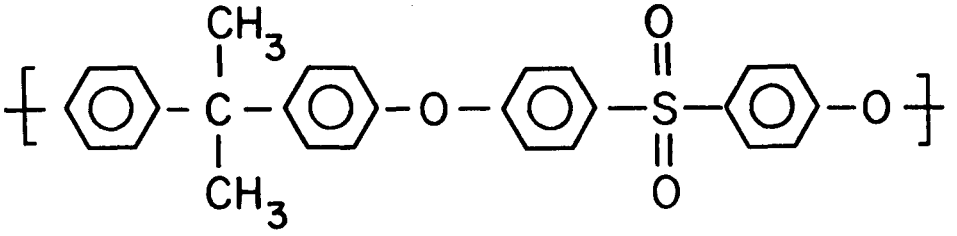

P1700

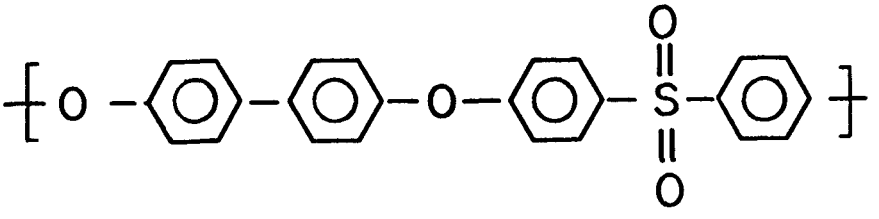

RADEL

Figure 2. Sulfone Structures

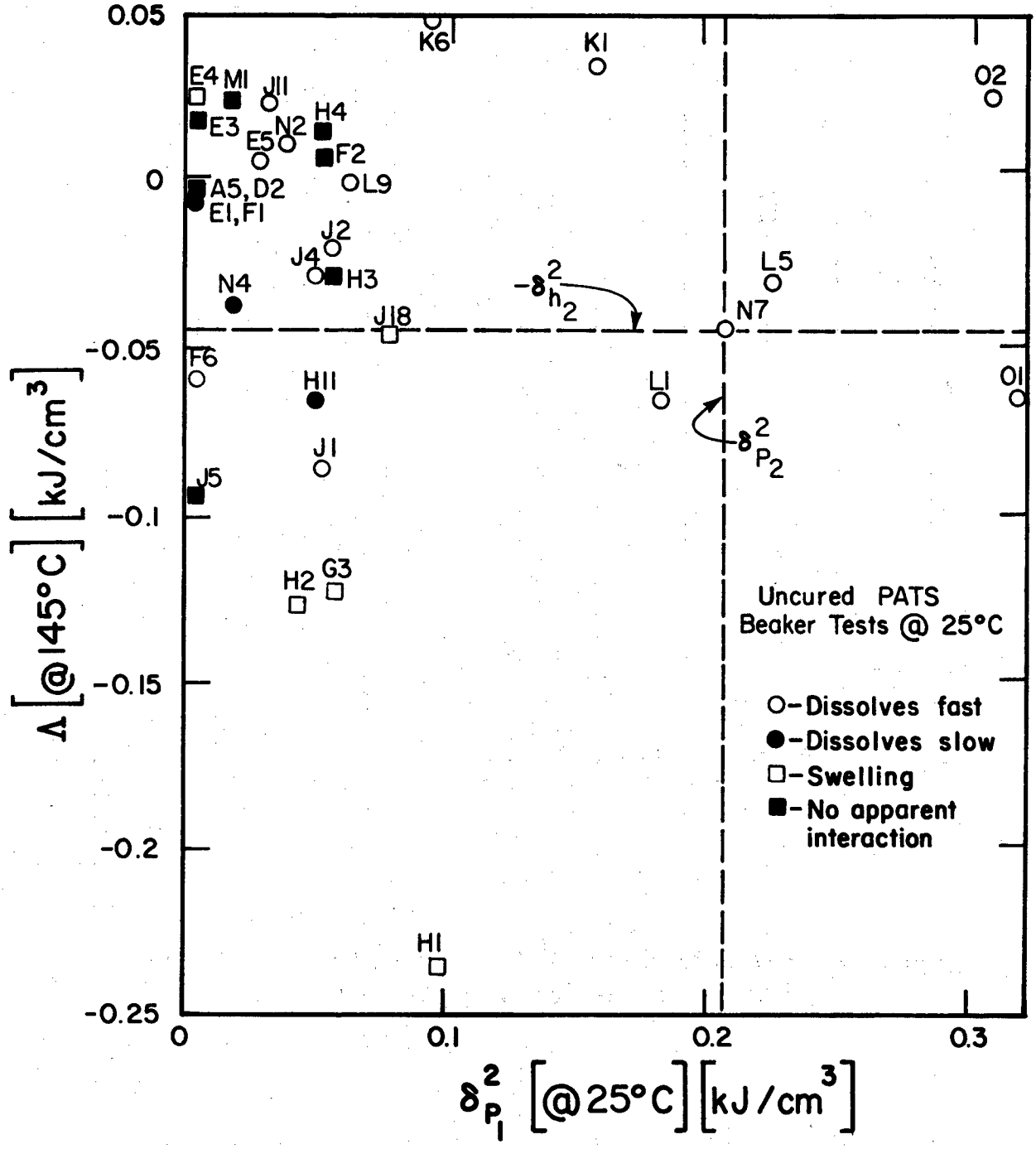

Figure 3. Uncured PATS Solubility Plot (145°C).

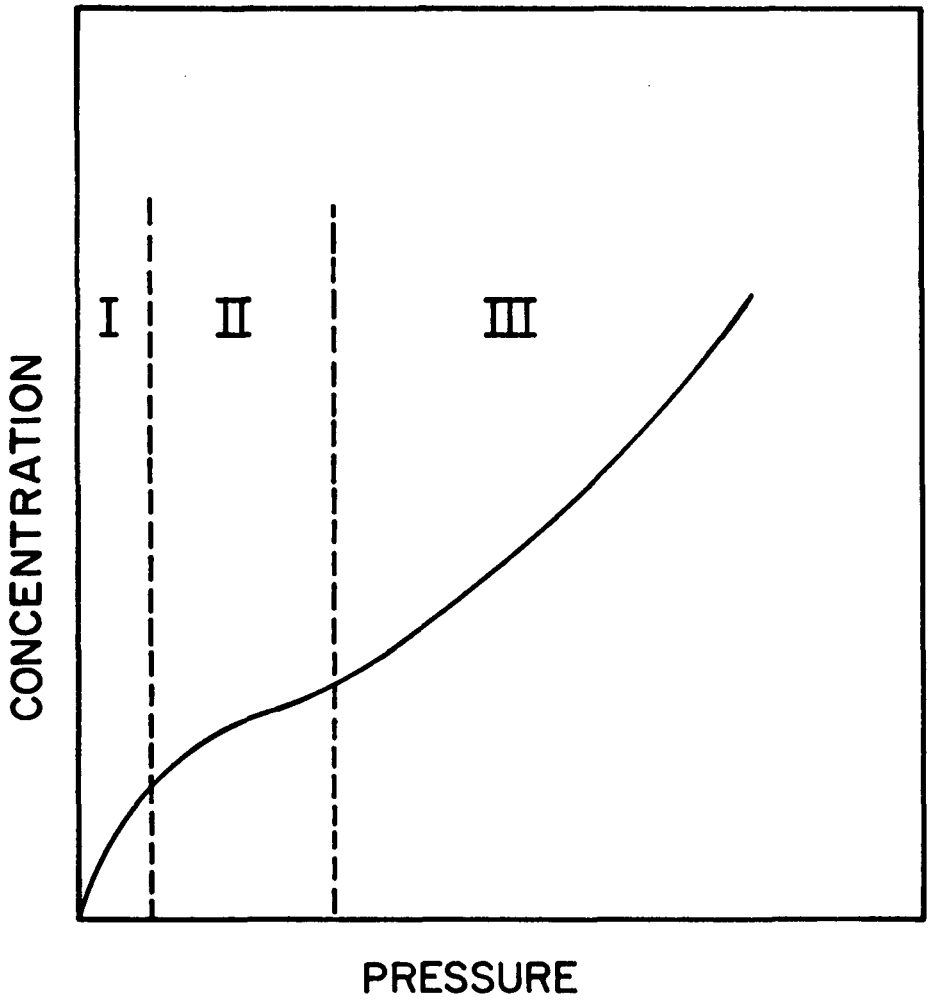

Figure 4. Pressure Dependence of Vinyl Chloride Monomer Concentration for Sorption in Glassy PVC.

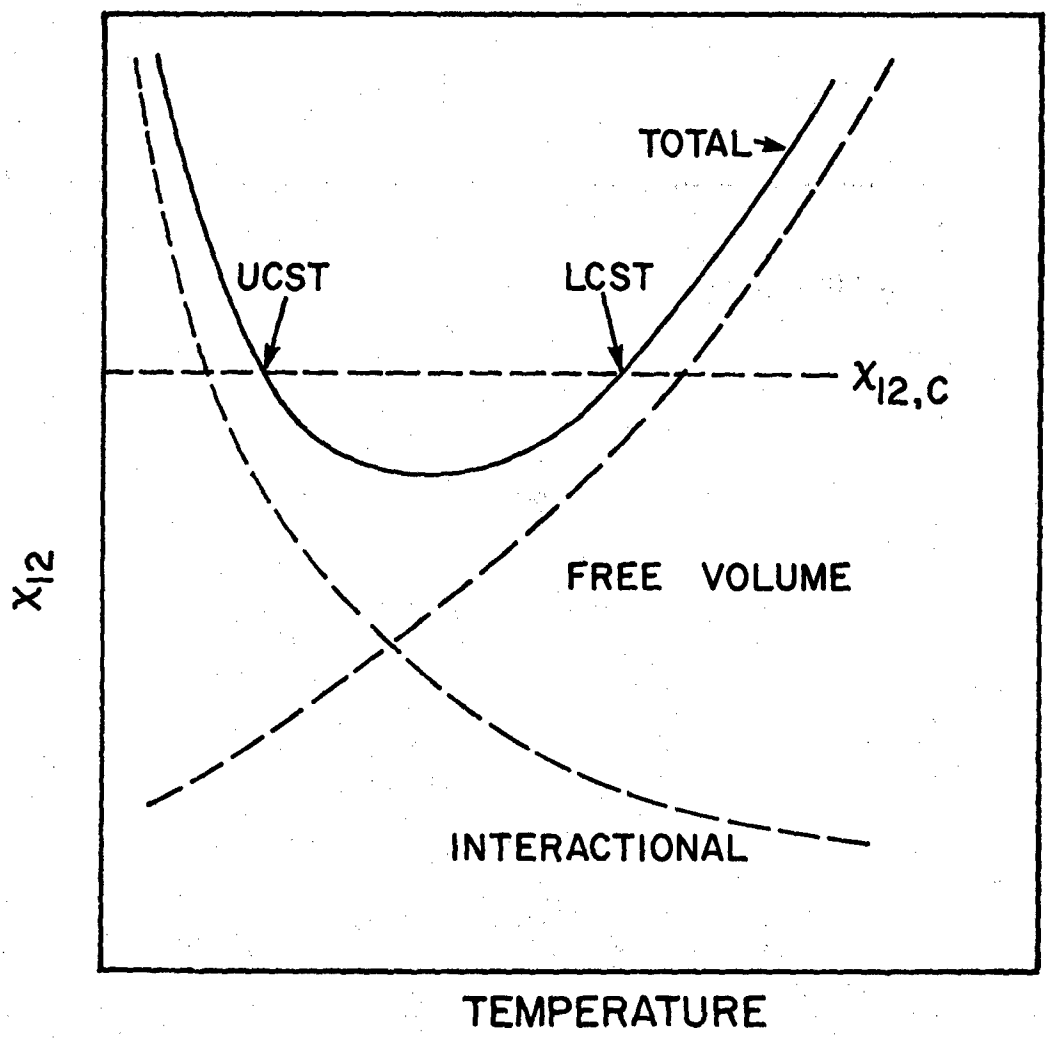

Figure 5. Temperature Dependence of the Flory–Huggins Interaction Parameters (After Patterson[47]).

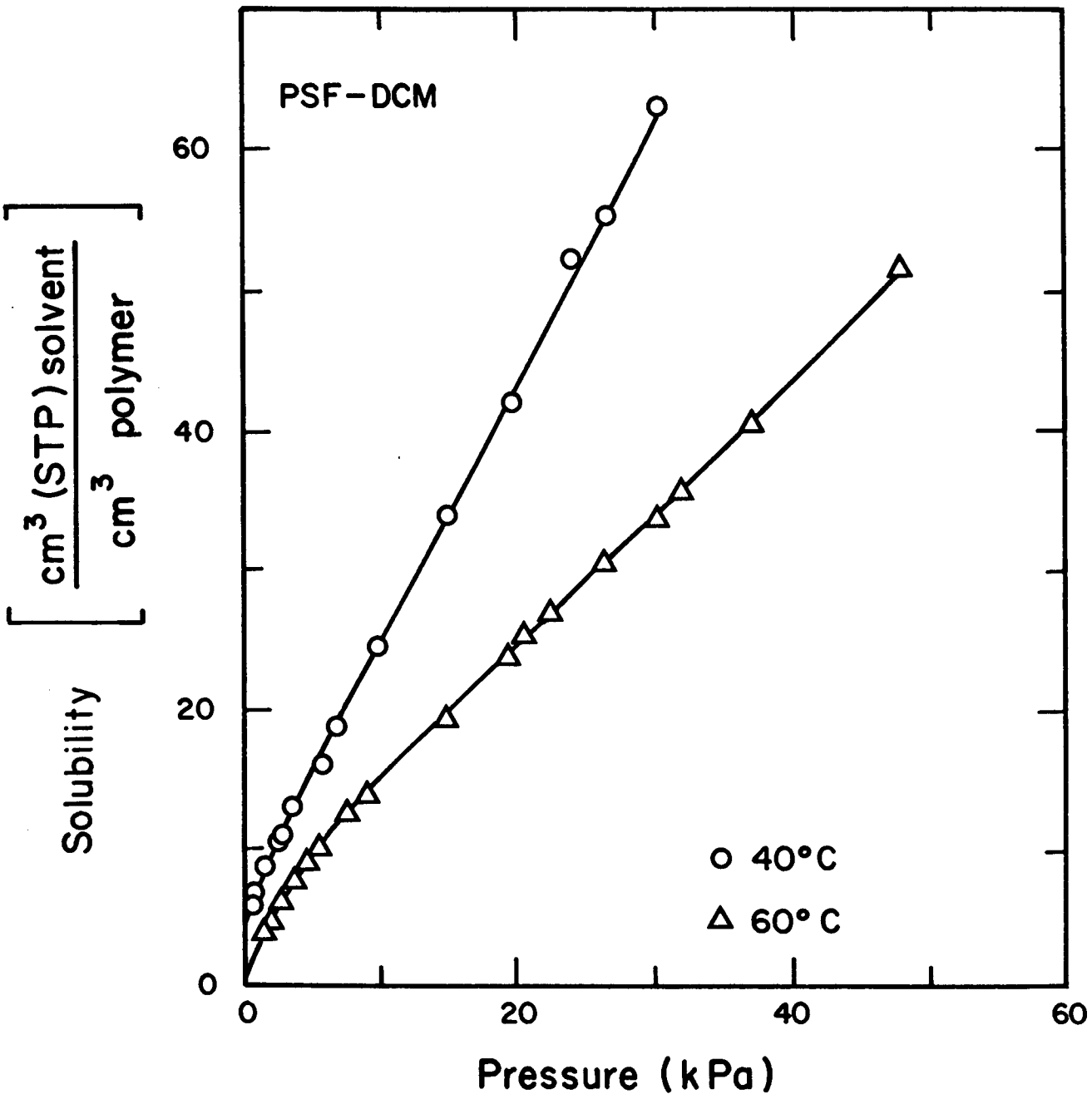

Figure 6. Solubility of Dichloromethane in Polysulfone.

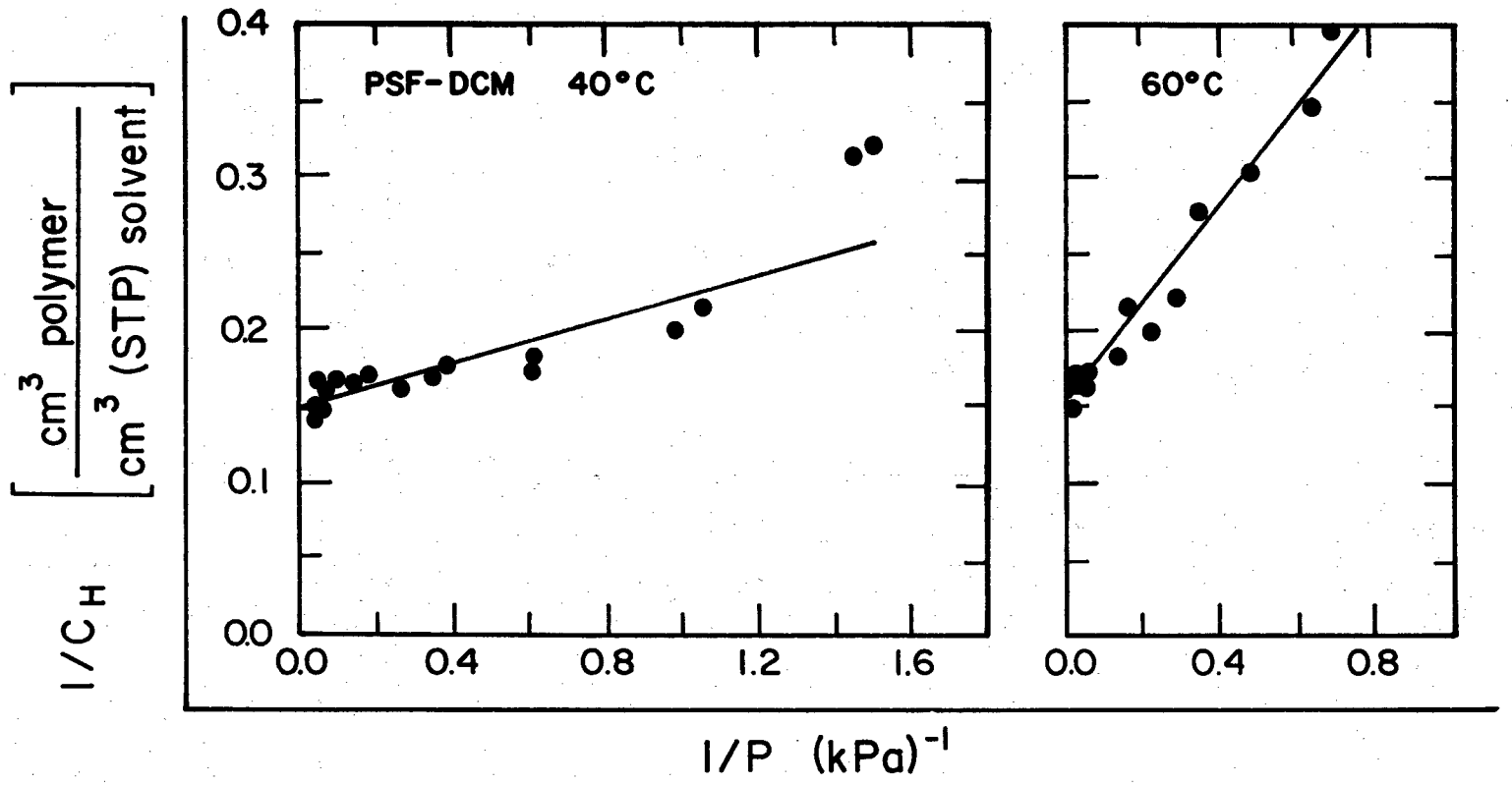

Figure 7. Test of Applicability of the Langmuir Equation for Describing Sorption Data.

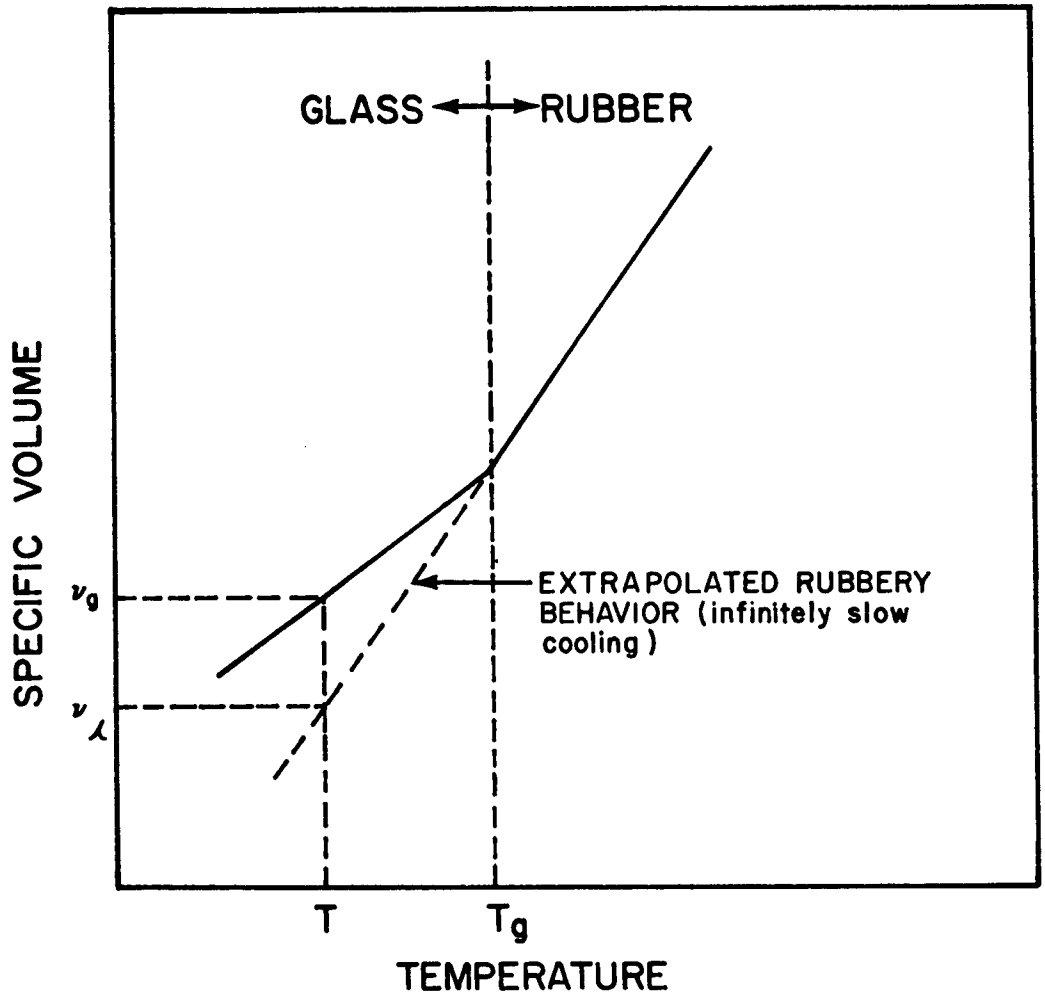

Figure 8. Temperature Dependence of the Specific Volume of an Amorphous Polymer.

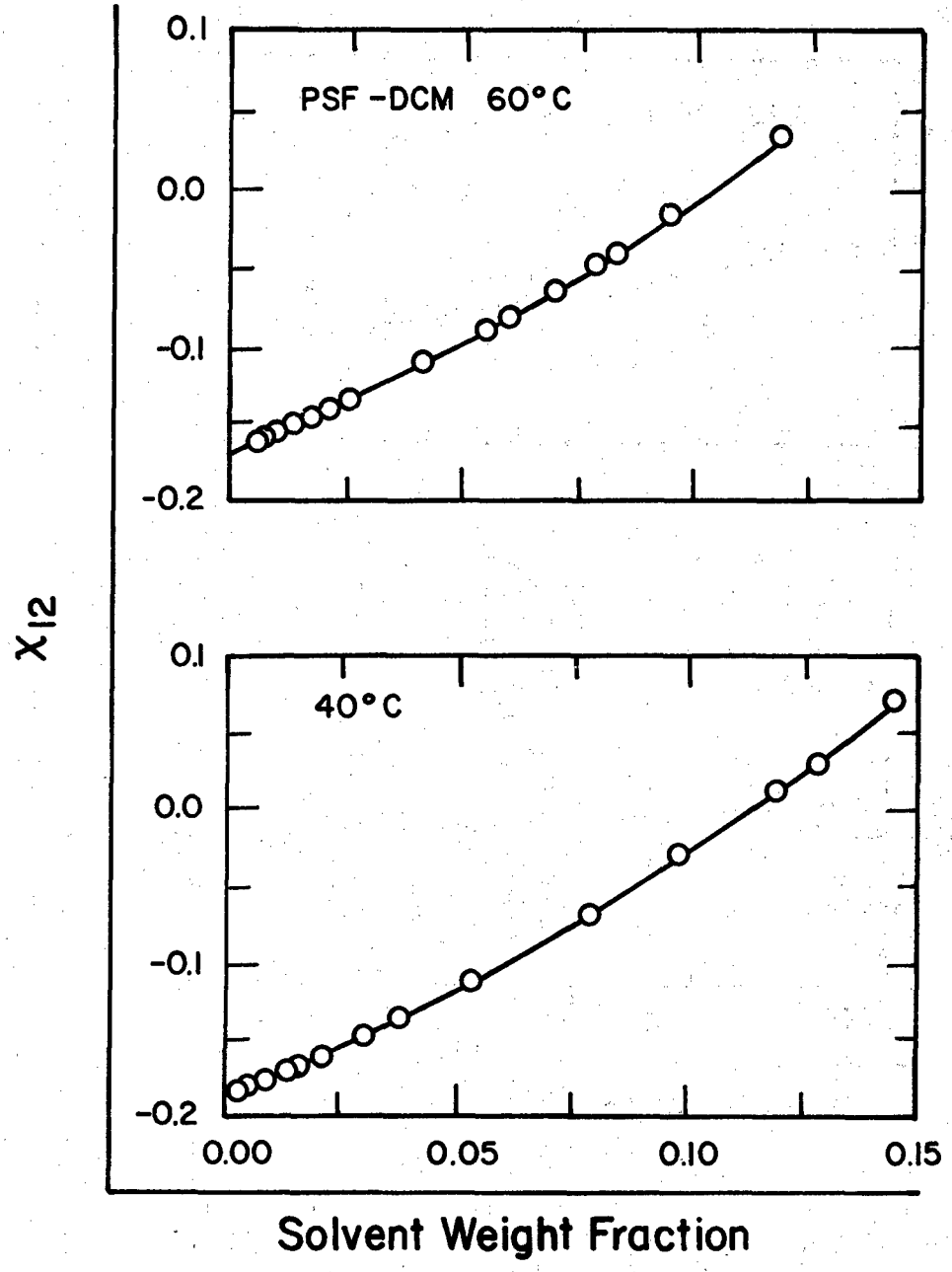

Figure 9. Flory- Huggins Interaction Parameter for Polysulfone – Dichloromethane.

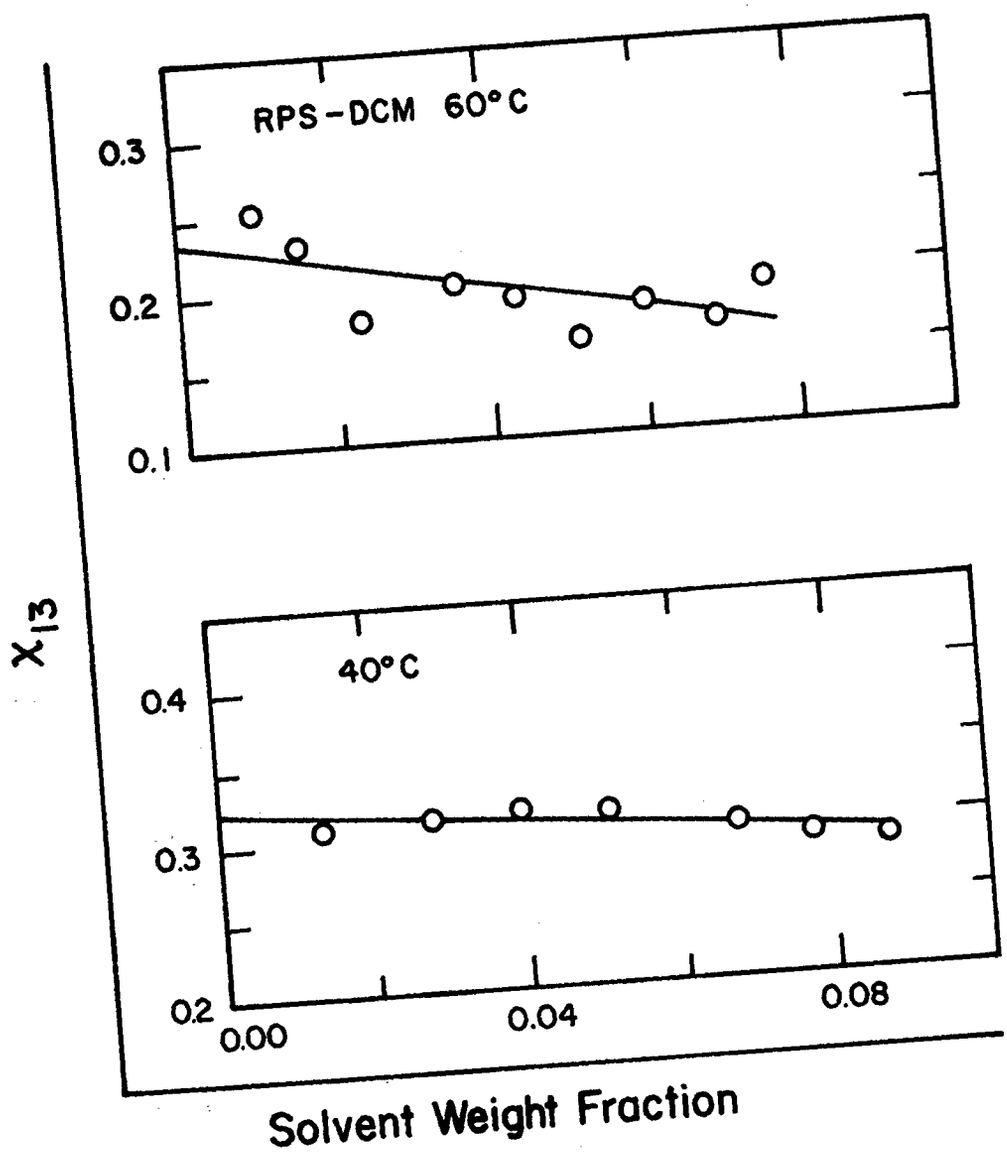

Figure 10. Flory-Huggins Interaction Parameter for Reactive Plasticizer - Dichloromethane.

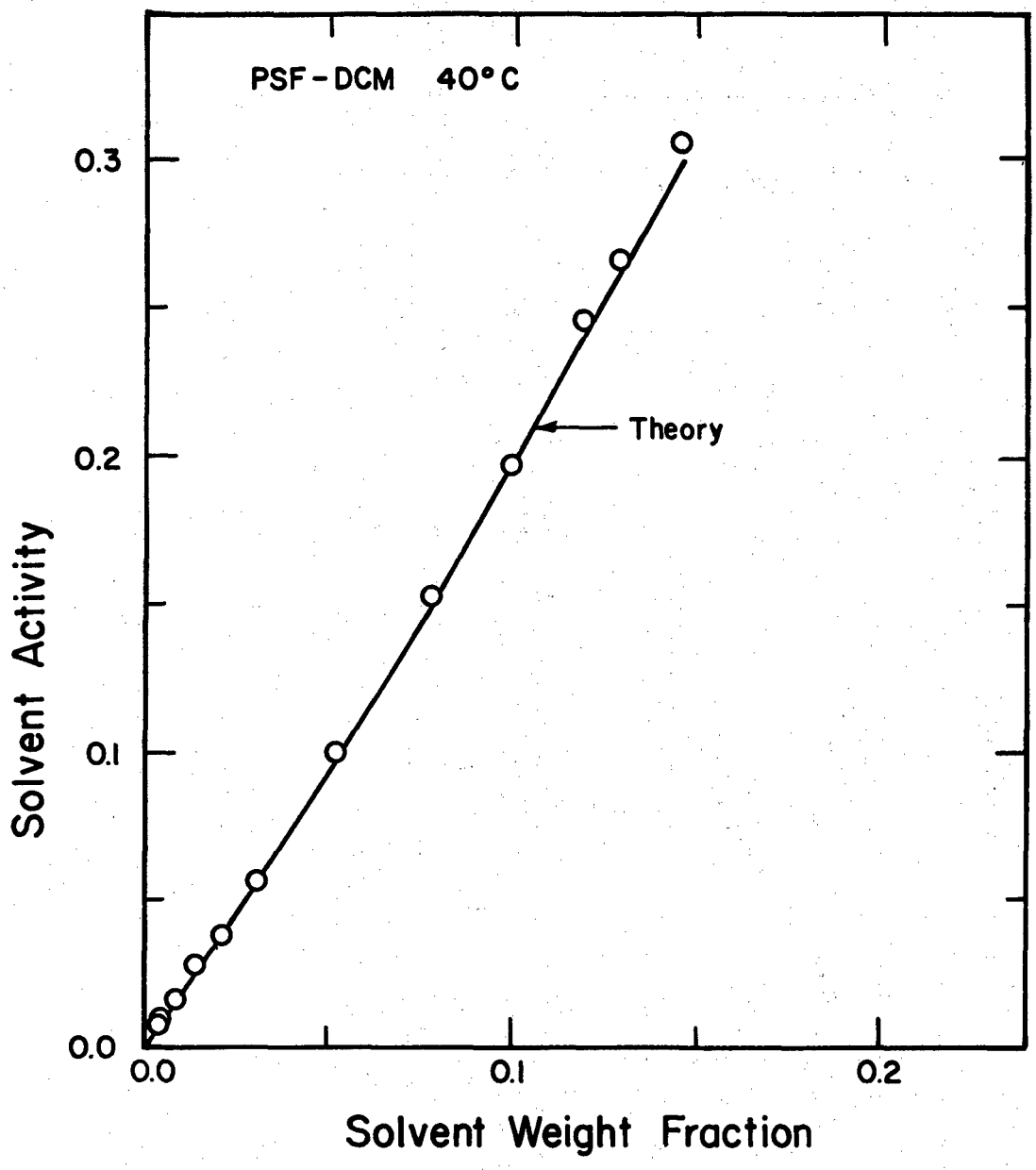

Figure II. Activity of Dichloromethane (Corrected for Langmuir Term) in Polysulfone at 40°C.

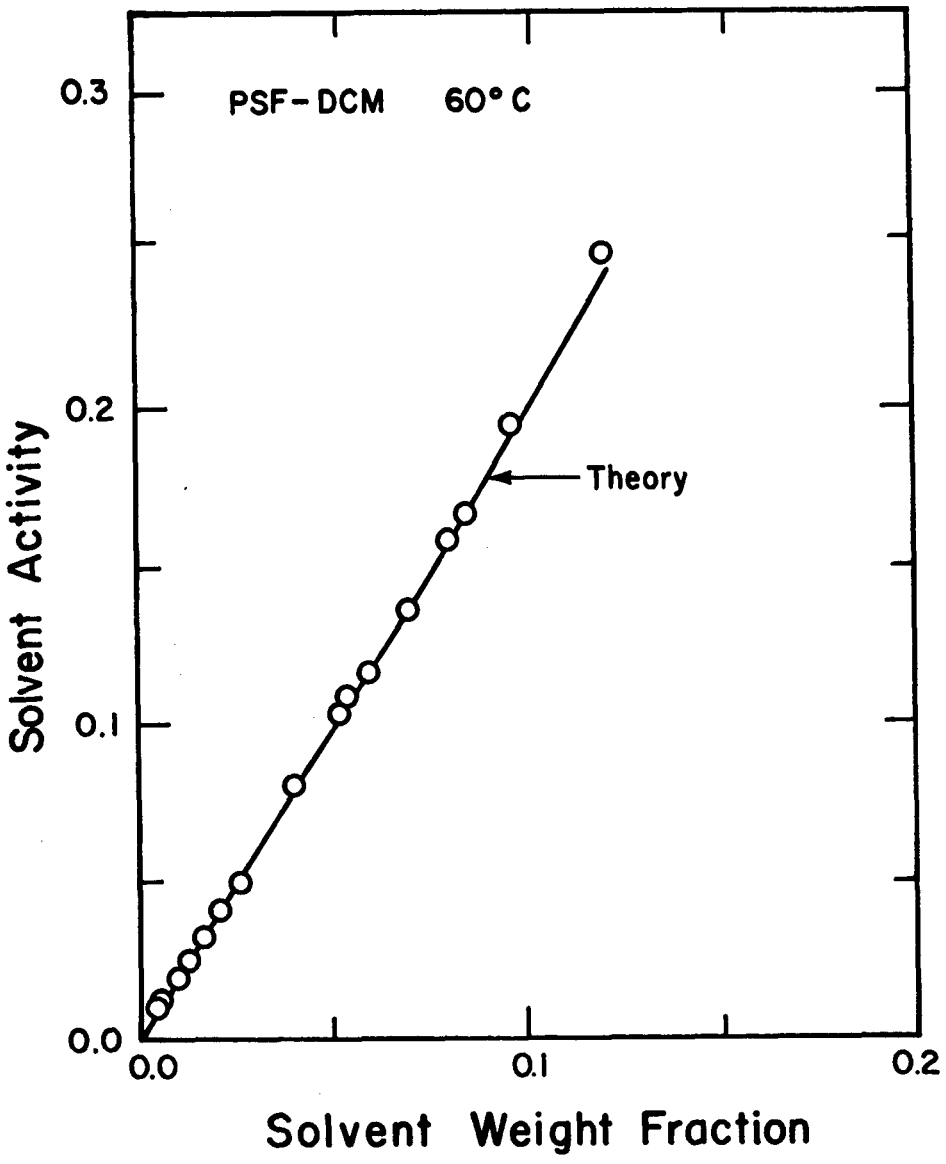

Figure 12. Activity of Dichloromethane (Corrected for Langmuir Term) in Polysulfone at 60° C.

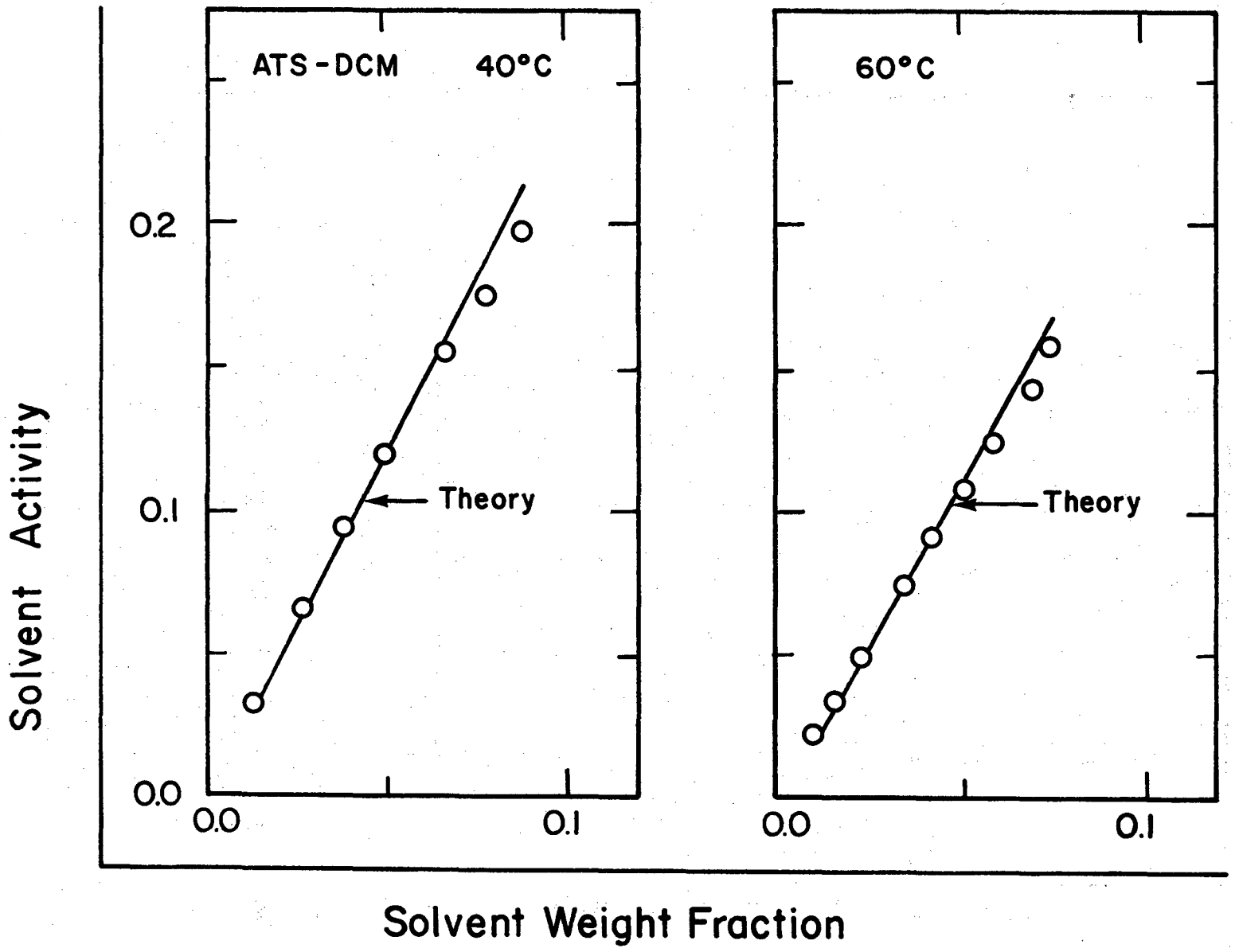

Figure 13. Activity of Dichloromethane in ATS.

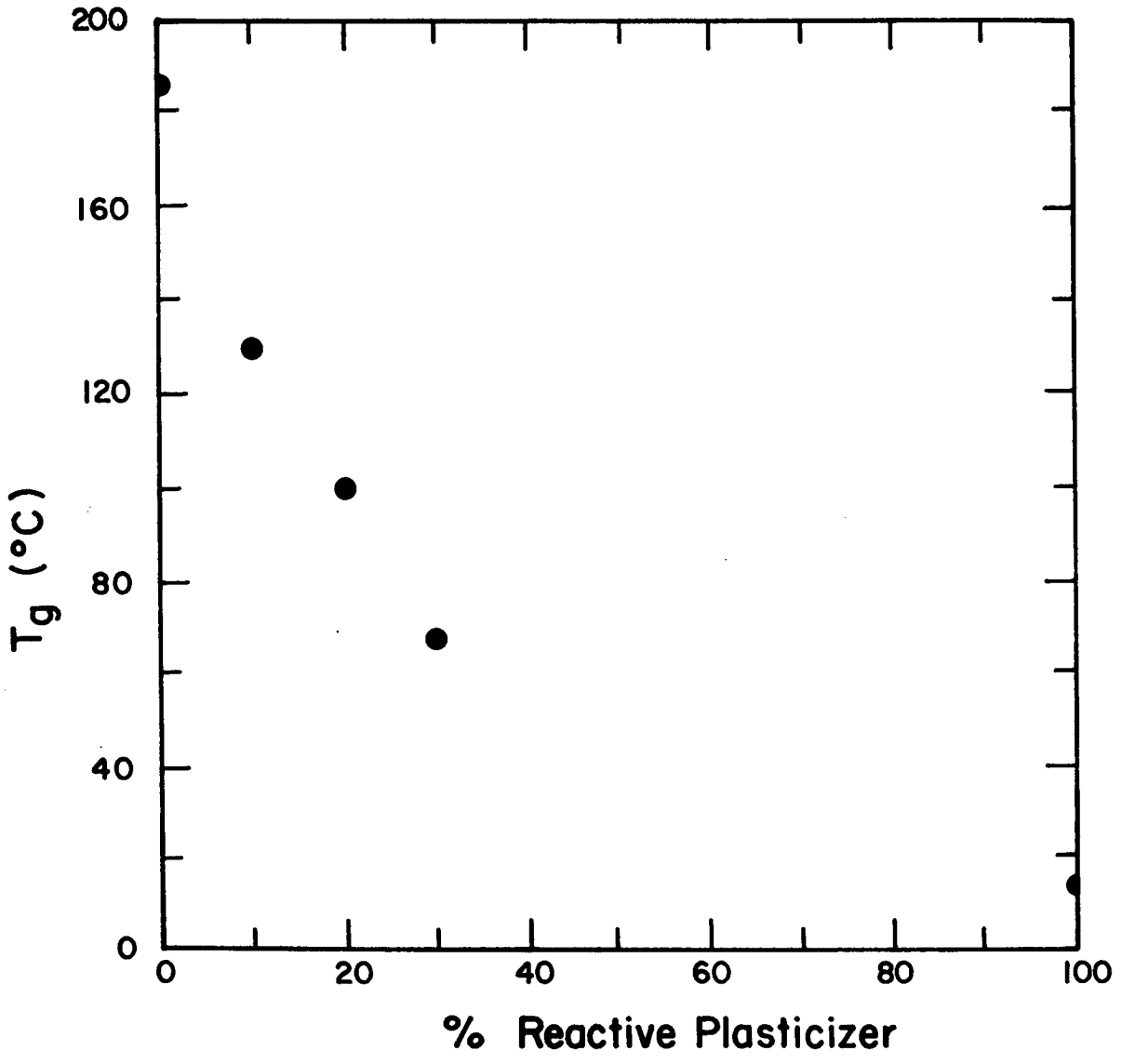

Figure 14. Glass Transition Temperature of P1700-ATS Mixtures as a Function of Composition.

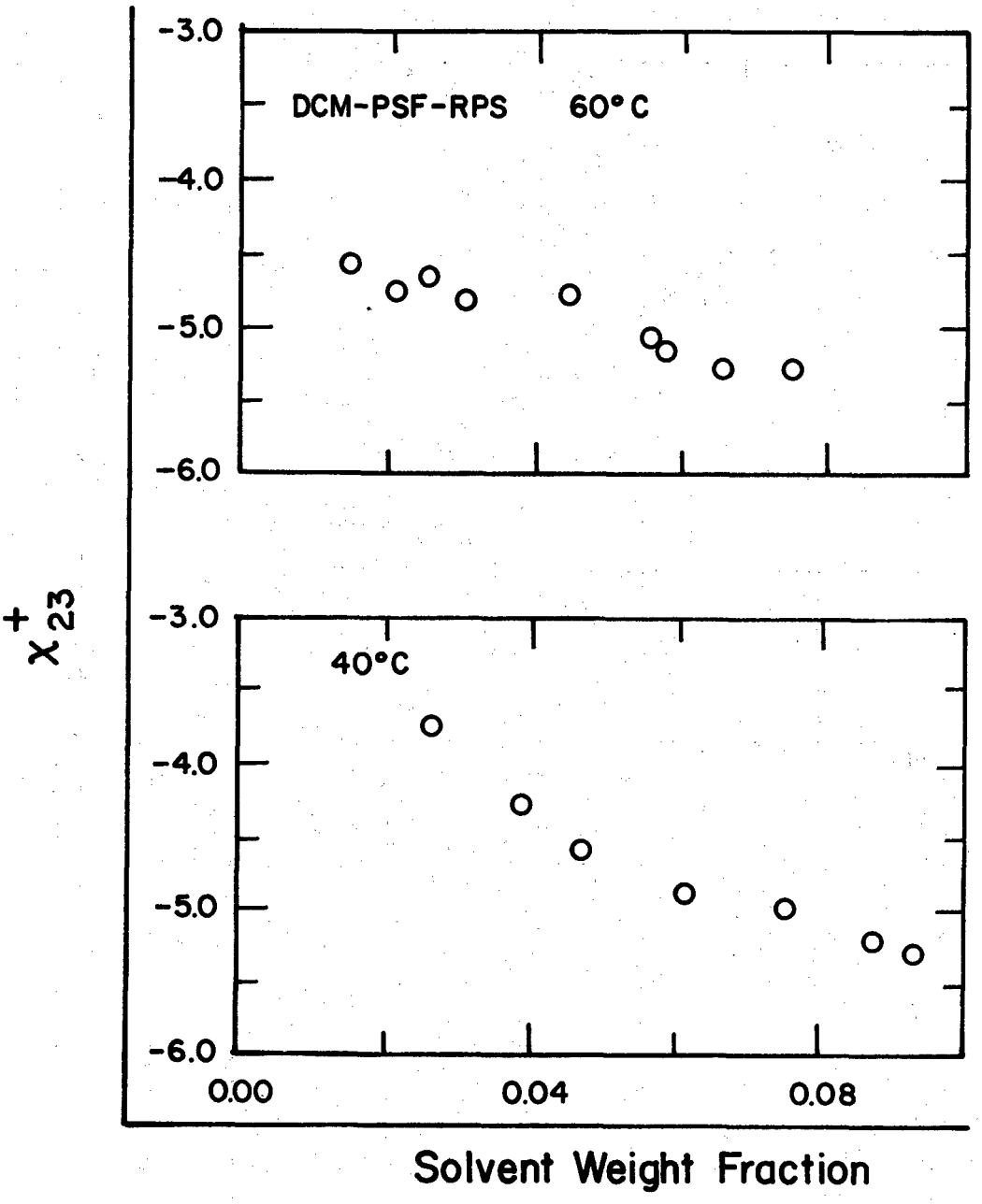

Figure 15. The Modified Flory-Huggins Interaction Parameter for P1700 ATS in Dichloromethane

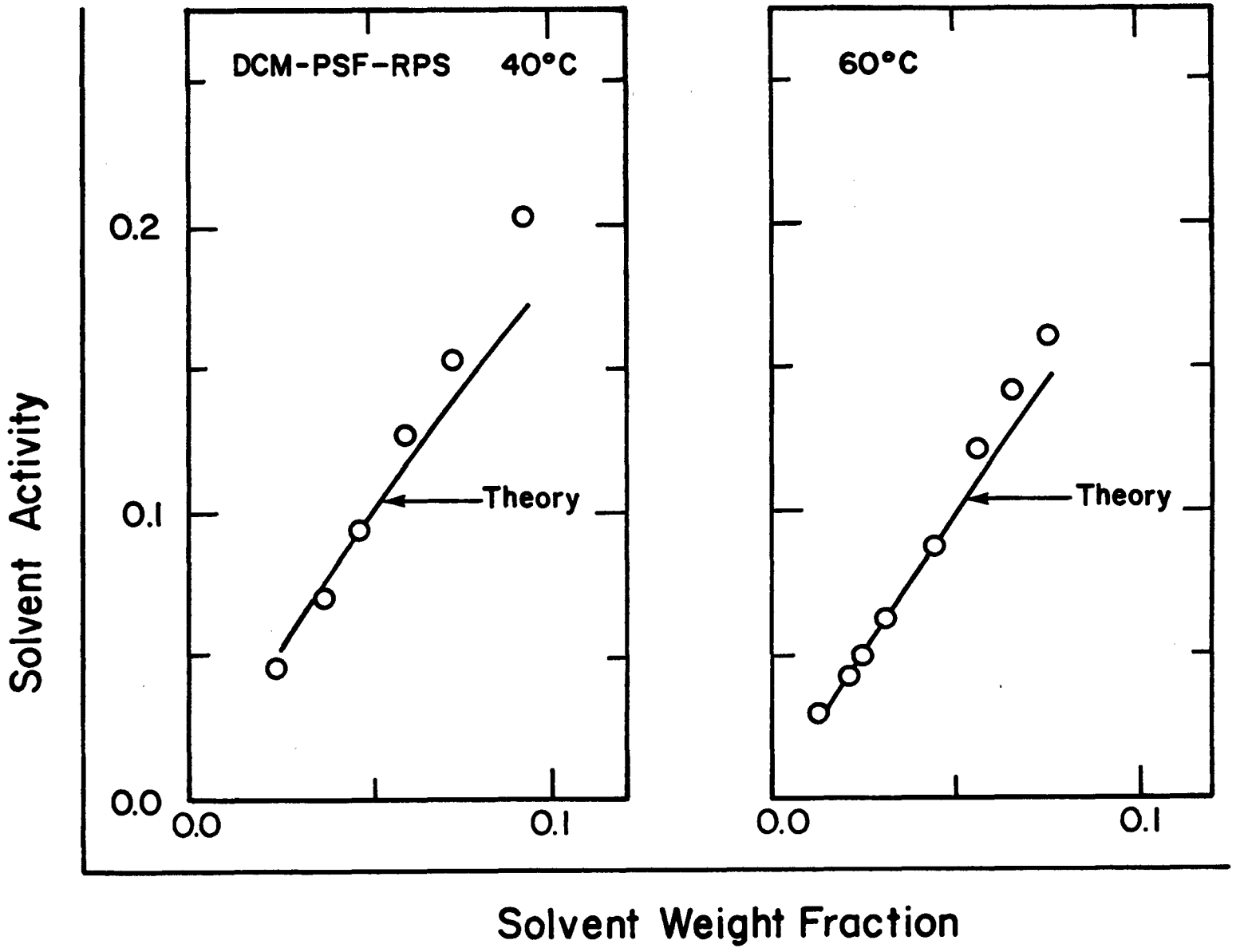

Figure 16. Activity of Dichloromethane in P1700-ATS Mixture.

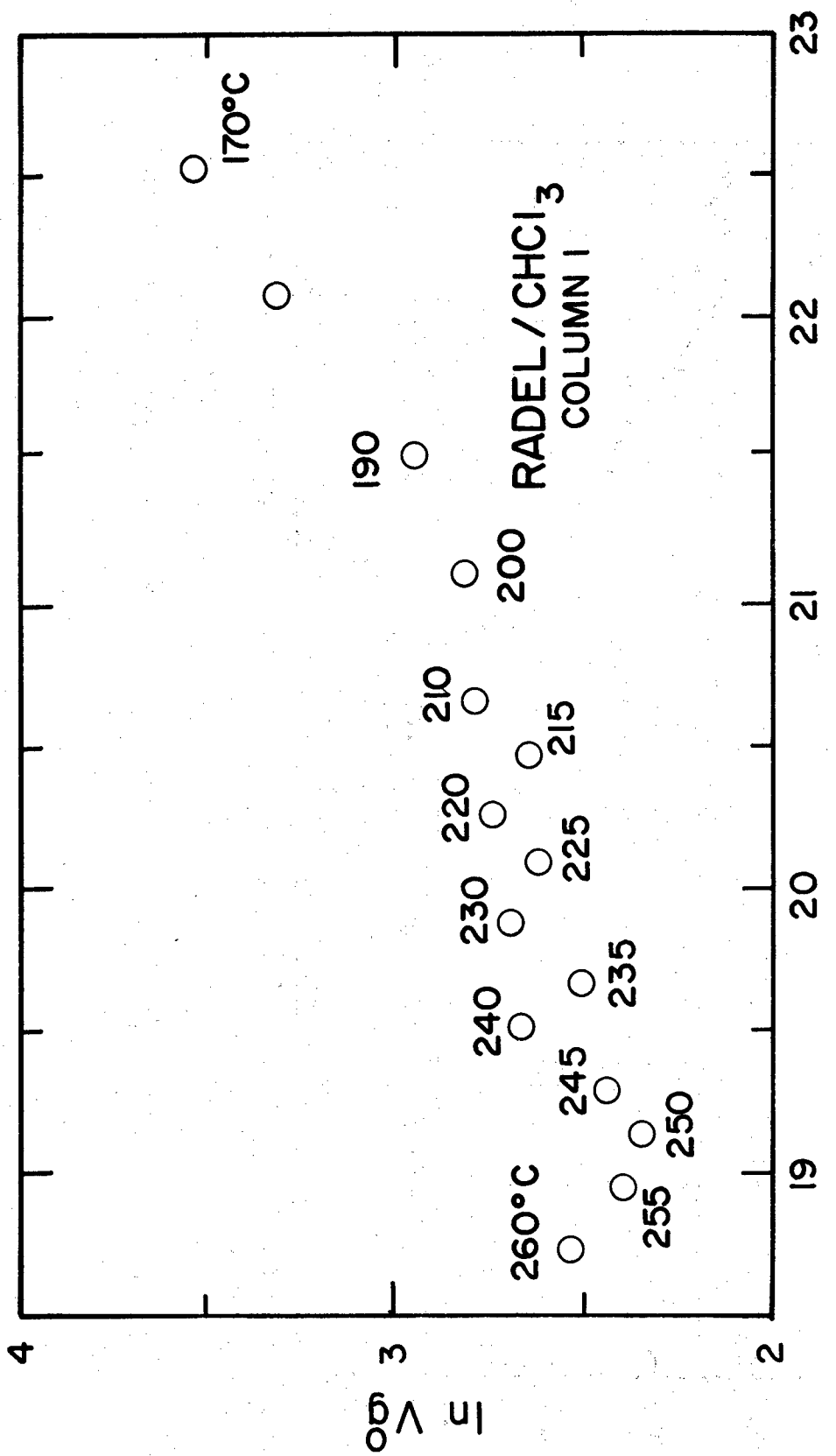

Figure 17. Radel / Chloroform Results for Column I.

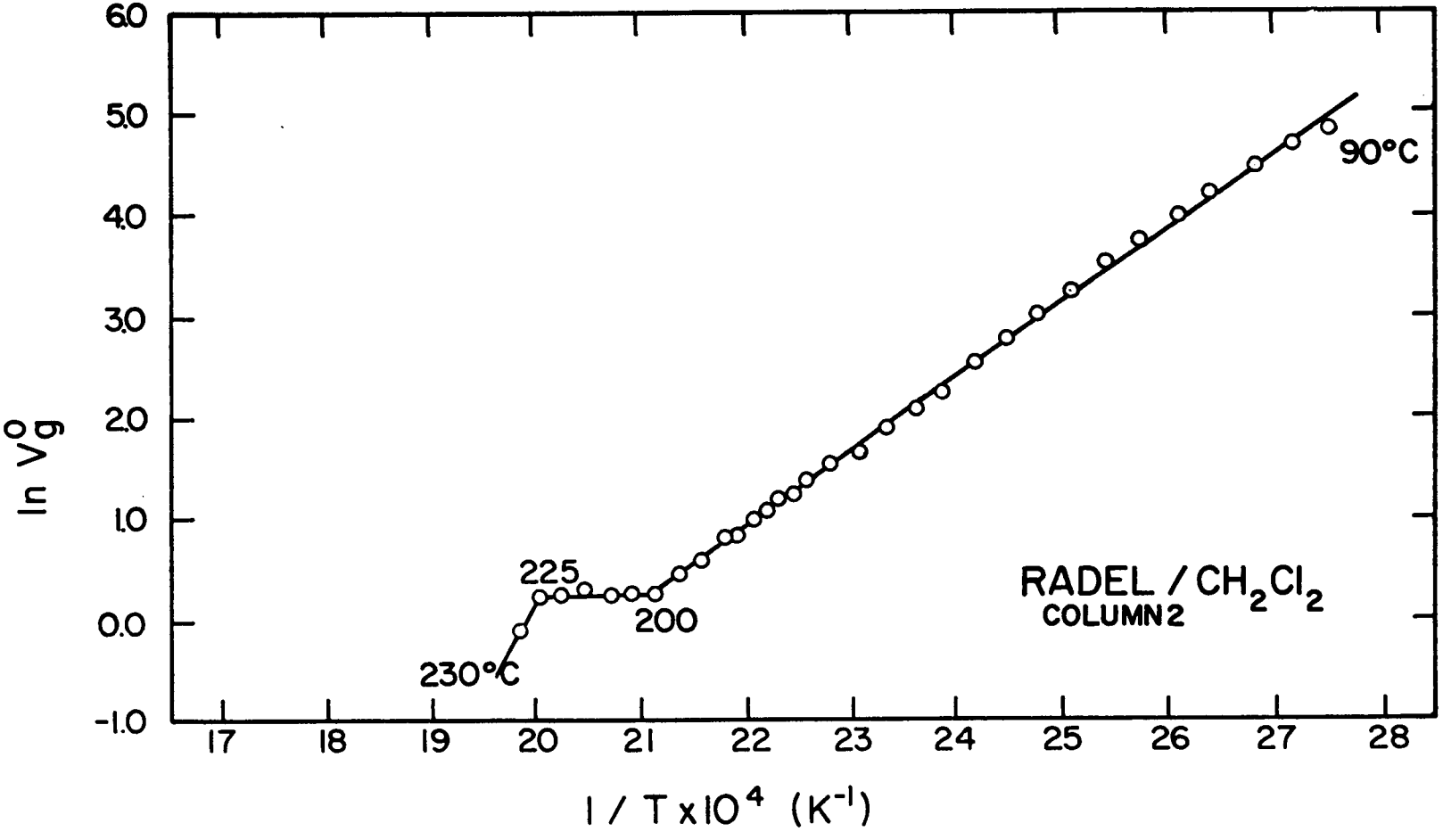

Figure 18. Radel / Dichloromethane Results for Column 2.

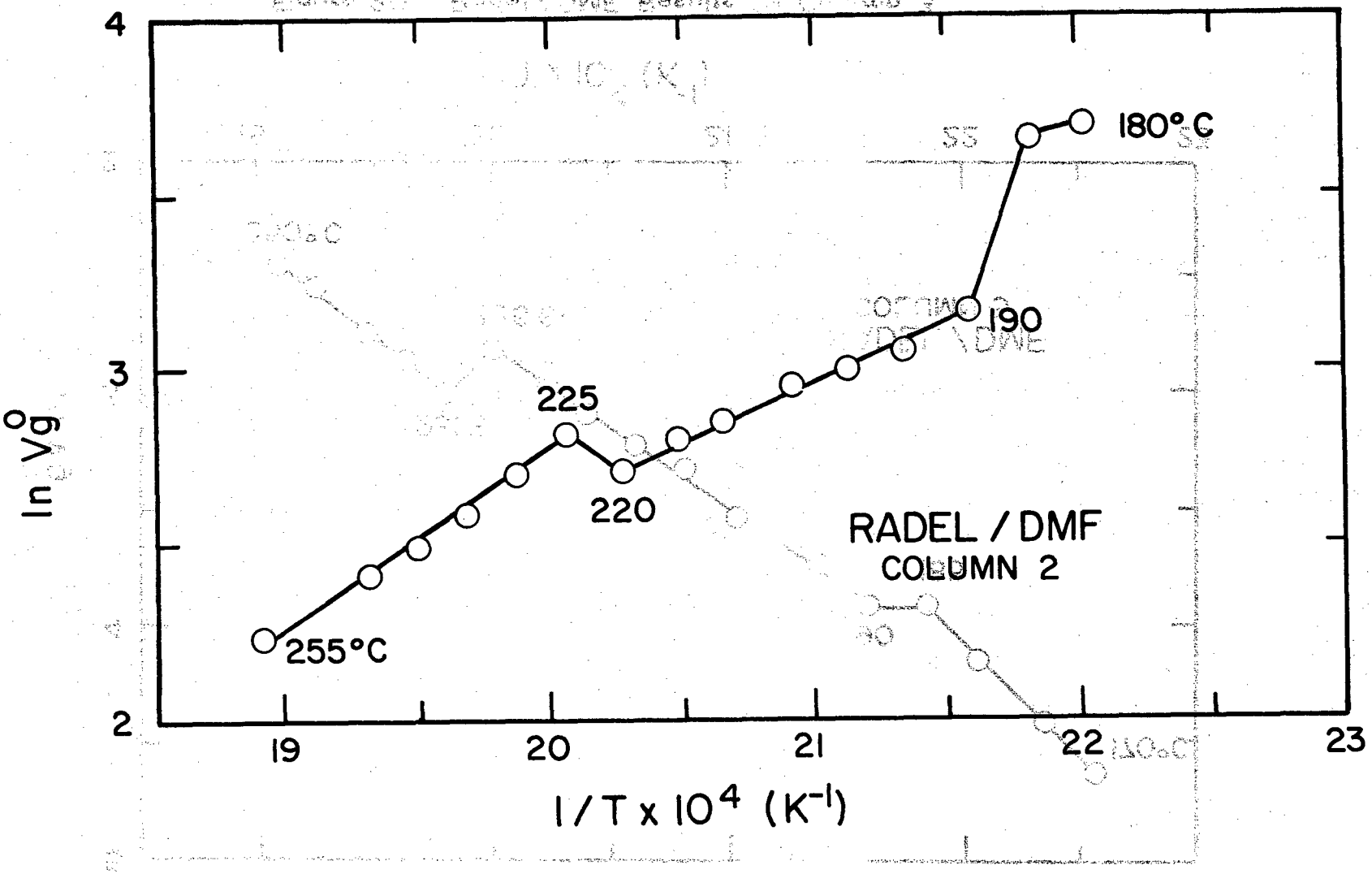

Figure 19. Radel / DMF Results for Column 2.

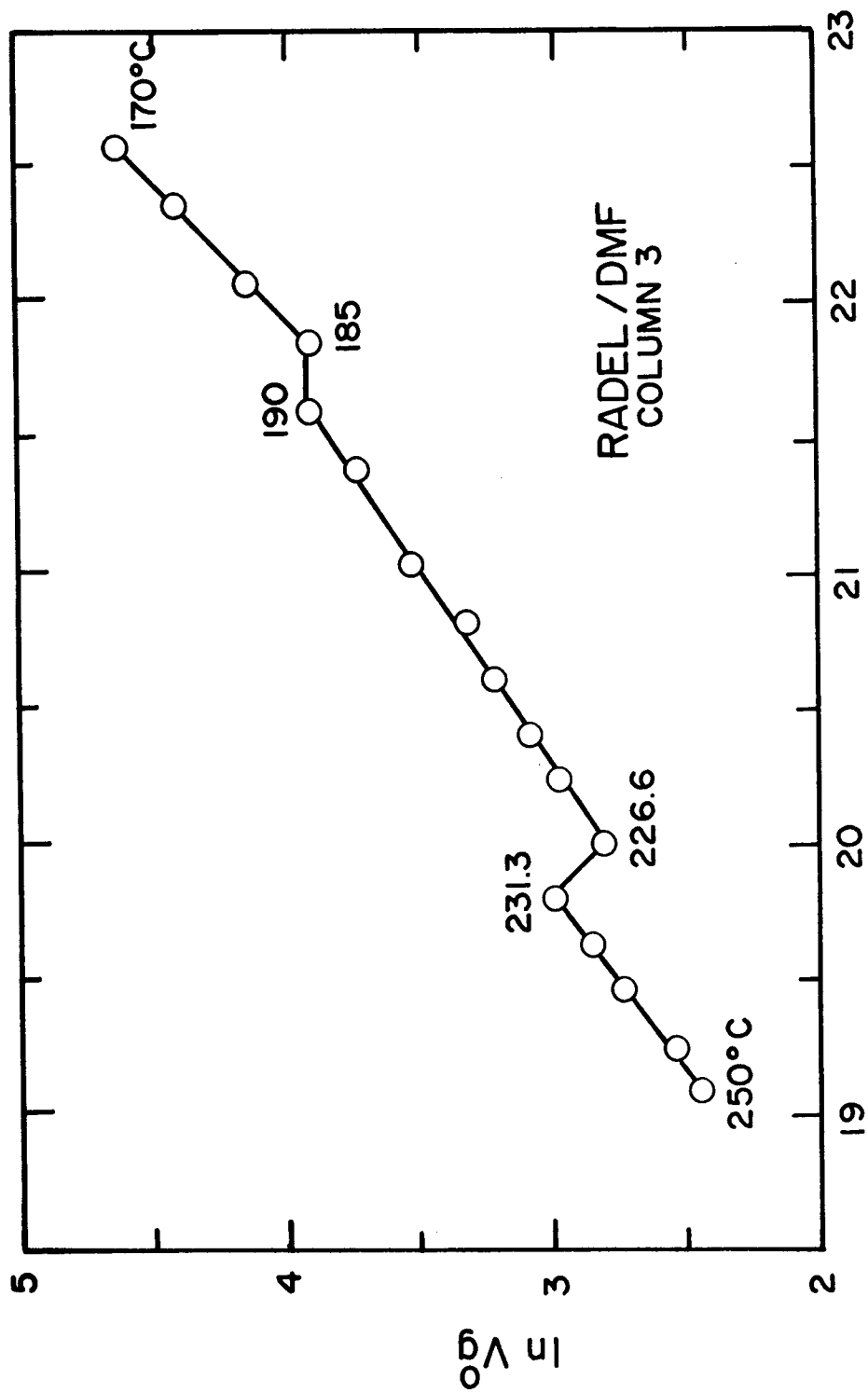

Figure 20. Radel / DMF Results for Column 3.

☆U.S.Government Printing Office: 1981 — 757-002/471